WADC TECHNICAL REPORT 55-243
PART II

# DEVELOPMENT OF ALLOYS HAVING GOOD HIGH TEMPERATURE PROPERTIES THROUGH POWDER METALLURGY TECHNIQUES

*Dr. R. Kieffer*
*Dr. F. Benesovsky*

*Metallwerk Plansee*

*SEPTEMBER 1959*

Materials Laboratory
Contract Number AF 61(514)-1144
Project No. 7351

WRIGHT AIR DEVELOPMENT CENTER
AIR RESEARCH AND DEVELOPMENT COMMAND
UNITED STATES AIR FORCE
WRIGHT-PATTERSON AIR FORCE BASE, OHIO

300 — November 1959 — 10-311

# FOREWORD

This report was prepared by Metallwerk Plansee, Reutte/Tyrol, under USAF Contract No. AF 61(514)-1144. The contract was initiated under Project number 7351, "Metallic Materials", Task number 73512, "Refractory Metals." It was administered under the direction of the Materials Laboratory, Directorate of Laboratories, Wright Air Development Center, with Mr. C. B. Hartley acting as project engineer.

This report covers work conducted from 1 December 1956 to 31 December 1958.

## ABSTRACT

Wet milled powder mixtures of Fe-Al-Mo 80-14-5-TiC/$Cr_3C_2$ alloys with 0-30% of a 90-10 TiC/$Cr_3C_2$ mixed crystals were sintered in a vacuum and their properties were evaluated.

With increasing additions of carbide mixed crystals the hot strength increases; however, the alloys become brittle.

The reinforcing of these alloys by means of Ni-Cr, megapyr or molybdenum wire and nets pressed into the powder compacts increases the impact strength provided no reaction occurs between the alloy and the reinforcing structure.

## PUBLICATION REVIEW

The publication of this report does not constitute approval by the Air Force of the findings or conclusions contained herein. It is published only for the exchange and stimulation of ideas.

FOR THE COMMANDER:

I. Perlmutter
I. PERLMUTTER
Chief, Physical Metallurgy Branch
Metals and Ceramics Division
Materials Laboratory

TABLE OF CONTENTS

LIST OF ILLUSTRATIONS

LIST OF ILLUSTRATIONS CONTINUED

LIST OF ILLUSTRATIONS CONTINUED

LIST OF ILLUSTRATIONS CONTINUED

LIST OF TABLES

LIST OF TABLES CONTINUED

LIST OF TABLES CONTINUED

LIST OF TABLE CONTINUED

LIST OF TABLES CONTINUED

# I. INTRODUCTION

The purpose of this research project was to continue the investigation of a series of highly refractory and scale resistant materials developed and evaluated under Contract AF 61(514)-741C. The results of this investigation were reported in WADC Technical Report 55-243 Pt. I.

To achieve this objective the program was conducted in the following manner:

a. Research on the influence of the grade of milling or grinding on the properties, especially on the toughness of the materials of the alloys Fe-Al-Mo-TiC/$Cr_3C_2$ 90/10-B.

b. Influencing the toughness of the above mentioned alloys by embedding the following materials into the greens: wire, braids and netting wire of molybdenum or other refractory metals as well as nickel-chromium and iron-chromium-aluminum alloys of the type used for heating elements. We call this reinforcement.

c. Influencing the toughness by coating the sintered specimens either electrolytically or by some other process. A recommendable coating consists of a nickel-chromium layer. Combining this process with the reinforcement according to item b).

d. Application of new binding alloys especially on the basis of:

Fe-Al-Ti
Ni-Al
Co-Al
Ni-Al-Si and Co-Al-Si

e. Improvement of the toughness of such alloys by the process as described under items a to c.

The metal powders and powdered alloys necessary for the manufacture of the compounds showed the following chemical compositions and physical properties:

1. Carbonyl Iron Powder (Badische Anilin und Sodafabrik Ludwigshafen)

Loss in hydrogen: 0,10%
Carbon 0,05%
Silicon 0,01%
Manganese 0,008%
Phosphorus, sulphur 0,002%
Bulk volume 32 $cm.^3$/100 gms.
Tap volume 24 $cm.^3$/100 gms.
Grain size 10 $\mu$

Manuscript released by the authors 31 December 1958 for publication as a WADC Technical Report.

2. Ferro-Aluminum (Hütte Liezen)

Aluminum 49,7%
Iron remainder
Bulk volume 47 $cm^3$/100 gms.
Tap volume 33 $cm.^3$/100 gms.
Grain size $>$ 0,15 20%
$>$ 0,06 30%
$<$ 0,06 50%

3. Molybdenum (Metallwerk Plansee Ges. m.b.H., Reutte/Tirol)

Molybdenum $>$ 99,95%
Grain size $<$ 20 $\mu$

4. Ferroboron (Gesellschaft für Elektrometallurgie, Düsseldorf)

Boron 17,8%
Carbon 0,05%
Iron remainder
Bulk volume 43 $cm.^3$/100 gms.
Tap volume 23 $cm.^3$/100 gms.
Grain size $<$ 60

5. Titanium Hydride (Metal Hydrides Incorp., Beverly)

Titanium 93-94% Hydrogen 3,4 - 3,6%
Nitrogen 1,0 max. Calcium 0,1 max.
Magnesium 0,05 max. Carbon 0,1 max.
Iron 0,1 max Aluminum 0,1 - 0,3
Silicon 0,2 max Zirconium 0,2 max.
Grain size $<$ 5 $\mu$

6. Titanium Carbide - Chromium Carbide 90/10 (Own Production)

90 parts of pure TiC and 10 parts of $Cr_3C_2$ produced by carburization of chromium powder, intimately mixed by hand and dry milled for 20 hrs. Ingots were pressed and annealed in a high-frequency vacuum furnace for 30 minutes at 1500°C. The reaction cakes were crushed and wet milled with acetone for 48 hrs.

The following analysis was determined:

Carbon total 17,95%
Carbon free 0,13%
Bulk volume 65 $cm.^3$/100 gms.
Tap volume 40 $cm.^3$/100 gms.
Grain size $<$ 10 $\mu$

The X-ray diagram showed a mixed crystal with a B1 structure with a lattice constant:

$a = 4{,}292 \pm 0{,}005$ kX.E.

7. Molybdenum Wire (Metallwerk Plansee Production)

We made use of soft annealed wire of purest molybdenum (Mo > 99.9%) of the following diameters and tensile strength:

| Diameter: (mm.) | Tensile strength: (kg./mm.$^2$) | Elongation: (%) |
|---|---|---|
| 0,2 | 90-100 | 15-20 |
| 0,4 | 90-95 | 15-18 |
| 0,8 | 80 | 16-19 |

We put individual pieces of the wire of a diameter of 0.8 mm. into the compacts. On the other hand we employed the wire of 0.2 mm. dia. as embedding material in the shape of 4 wired braids and produced 3 wired braids from the dia. 0.4 mm. for the same purpose.

8. Molybdenum Netting Wire

The following netting was made of the above mentioned molybdenum wire:

| Diameter of wire: (mm.) | Width of mesh: (mm.) |
|---|---|
| 0,2 | 1,6 |
| 0,4 | 1,4 |
| 0,8 | 1,6 |

Pieces of these gauzes were placed into the compacts and consisted of 4 wires for the mesh of 0.2 dia. wire, of 4 wires for the mesh of 0.4 dia. wire and of 3 wires for the mesh of 0.8 dia. wire. The length was according to that one of the compact.

9. Nickel-Chromium and Megapyr Wire (Vacuumschmelze, Hanau/Main)

| Diameter mm. | | Tensile strength kg./mm.$^2$ | Elongation % |
|---|---|---|---|
| Nickel-chromium | 0,2 | 85 | 27 |
| Nickel-chromium | 0,4 | 83 | 34 |
| Nickel-chromium | 0,8 | 74 | 46 |
| Nickel-chromium | 1,5 | 75 | 40 |
| Megapyr | 0,2 | 92 | 17 |
| Megapyr | 0,4 | 83 | 20 |
| Megapyr | 0,8 | 77 | 20 |

## II. MANUFACTURE OF THE SPECIMENS

For the manufacture of the powder batches we exclusively employed the wet milling process. This process produces much finer grained and denser materials. Batches of 1 or 2 kgs. were ground during 24, 48 or 96 hours in cemented carbide lined mills with the aid of balls of cemented carbides and acetone acting as the liquid. After the evaporization of the acetone we mixed the fine powder batches in a mortar together with a solution of camphor in ether for easier compaction. The compacting was done in cemented carbide lined dies by means of a uniform pressure of 6 tons per sq.cm. We produced flat specimens of approx. 5 to 6 mm. in height and Charpy specimens of 12 x 12 x 60 mm. The Charpy specimens shrank during sintering to the approximate standard dimensions of 10 x 10 x 55 mm.

The embedding of wire, braids or netting was done as follows: One part of the specimen was compacted with 2 wires each, 2 braids each or 1 piece of netting wire embedded in such a manner that the material was right in the middle, i.e. in the neutral zone of the compact. We filled first the half amount of powder in the dies, put then the wires or netting on it and filled the second half of the powder into the die. We compacted subsequently with a pressure of 6 tons per sq.cm. The process of compacting the Charpy specimens, containing 4 wires or braids each was done similarly. We divided the necessary individual amount of powder into 3 parts and after having filled in one third we placed 2 wires or braids upon the powder. By so doing the embedded material was not in the neutral zone but approximately in 1/3 and 2/3 of the height of the compact. The properties of these specimens layout and the placing of the embedded materials are shown in Table 1.

There were no difficulties in compacting the specimens with the embedded wire, braids and netting. The fine powder completely coated the embedded material - as will be shown later on by micro-photos. During compacting we also could find out any fissures in the specimens with embedded netting of 0,8 mm. dia. wire. The sintering, however, produced fissures along some wires of embedded netting and for later investigations we did not use netting of 0,8 mm. dia. wire.

The sintering of the specimens was done in molybdenum wound vacuum furnaces at 1250°C. to 1300°C., resp. according to composition, during 2 hours in a vacuum of $< 10^{-2}$ Torr. The sintering facilities and the placing of the specimens in the furnace are described in WADC TR 55-243 Pt. I.

## III. EXAMINATION

The examination was done in the same way and with the aid of the same equipment as described in WADC TR 55-243, Pt. I. The only exception was the impact test where we also made use of Charpy specimens besides the flat test bars but also without notches. Besides the impact strength at room

Table 1: Impact Strength of Reinforced Charpy Specimens $Fe$-$Al$-$Mo$-$TiC/Cr_3C_2$ 90-B
(wet milled 24 hours)

| Specimen No. | Impact strength Charpy mkg./cm.$^2$ (1) | (2) | (3) | (4) | (5) | (6) | (7) |
|---|---|---|---|---|---|---|---|
| 22 | 1,1 | 1,49 | 1,62 | 1,30 | 1,53 | 1,44 | 1,68 |
| 23 | 1,0 | 1,57 | 1,65 | 1,71 | 1,70 | 1,76 | 1,58 |
| 24 | 0,94 | 0,98 | 1,05 | 0,83 | 0,94 | 1,16 | 1,07 |
| 25 | 0,82 | 0,86 | 0,86 | 0,78 | 0,98 | 0,86 | 1,00 |
| 26 | 0,74 | 0,61 | 0,59 | 0,72 | 0,77 | 0,69 | 0,79 |
| 27 | 0,54 | 0,50 | 0,59 | 0,71 | 0,71 | 0,63 | 0,59 |
| 28 | 0,51 | 0,49 | 0,42 | 0,45 | 0,44 | 0,51 | 0,43 |

(1) without reinforcement
(2) 2 molybdenum wires 0,8 mm. dia.
(3) 4 molybdenum wires 0,8 mm. dia.
(4) 2 molybdenum braids from 0,2 mm. dia. wire
(5) 4 molybdenum braids from 0,2 mm. dia. wire
(6) 2 molybdenum braids from 0,4 mm. dia. wire
(7) 4 molybdenum braids from 0,4 mm. dia. wire

temperature we also determined the values at 400,600,800 and 1000°C. For this purpose we heated the specimens in a muffle furnace in air to the temperature wanted, placing the specimens speedily into the impact tester and striking with a hammer of 3 m./kgs. For some specimens, however, the force of the hammer was unsatisfactory at 400°C. In these cases a notch would have been necessary.

a. Fe-Al-Mo-TiC/$Cr_3C_2$ Alloys, Influence of Wet Milling

Wet milling during 24, 48 and 96 hours was done with alloy batches containing 0,5,10,15,20,25 or 30% TiC/$Cr_3C_2$ besides the binding alloy consisting of approx. 80% Fe, 14% Al and 5% Mo as well as 0,5% B.

1. Pressed Density

The density of the compact decreases with increasing time of milling, in other words, the finer the powder batch the lower is the green density, which is an effect well known in powder metallurgy.

2. Sintered Density and Shrinkage

The sintered density as well is somewhat lower with batches which were subject to a longer milling, but the shrinkage is clearly higher, especially with samples containing low additions of carbides. A short milling term and a higher content of carbide provoke a lower shrinkage, higher porosity and at the same time, worse mechanical properties. This effect is probably due to a certain oxidation of the very fine particles thus inhibiting sintering.

3. Hardness

According to Figure 1 hardness increases with rising carbide content. The influence of the time of milling is not great, on the contrary, after a milling of 96 hours the values of hardness decreased to a certain extent due to higher porosity.

4. Tensile Strength at Room Temperature

The tensile strength of the materials rapidly decreases with increasing carbide content and if we take these values as a basis for the consideration of these materials, which is doubtful because of their brittleness, the influence on the values is positive if we extend the milling term from 24 to 48 hours. A further extension of the milling is, due to the reasons given above, negative and variations of the values obtained are greater. (Figure 2).

5. Impact Strength at Room Temperature

We determined the impact strength with flat samples as well as with Charpy like samples without notches and, as expected, the values

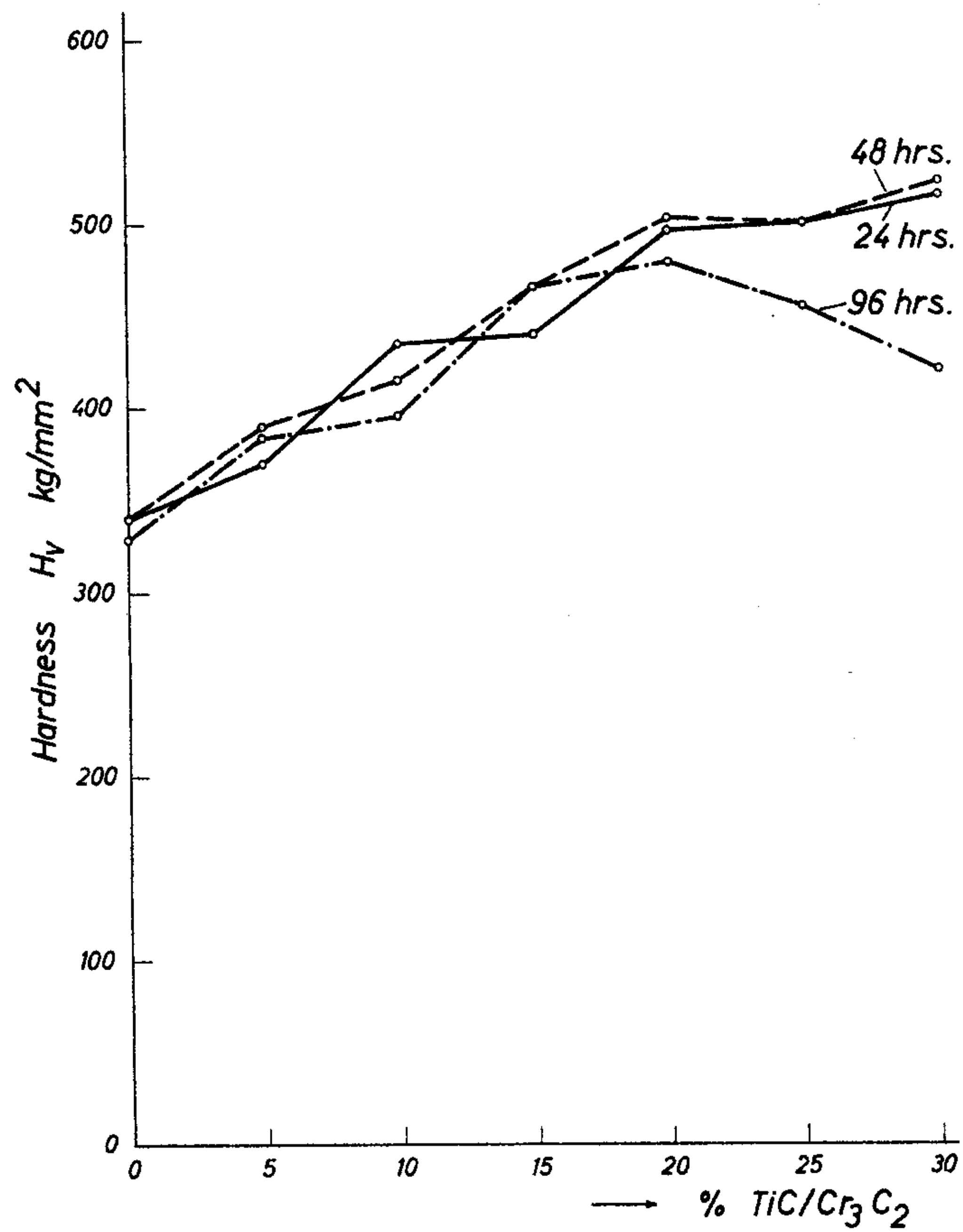


Fig. 1: Hardness of Wet Milled Fe-Al-Mo-$TiC/Cr_3C_2$ Alloys

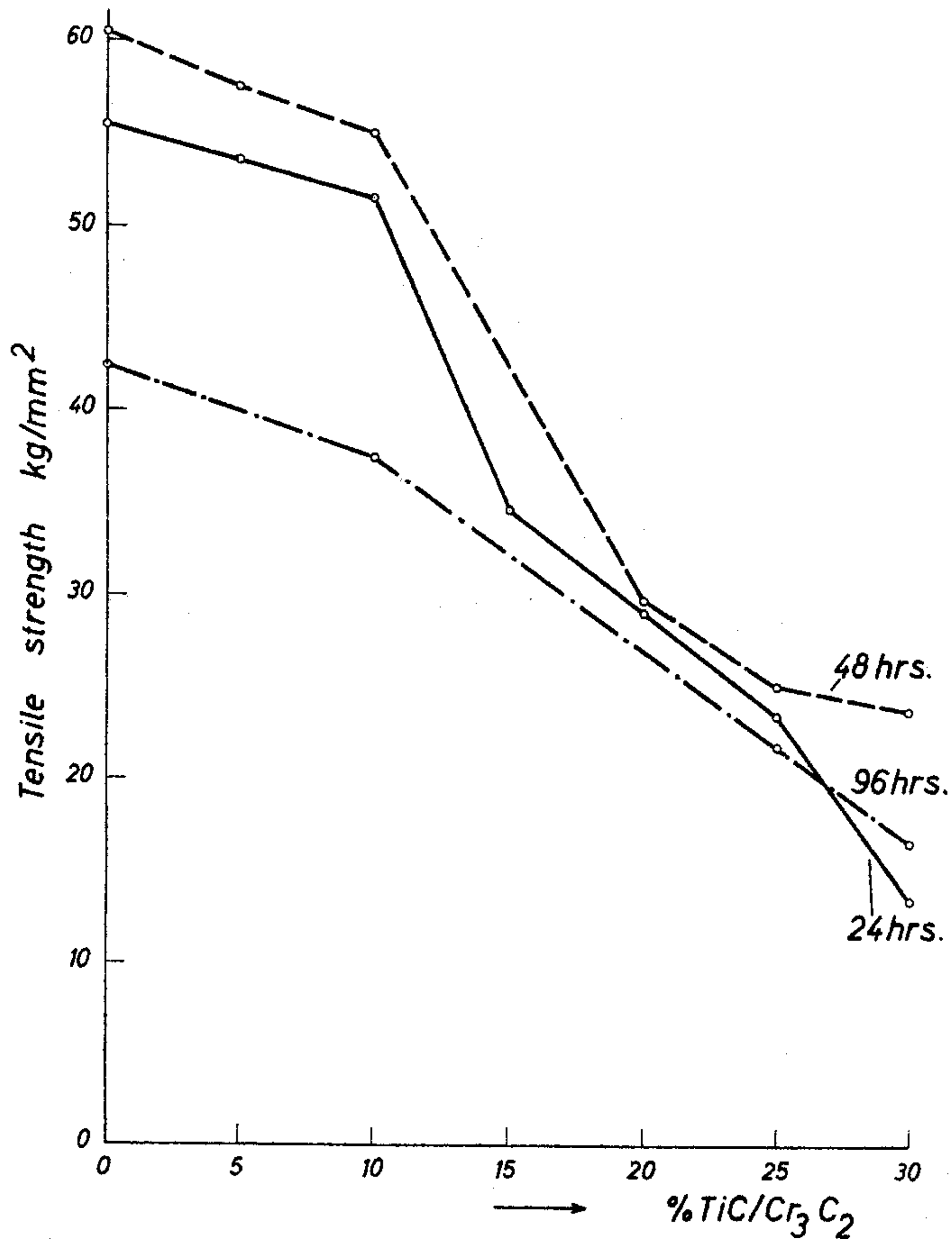


Fig. 2: Tensile Strength of Wet Milled Fe-Al-Mo-TiC/$Cr_3C_2$ Alloys

decreased with increasing carbide content. In any case, even the specimens with high carbide content are considerably tough. A long term milling provokes a certain rise of the values, even if the milling is extended to 96 hours (Figure 3). The values, however, are subject to variations.

6. Non-Scaling Properties

The property is excellent at 800 to 900°C. At 1100°C. a scale layer appears, especially with specimens of low carbide content, which has poor adhesion. Specimens, containing 20 to 30% $TiC/Cr_3C_2$ are relatively non-scaling even at this temperature. An extension of the time of milling results in a generally worse scaling property. The scale layer is less adhesive with samples made from long term milled batches.

7. Transverse Rupture Strength at Elevated Temperature

The transverse rupture strength at elevated temperature shows better values the higher the carbide content (Figure 4). Many samples show a certain increase in tensile strength at medium test temperatures which is certainly due to the increased ductility in this range. We could observe this effect specially with samples made of long term milled batches. Generally speaking, the influence of the milling time is not too great. All values are somehow decrease and are rather variable if the milling is extended to 96 hours.

8. Hot Hardness

The hot hardness increases considerably with increasing carbide content (Figure 5). The batches milled 48 hours show a slightly increased hot hardness whereas the values of samples made of batches milled for 96 hours are varying and somewhat lower.

9. Hot Tensile Strength

As already previously mentioned, the values of the tensile strength of materials, especially with higher additions of carbides, vary considerably due to their brittleness. A consideration of these values is not very informative (Figure 6). A short time test shows a decrease of the tensile strength with increasing temperatures, as expected. The specimens of higher carbide content show even at the highest test temperature of 900°C. the relatively highest tensile strength. There is also an apparent increase of the tensile strength of many samples in the range of 500 to 700°C. This is comparable to the hot transverse rupture strength. The reason is certainly the increased ductility. The samples made of batches milled 96 hours show again variable and somewhat lower values.

10. Impact Strength at Elevated Temperatures

The previous tests proved that an extended milling term does not exercise a too favorable influence on the properties. By these

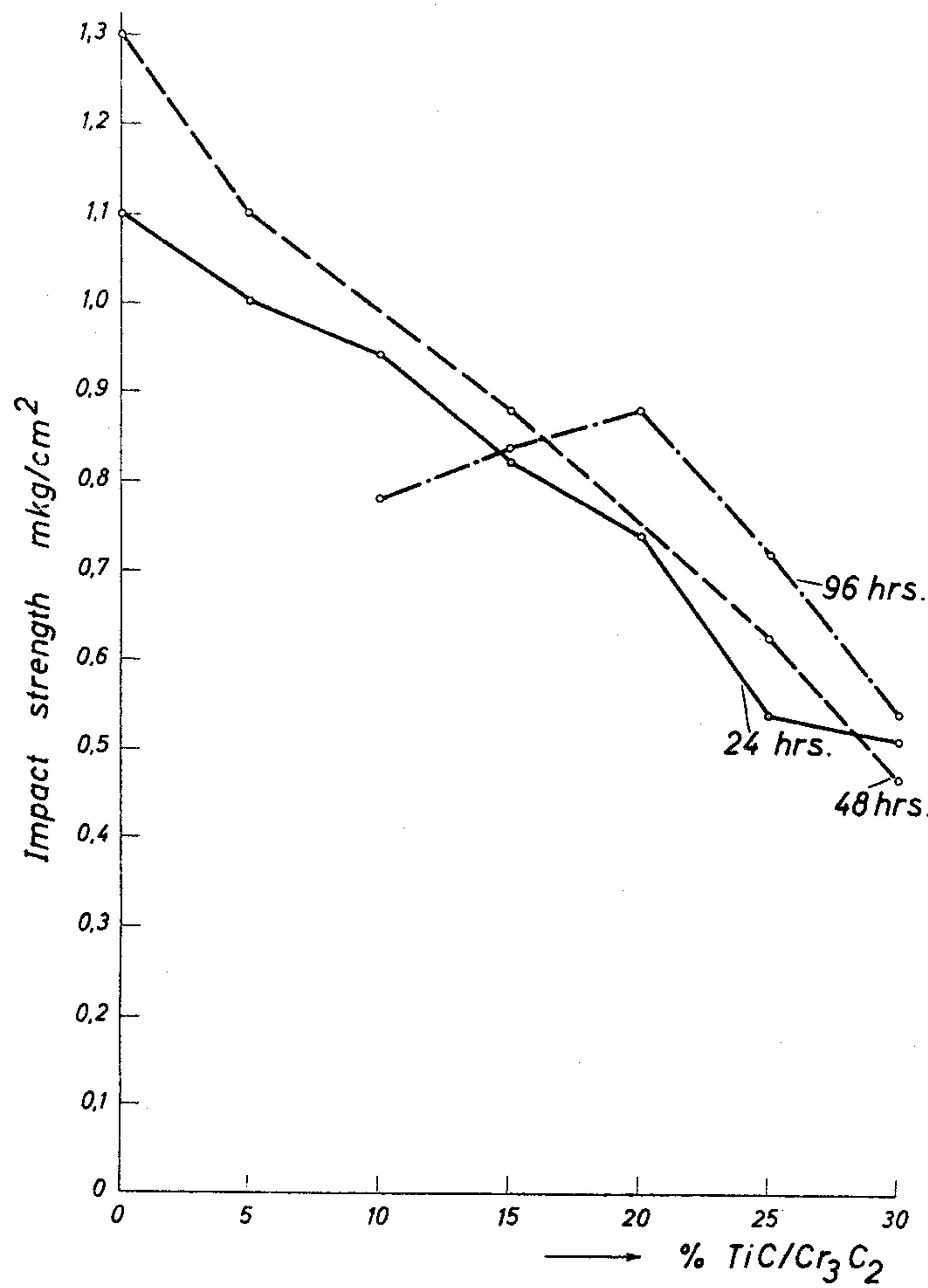


Fig. 3: Impact Strength of Wet Milled Fe-Al-Mo-TiC/$Cr_3C_2$ Alloys

| AF 61(514)-1144 Techn.Note | Metallwerk Plansee Ges.m.b.H. Reutte/Tirol | |
|---|---|---|

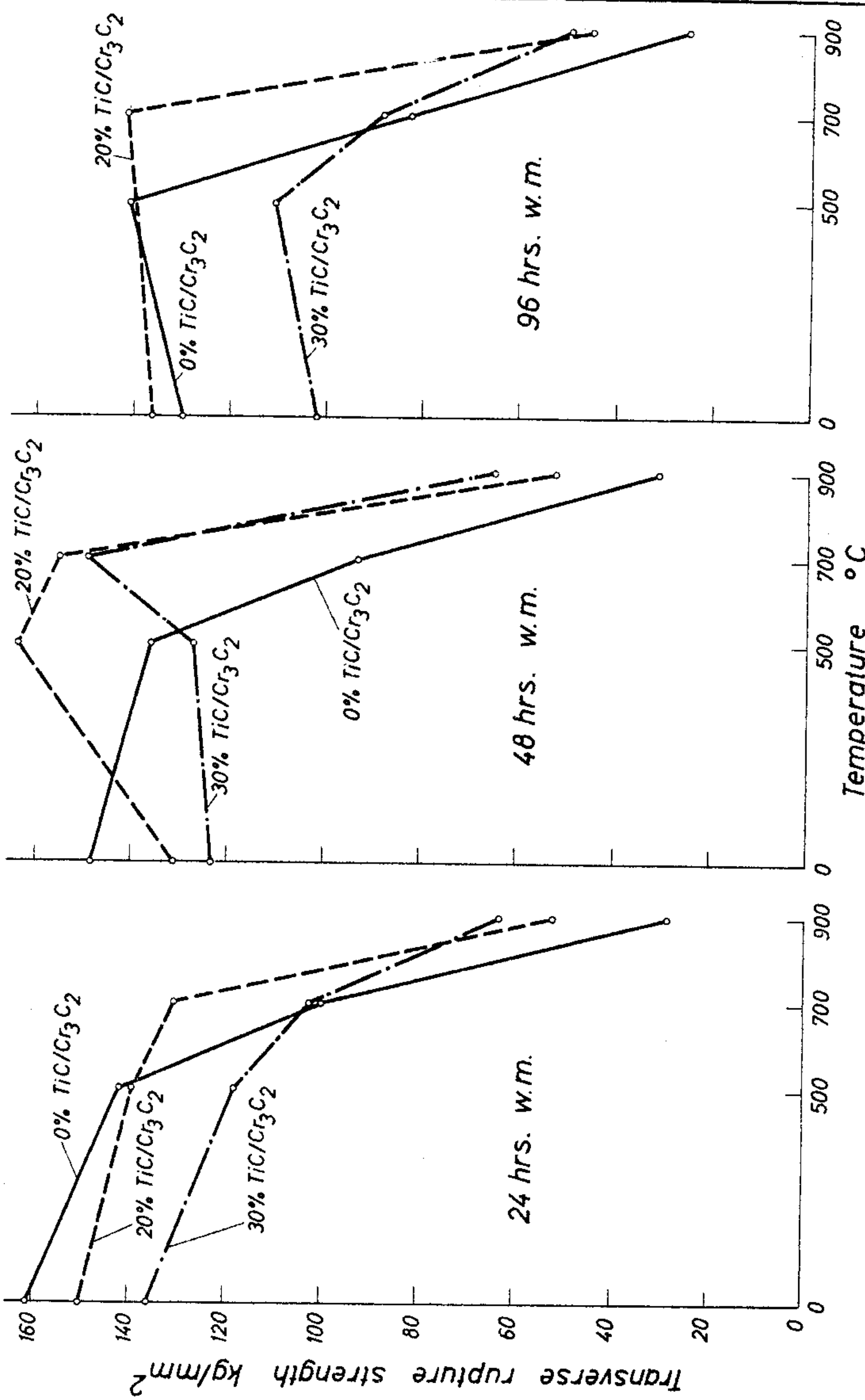


Fig. 4: Transverse Rupture Strength at Elevated Temperatures of Wet Milled Fe-Al-Mo-TiC/$Cr_3C_2$ Alloys

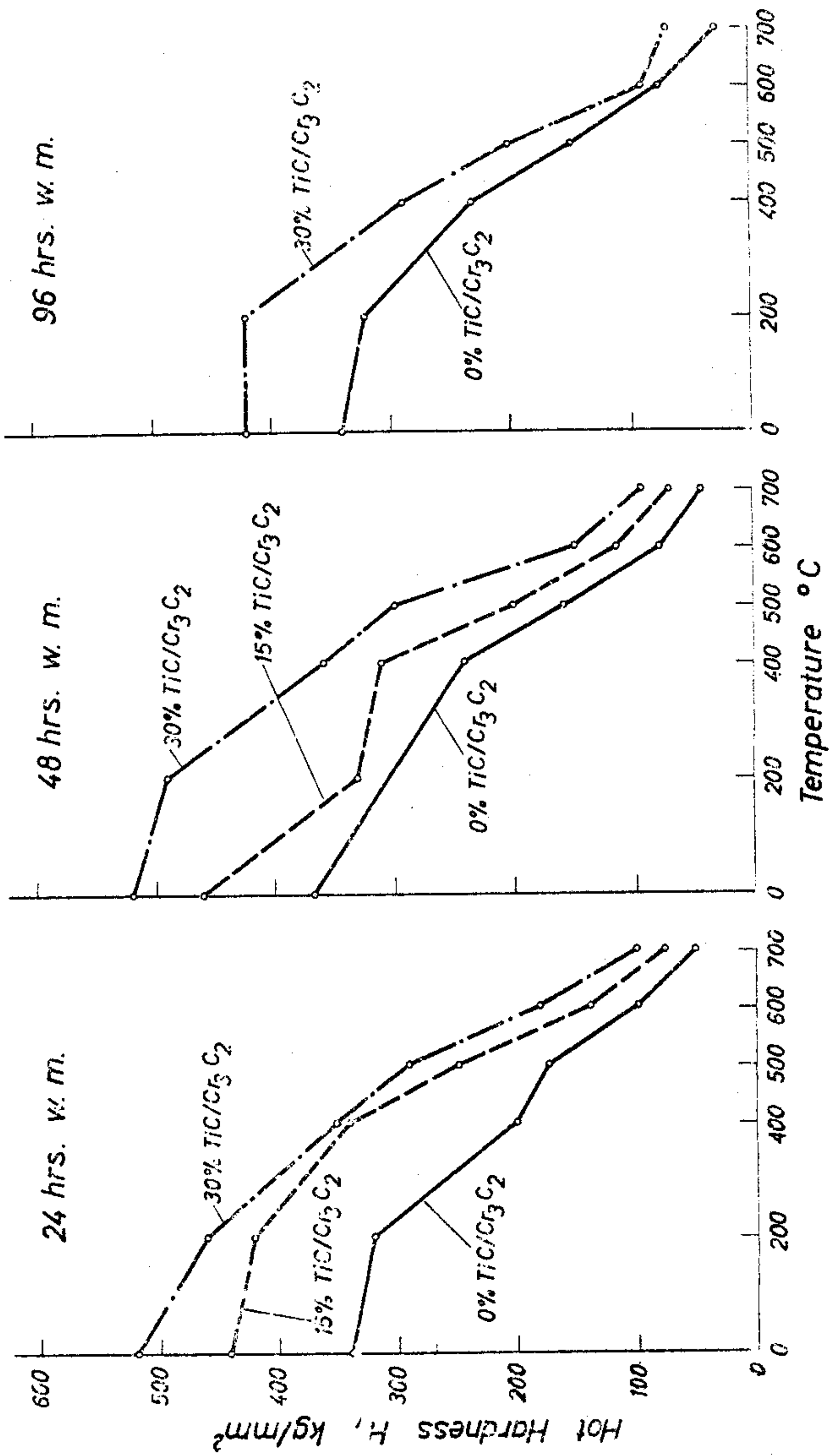


Fig. 5: Hot Hardness of Wet Milled Fe-Al-Mo-TiC/$Cr_3C_2$ Alloys

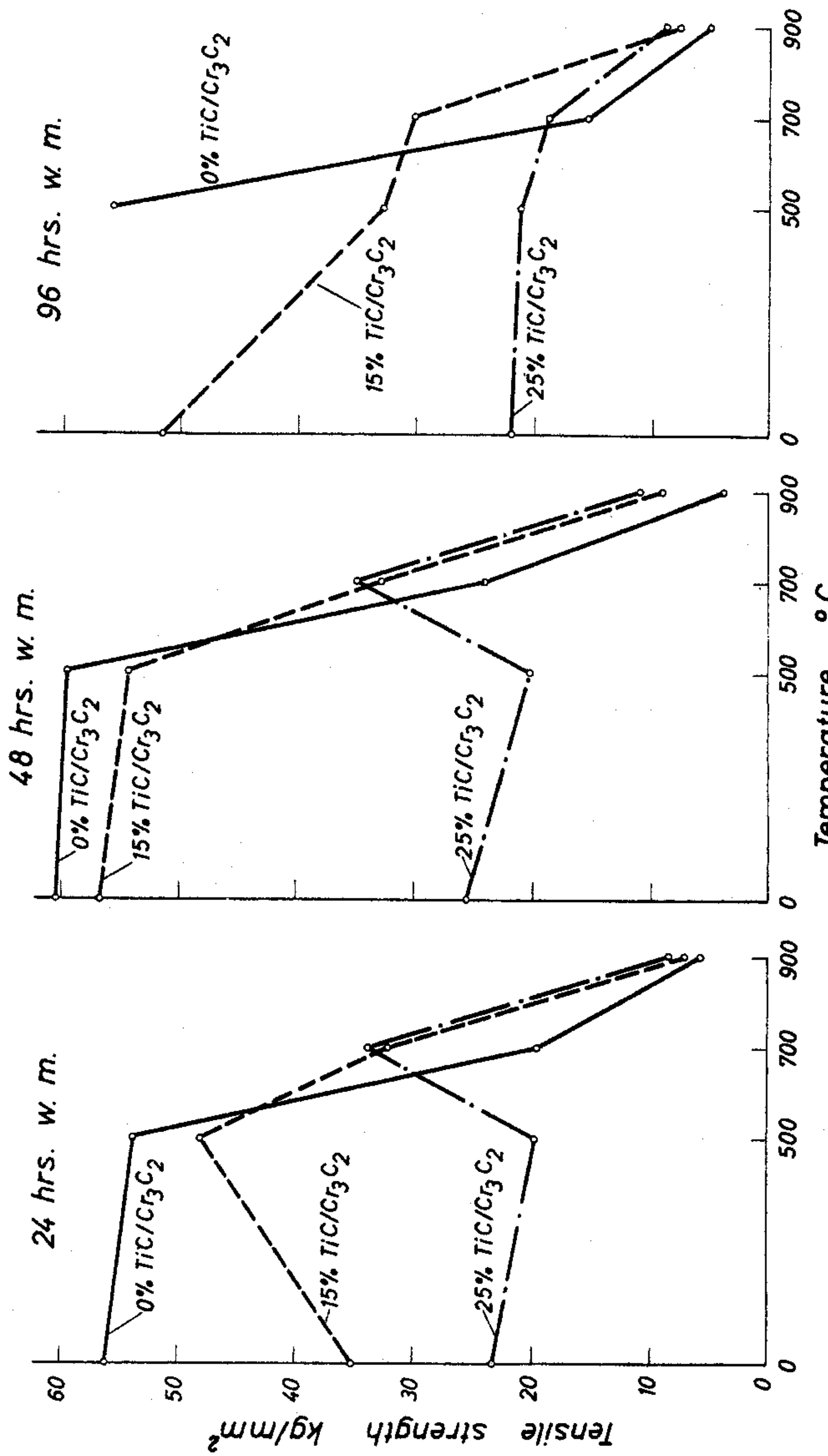


Fig. 6: Tensile Strength at Elevated Temperatures of Wet Milled Fe-Al-Mo-TiC/$Cr_3C_2$ Alloys

reasons and for a simplified production of powder batches for further research they were only wet milled for 24 hours.

The impact strength showed generally an increasing tendency in the temperature range of 20 to 600°C. with specimens of carbide content. At 800°C. there is a certain decrease and at 1000°C. all specimens with the exception of those of high carbide content are getting so tough that we could no longer destroy them with the 3mkg hammer available and they showed only a strong deformation (Figure 7). The specimen with 30% $TiC/Cr_3C_2$ did not change very much in its impact strength showing that the relatively brittle alloy remains rigid and may, therefore, have a high stress to rupture strength.

If high impact strength is desirable we have to chose alloys with lower additions of carbides; in this case we have to put up with lower stress to rupture strength and increased creep.

b. Fe-Al-$TiC/Cr_3C_2$ Alloys, Influence of Reinforcements on Impact Strength

1. Reinforcement by Molybdenum

Tables 1 and 2 (impact strength at room temperature), Tables 3 to 6 (hot impact strength) and Tables 7 to 10 (transverse rupture strength and tensile strength at room temperature and at elevated temperatures) show the influence of a reinforcement on the impact strength by using molybdenum wire of 0,8 mm diameter, as well as of braids of molybdenum wire 0,2 and 0,4 mm dia. and gauzes made of molybdenum wire of 0,2, 0,4 and 0,8 mm. Figures 8 and 9 evidence the strong rise of the impact strength by a reinforcement of molybdenum wire, braids and gauzes embedded in specimens containing small additions of carbides. Samples of high carbide content show a low influence, a fact which is probably due to transpositions of the molybdenum with the embedding alloy probably creating brittle phases. Microscopic investigations shown in Figures 10 thru 13 proved this fact.

When testing the reinforced samples for their hot impact strength, the samples of low carbide content showed according to the previously mentioned results a certain increase of the impact strength whereas there was no observable effect with alloys of high carbide content. The transverse rupture strength at room temperature and at temperatures between 500 to 900°C., as determined with flat specimens reinforced by embedded molybdenum wire and gauzes, increases somewhat with increasing carbide content as illustrated in Figure 14. The transverse rupture strength at room temperature of reinforced rods made of alloys with low carbide content is higher than with not reinforced rods (See Figure 4). On the contrary, specimens of higher carbide content show a decrease in values at both room and increased temperature, probably due to the transposition of the molybdenum with the embedding alloy, producing brittle phases. These results are in accordance with findings made on hot impact tests.

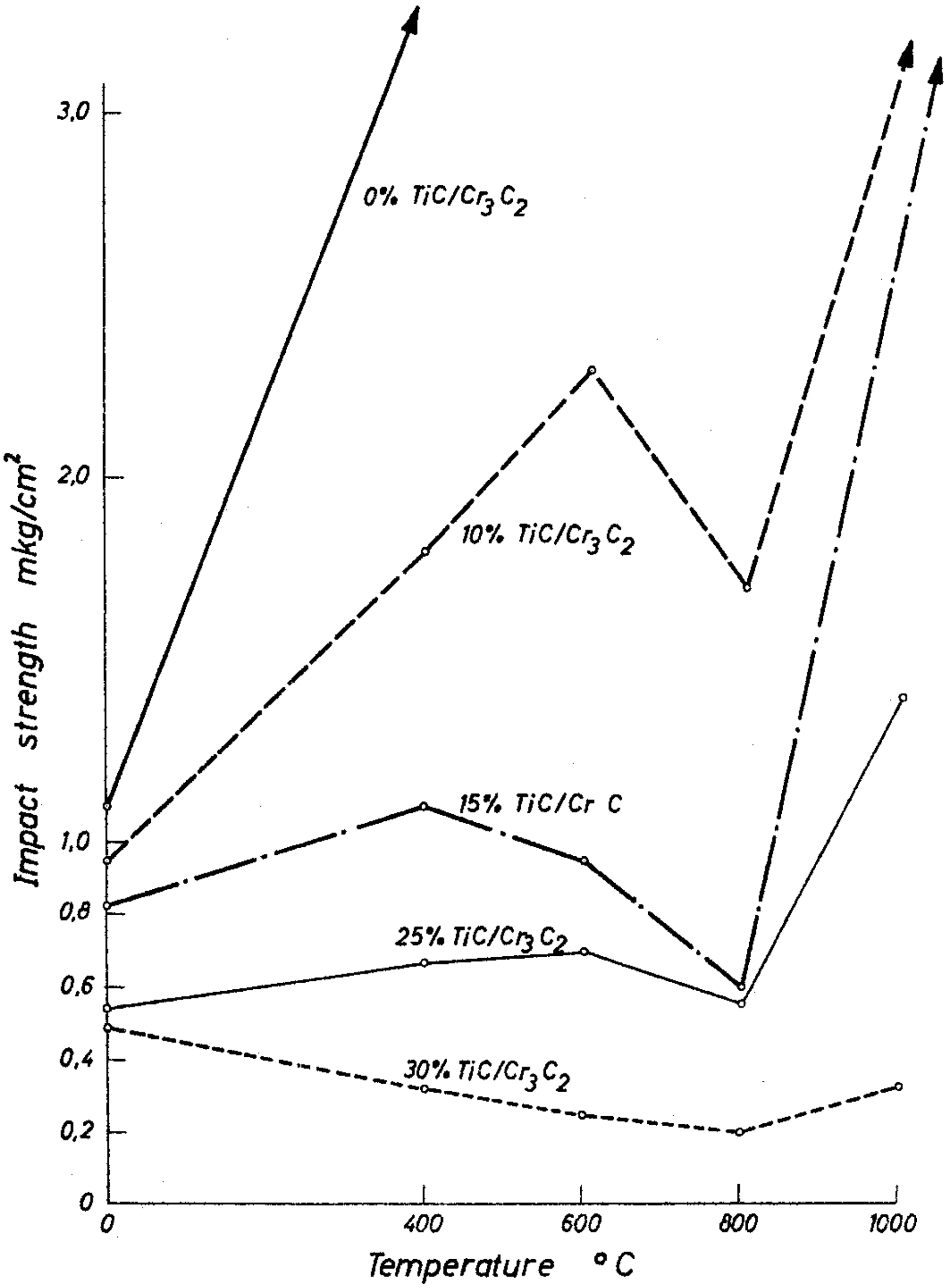


Fig. 7: Impact Strength of Charpy Bars at Elevated Temperatures (24 hrs. wet milled, without reinforcement)

Table 2: Impact Strength of Reinforced Charpy Specimens
$Fe-Al-Mo-Cr_3C_2$ 90/10-B (wet milled 24 hours)

| Specimen No. | Impact strength Charpy $mkg./cm.^2$ | | | |
|---|---|---|---|---|
| | (1) | (2) | (3) | (4) |
| 22 | 1,1 | 1,58 | 1,72 | 1,85 |
| 23 | 1,0 | 1,95 | 1,83 | 1,83 |
| 24 | 0,94 | 1,09 | 1,80 | 1,15 |
| 25 | 0,82 | 0,87 | 0,87 | 0,96 |
| 26 | 0,74 | 0,57 | -- | -- |
| 27 | 0,54 | 0,42 | -- | -- |
| 28 | 0,51 | 0,36 | -- | -- |

(1) without reinforcement
(2) molybdenum netting from 0,2 mm. dia. wire
(3) molybdenum netting from 0,4 mm. dia. wire
(4) molybdenum netting from 0,8 mm. dia. wire

Table 3: Impact Strength of Reinforced Charpy Bars at Elevated Temperatures

| Specimen No. |  (x) | | Impact strength mkg./cm.2 at °C. | | |
|---|---|---|---|---|---|
| | 20 | 400 | 600 | 800 | 1000 |
| 22 | 1,49 | > 3 | > 3 | > 3 | > 3 |
| 23 | 1,57 | > 3 | > 3 | > 3 | > 3 |
| 24 | 0,98 | 1,8 | 1,6 | 1,3 | > 3 |
| 25 | 0,86 | 1,4 | 1,7 | 1,1 | 2,7 |
| 26 | 0,61 | 1,3 | 0,32 | 0,43 | 1,5 |
| 27 | 0,50 | 0,87 | 0,56 | 0,61 | 2,0 |
| 28 | 0,49 | 0,38 | 0,30 | 0,27 | 0,34 |

(x) 2 molybdenum wires 0,8 mm. ∅.

Table 4: Impact Strength of Reinforced Charpy Bars at Elevated Temperatures

| Specimen No. | 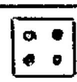 (x) Impact Strength mkg./cm.$^2$ at °C. | | | | |
|---|---|---|---|---|---|
| | 20 | 400 | 600 | 800 | 1000 |
| 22 | 1,62 | > 3 | > 3 | > 3 | > 3 |
| 23 | 1,65 | > 3 | > 3 | > 3 | > 3 |
| 24 | 1,05 | 2,2 | 3 | 2,6 | > 3 |
| 25 | 0,86 | 1,1 | 0,73 | 0,81 | > 3 |
| 26 | 0,59 | 1,4 | 1,6 | 1,3 | — |
| 27 | 0,59 | 0,68 | 0,55 | 0,43 | 2,5 |
| 28 | 0,42 | 0,35 | 0,37 | 0,48 | 0,3 |

(x) 4 molybdenum wires 0,8 mm. ∅

Table 5: Impact Strength of Reinforced Charpy Bars at Elevated Temperatures

| Specimen No. | [× ×] (x) | | Impact strength mkg./cm.$^2$ at °C. | | |
| --- | --- | --- | --- | --- | --- |
| | 20 | 400 | 600 | 800 | 1000 |
| 22 | 1,44 | > 3 | > 3 | > 3 | > 3 |
| 23 | 1,76 | > 3 | > 3 | > 3 | > 3 |
| 24 | 1,16 | 1,9 | 2,4 | 1,7 | > 3 |
| 25 | 0,86 | 1,2 | 0,77 | 0,59 | > 3 |
| 26 | 0,69 | 0,43 | 0,35 | 0,29 | 0,24 |
| 27 | 0,63 | 0,63 | 0,67 | 0,52 | 2 |
| 28 | 0,51 | 0,31 | 0,32 | 0,25 | 0,20 |

(x) 2 molybdenum braids from 0,4 mm. dia. wire

Table 6: Impact Strength of Reinforced Charpy Bars at Elevated Temperatures

| Specimen No. |  (x) Impact strength mkg/cm.$^2$ at °C. | | | | |
|---|---|---|---|---|---|
| | 20 | 400 | 600 | 800 | 1000 |
| 22 | 1,68 | > 3 | > 3 | > 3 | > 3 |
| 23 | 1,58 | > 3 | > 3 | > 3 | > 3 |
| 24 | 1,07 | 2,6 | 2,7 | > 3 | > 3 |
| 25 | 1,00 | 1,2 | 1,1 | 0,55 | > 3 |
| 26 | 0,79 | 0,38 | 0,32 | 0,27 | 1,8 |
| 27 | 0,59 | 0,68 | 0,53 | 0,37 | 0,38 |
| 28 | 0,43 | 0,35 | 0,31 | 0,32 | 0,29 |

(x) 4 molybdenum braids from 0,4 mm dia. wire

Table 7: Transverse Rupture Strength and Tensile Strength of Reinforced Tensile Bars at Elevated Temperatures

| Specimen No. | [• •] (x) Transverse rupture strength kg./mm.² at °C. | | | | Tensile strength kg./mm.² at °C. | | | |
|---|---|---|---|---|---|---|---|---|
| | 20 | 500 | 700 | 900 | 20 | 500 | 700 | 900 |
| 22 | 183 | 129 | 44 | 10 | 64.4 | 47.3 | - | - |
| 23 | 182 | 153 | 45 | 11 | 63.9 | 59.3 | 16.8 | 4.8 |
| 24 | 157 | 162 | 54 | 14 | 60.2 | 69.2 | 22.5 | - |
| 25 | 157 | 119 | 61 | 17 | 47.8 | 65.2 | 26.5 | - |
| 26 | 148 | 141 | 70 | n.b.(xx) | 55.6 | 61.1 | 29.5 | 7.8 |
| 27 | 120 | 97 | 81 | 21 | 32.1 | 28.8 | 32.4 | - |
| 28 | 94 | 93 | 70 | 22 | 27.6 | 23.2 | 22.1 | 7.3 |

(x) 2 molybdenum wires 0.8 mm Ø
(xx) not broken

Table 8: Transverse Rupture Strength and Tensile Strength of Reinforced Tensile Bars at Elevated Temperatures

| Specimen No. | [• • •] (x) Transverse rupture strength kg/mm.$^2$ at °C. | | | | Tensile strength kg./mm.$^2$ at °C. | | | |
|---|---|---|---|---|---|---|---|---|
| | 20 | 500 | 700 | 900 | 20 | 500 | 700 | 900 |
| 22 | 181 | 136 | 39 | 10 | 56,1 | -- | -- | -- |
| 23 | 171 | 139 | 48 | 11 | 51,3 | -- | -- | -- |
| 24 | 152 | 163 | 55 | 14 | 60,3 | 69,2 | 25,0 | -- |
| 25 | 162 | 161 | 65 | 17 | 61,2 | 63,6 | 26,4 | 7,3 |
| 26 | 138 | 157 | 65 | 19 | 55,7 | 59,8 | -- | -- |
| 27 | 128 | 116 | 80 | 24 | 34,2 | 38,6 | 30,3 | -- |
| 28 | 80 | 103 | 72 | 23 | 25,6 | 32,7 | 28,7 | -- |

(x) 3 molybdenum wires 0,8 mm ∅

Table 9: Transverse Rupture Strength and Tensile Strength of Reinforced Tensile Bars at Elevated Temperatures

| Specimen | (x) Transverse rupture strength kg./mm.$^2$ at °C | | | | Tensile Strength kg./mm.$^2$ at °C. | | | |
|---|---|---|---|---|---|---|---|---|
| | 20 | 500 | 700 | 900 | 20 | 500 | 700 | 900 |
| 22 | 184 | 147 | 40 | 8 | 62,2 | 61,7 | 14,6 | - |
| 23 | 174 | 150 | 47 | 10 | 60,1 | - | - | - |
| 24 | 153 | 162 | 57 | 13 | 55,9 | 65,3 | - | - |
| 25 | 147 | 129 | 65 | 16 | 48,9 | 63,2 | 27,0 | - |
| 26 | 150 | 154 | 71 | 17 | 31,5 | - | - | - |
| 27 | 124 | 89 | 72 | 21 | 25,3 | - | - | - |
| 28 | 107 | 80 | 75 | 25 | 15,3 | - | - | - |

(x) molybdenum netting from 0,2 mm dia. wire

Table 10: Transverse Rupture Strength and Tensile Strength of Reinforced Tensile Bars at Elevated Temperatures

| Specimen No. | (x) Transverse rupture strength kg./mm.$^2$ at °C | | | | Tensile Strength kg./mm.$^2$ at °C | | | |
|---|---|---|---|---|---|---|---|---|
| | 20 | 500 | 700 | 900 | 20 | 500 | 700 | 900 |
| 22 | 179 | 121 | 43 | 9 | 68.4 | 59.6 | 17.4 | 4.2 |
| 23 | 169 | 163 | 46 | 11 | 54.5 | 64.0 | 19.8 | 4.6 |
| 24 | 160 | 136 | 49 | 14 | 58.3 | 54.3 | 18.4 | 5.9 |
| 25 | 164 | 140 | 56 | 16 | 35.9 | 26.3 | 25.0 | 7.1 |
| 26 | 155 | 159 | 71 | 19 | 36.0 | - | - | - |
| 27 | 146 | 139 | 100 | 20 | 18.6 | - | - | - |
| 28 | - | - | - | - | - | - | - | - |

(x) molybdenum netting from 0.4 mm dia. wire

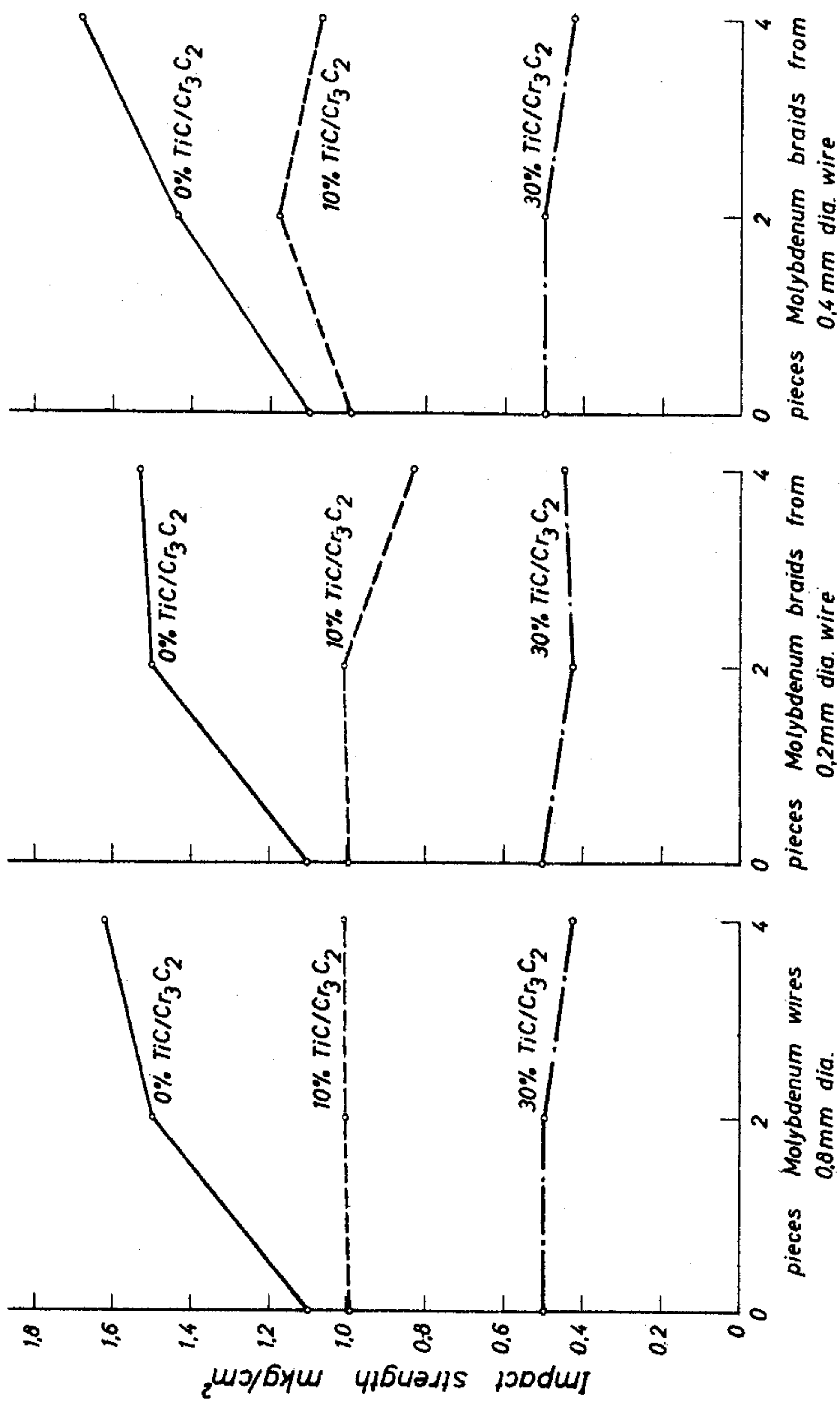


Fig. 8: Impact Strength of Reinforced Charpy Bars (molybdenum wires and braids) from Fe-Al-Mo-$TiC/Cr_3C_2$ Alloys

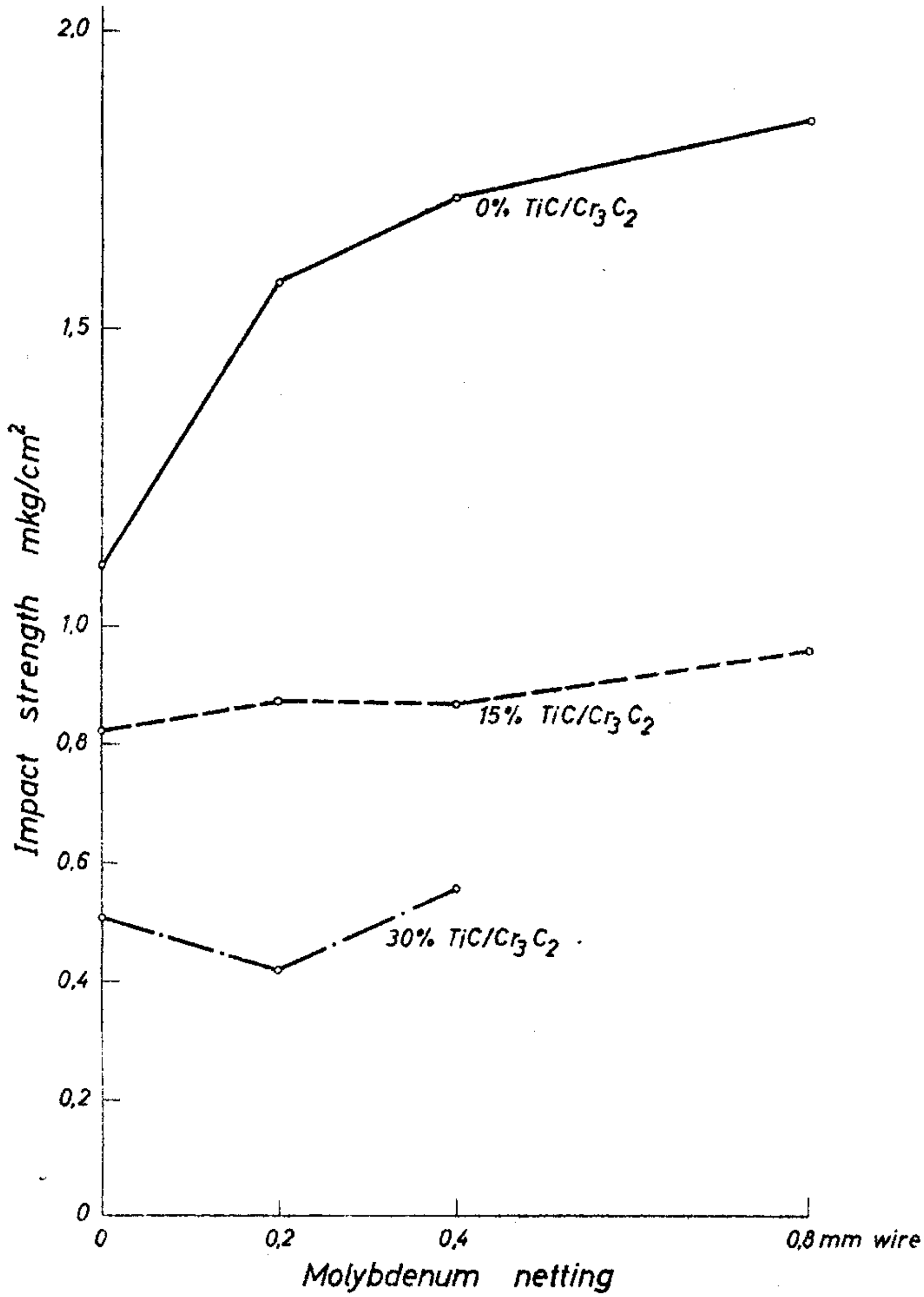


Fig. 9: Impact Strength of Reinforced Charpy Bars (molybdenum nettings) from Fe-Al-Mo-TiC/$Cr_3C_2$ Alloys

PHOTOMICROGRAPH DOUBLE MOUNTING SHEET

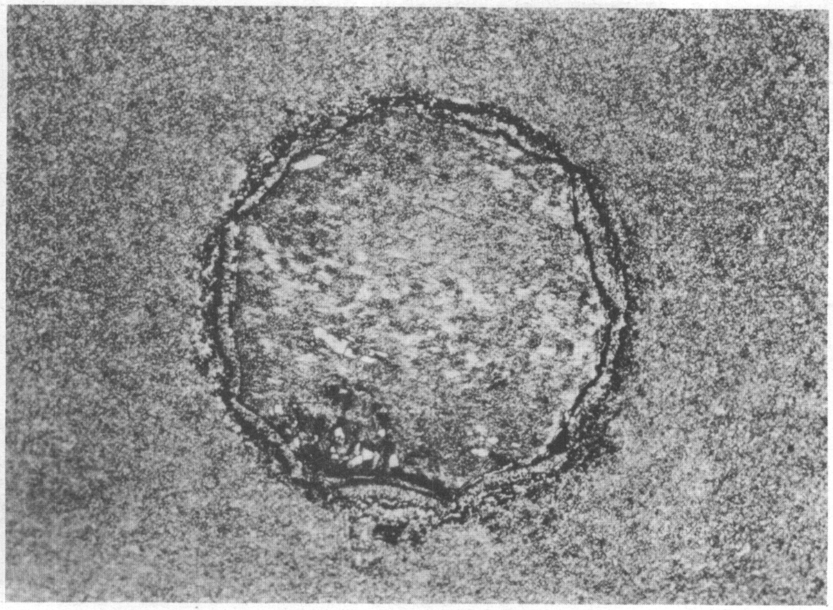

**Fig**....10........ **Plate**...............

**Magn**..70X...... **Diam Etch**...............

**Remarks:**

Section through reinforced charpy bar, 0.8 mm dia. molybdenum wire, composition 28 (30 % $TiC/Cr_3C_2$)

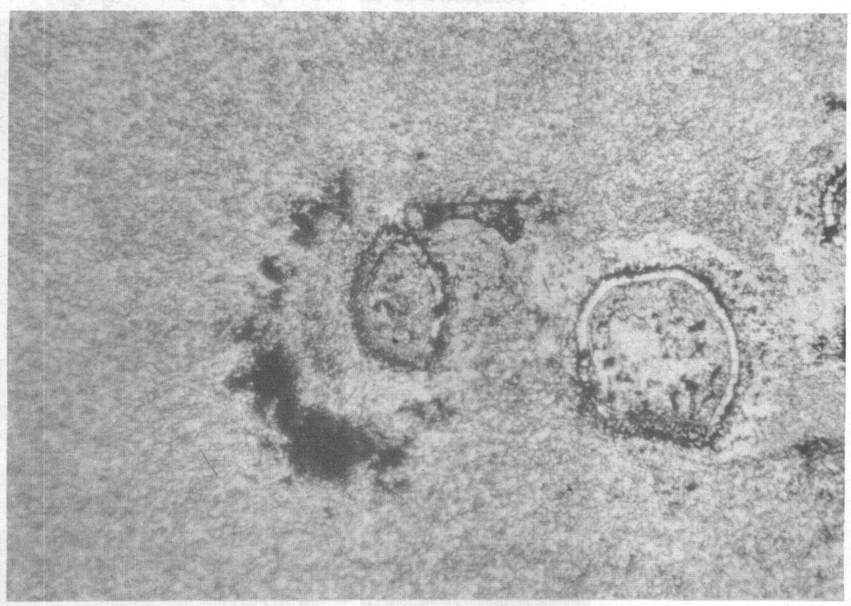

**Fig**....11......... **Plate**.............

**Magn**..100X..... **Diam Etch**.............

**Remarks:**

Section through reinforced charpy bar. Braid from 0.2 mm dia. molybdenum wire. Composition 28 (30% $TiC/Cr_3C_2$)

PHOTOMICROGRAPH DOUBLE MOUNTING SHEET

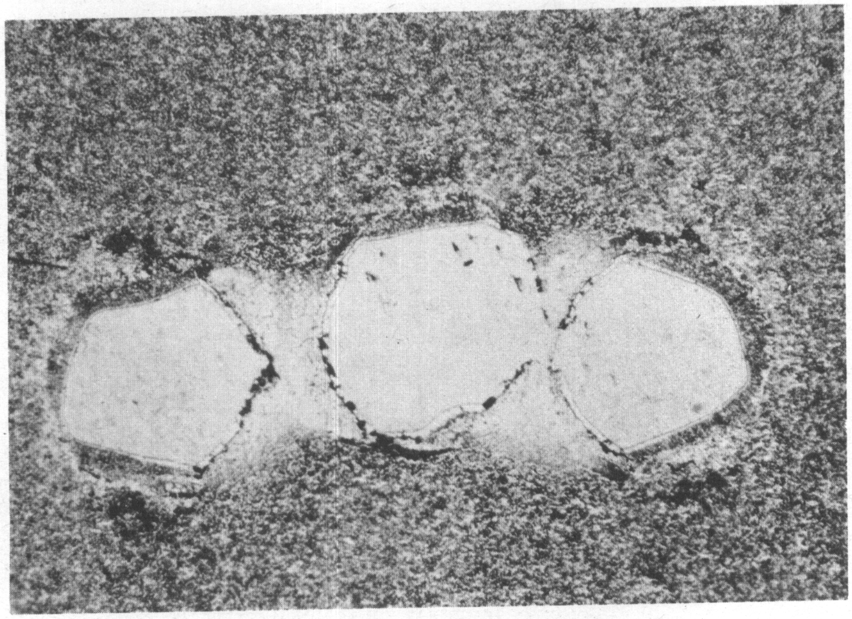

Fig. 12 Plate

Magn. 70X Diam Etch

Remarks:

Section through reinforced charpy bar. Braid from 0.4 mm. dia. molybdenum wire. Composition 28 (30% $TiC/Cr_3C_2$)

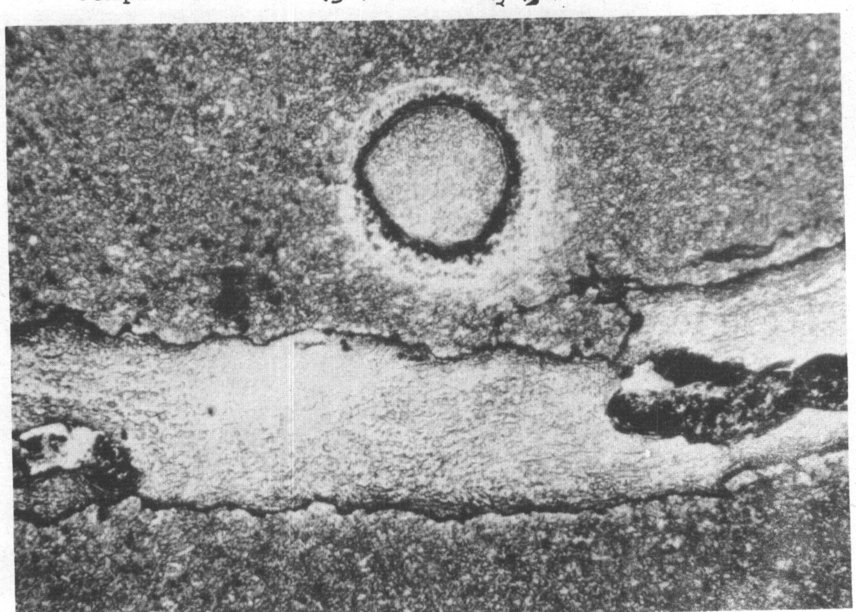

Fig. 13 Plate

Magn. 100X Diam Etch

Remarks:

Section through reinforced charpy bar. Netting from 0.2 mm. dia, molybdenum wire. Composition 28. (30% $TiC/Cr_3C_2$)

| | | |
|---|---|---|
| AF 61(514)-1144 Techn.Note | Metallwerk Plansee Ges.m.b.H. Reutte/Tirol | |

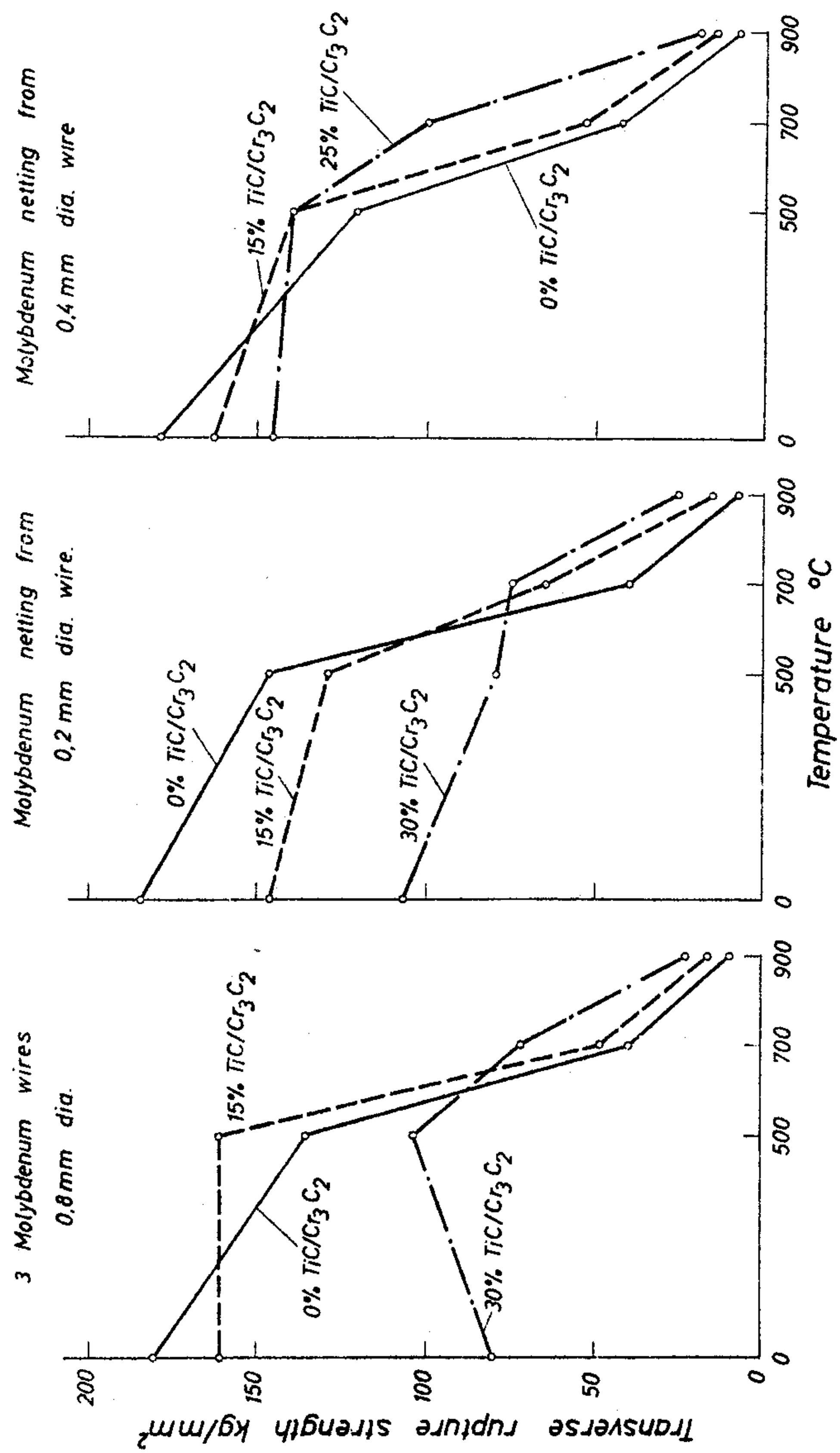


**Fig. 14:** Transverse Rupture Strength of Reinforced Tensile Bars from Fe-Al-Mo-TiC/$Cr_3C_2$ Alloys at Elevated Temperatures

2. Reinforcements with Megapyr (FeCrAl) and Nickel-Chromium

The influence of reinforcements on the impact strength by Megapyr wires 0,8 mm dia. and braids of Megapyr made of wire of a dia. of 0,2 and 0,4 mm as well as of nickel chromium wires of 0,8 and 1,5 mm dia. at both room and elevated temperatures is condensed in Tables 11 to 16 (Megapyr) and 17 to 20 (Ni-Cr). Fig. 15 and 16 indicate that, similar to molybdenum, a reinforcement by Megapyr and nickel-chromium wire and braids result in an increase in the impact strength with samples of low carbide content. The values are somewhat higher than those obtained by a reinforcement with molybdenum. This is especially the case with a reinforcement by nickel-chromium (to be compared with Fig. 8). The reinforcements have no influence if there is a higher carbide content. (This is illustrated in Figs. 17 to 24). The reason is an unsatisfactory binding of the reinforcing wires or embrittlement, probably by an absorption of carbon from the embedding alloy. On investigating the hot impact strength, the values are approximately comparable to the specimens reinforced by molybdenum. There is a certain rise with specimens of low carbide content whereas the effect is low with specimens of high carbide content. The reinforced specimens as well as the not reinforced, both of a carbide content up to approx. 15%, show impact strengths exceeding partly 3 mkg. if tested at a temperature of more than 600°C. It was impossible to destroy the specimens with the 3 mkg hammer without having notched them as they only showed a strong deformation.

c. Improvement of the Impact Strength by Surface Layers

We first carried out some preliminary research. We adopted two methods. First, after a suitable preparation of the surface, we coated it electrolytically with a nickel layer, annealed it subsequently at 1000°C. thus solidifying it. The layers produced this way were too thin to exercise an influence for an improved impact strength because the samples themselves had good impact strength. Second, we took a spray gun spraying nickel wire and also a Colmonoy powder gun (alloy Ni-Cr-B-Si) producing a layer of 0,1 to 0,5 mm thickness. Subsequently, both coatings were melted onto the material by means of a blowpipe thus producing a smooth, continuous layer of good adhesion. There was a relatively small effect with specimens of low carbide content as they originally had a good impace strength. On the contrary, the more brittle specimens of high carbide content showed a distinct improvement which was more effective compared to the reinforcement by embedded wire. Investigations in this field are, therefore, promising and we shall take them into consideration when continuing our research work.

d. Alloys on the Base of Fe-Al-Ti

The binding alloy contained roughly 81% Fe, 14% Al, 5% Ti and we added the solid solution $TiC/Cr_3C_2$ in lots of 0,5,10,15,20,25 and 30% each (see Table 21). The production of the specimens was the same as used for the Fe-Al-Mo alloys. During the sintering process, however, the specimens didn't shrink as much as the alloys of molybdenum content. The

**Table 11:** Impact Strength of Reinforced Charpy Bars (Megapyr) at Elevated Temperatures

| Specimen No. | [• •] *) Impact strength mkg./cm.$^2$ at $^{o}$C. 20 | 400 | 600 | 800 | 1000 |
|---|---|---|---|---|---|
| 22 | 1,8 | > 3 | > 3 | > 3 | > 3 |
| 23 | 0,86 | > 3 | > 3 | > 3 | > 3 |
| 24 | 0,81 | 1,4 | 1,3 | 1,7 | > 3 |
| 25 | 0,77 | 1,2 | 0,94 | 1,3 | > 3 |
| 26 | 0,48 | 0,77 | 0,61 | 0,94 | > 3 |
| 27 | 0,38 | 0,47 | 0,44 | 0,49 | 0,92 |
| 28 | 0,35 | 0,32 | 0,32 | 0,26 | 0,29 |

*) 2 Megapyr wires 0,8 mm.dia.

Table 12: Impact Strength of Reinforced Charpy Bars (Megapyr) at Elevated Temperatures

| Specimen No. | 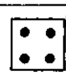 *) Impact strength mkg./cm.$^2$ at $^o$C. | | | | |
|---|---|---|---|---|---|
| | 20 | 400 | 600 | 800 | 1000 |
| 22 | 1,6 | > 3 | 2,6 | > 3 | > 3 |
| 23 | 1,3 | > 3 | 2,5 | 2,1 | > 3 |
| 24 | 0,81 | 1,7 | 1,7 | 1,5 | > 3 |
| 25 | 0,43 | 0,51 | 0,65 | 0,33 | > 3 |
| 26 | 0,69 | 0,42 | 0,62 | 0,39 | - |
| 27 | 0,39 | 0,43 | 0,45 | 0,42 | 1,1 |
| 28 | 0,29 | 0,32 | 0,32 | 0,23 | 0,26 |

*) 4 Megapyr wires 0,8 mm.dia.

**Table 13:** Impact Strength of Reinforced Charpy Bars (Megapyr) at Elevated Temperatures

| Specimen No. | ☒ *) Impact strength mkg./cm.$^2$ at $^\circ$C. | | | | |
|---|---|---|---|---|---|
| | 20 | 400 | 600 | 800 | 1000 |
| 22 | 1,6 | > 3 | > 3 | > 3 | > 3 |
| 23 | 1,6 | > 3 | > 3 | > 3 | > 3 |
| 24 | 0,92 | 1,3 | 2,1 | 1,3 | > 3 |
| 25 | 0,63 | 1,0 | 1,2 | 0,72 | > 3 |
| 26 | 0,62 | 0,75 | 0,41 | 0,58 | 1,2 |
| 27 | 0,42 | 0,49 | 0,43 | 0,44 | 0,94 |
| 28 | 0,31 | 0,39 | 0,33 | 0,35 | 0,34 |

*) 2 Megapyr braids from 0,2 dia. wire

| AF 61(514)-1144 2nd Techn.Rep. | Metallwerk Plansee Ges.m.b.H. Reutte/Tirol | |
|---|---|---|

**Table 14:** Impact Strength of Reinforced Charpy Bars (Megapyr) at Elevated Temperatures

| Specimen No. | *) Impact strength mkg./cm.$^2$ at $^{\circ}$C. | | | | |
|---|---|---|---|---|---|
| | 20 | 400 | 600 | 800 | 1000 |
| 22 | 1,4 | > 3 | > 3 | > 3 | > 3 |
| 23 | 1,5 | > 3 | > 3 | > 3 | > 3 |
| 24 | 1,1 | > 3 | 1,9 | 1,3 | > 3 |
| 25 | 0,67 | 1,1 | 1,2 | 0,43 | > 3 |
| 26 | 0,65 | 0,78 | 0,61 | 0,57 | 1,8 |
| 27 | 0,42 | 0,42 | 0,56 | 0,45 | 1,0 |
| 28 | 0,30 | 0,33 | 0,30 | 0,30 | 0,40 |

*) 4 Megapyr braids from 0,2 mm.dia. wire

**Table 15:** Impact Strength of Reinforced Charpy Bars (Megapyr) at Elevated Temperatures

| Specimen No. | xx *) Impact strength mkg./cm.² at °C. | | | | |
|---|---|---|---|---|---|
| | 20 | 400 | 600 | 800 | 1000 |
| 22 | 1,1 | > 3 | > 3 | > 3 | > 3 |
| 23 | 1,5 | 1,9 | > 3 | > 3 | > 3 |
| 24 | 0,82 | 1,4 | 1,9 | 1,6 | > 3 |
| 25 | 0,82 | 0,79 | 0,82 | 1,4 | > 3 |
| 26 | 0,39 | 0,69 | 0,40 | 0,48 | 0,40 |
| 27 | 0,45 | 0,31 | 0,37 | 0,37 | 0,39 |
| 28 | 0,29 | 0,40 | 0,25 | 0,19 | 0,18 |

*) 2 Megapyr braids from 0,4 mm.dia. wire

**Table 16:** Impact Strength of Reinforced Charpy Bars (Megapyr) at Elevated Temperatures

| Specimen No. | 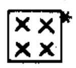*) Impact strength mkg./cm.$^2$ at °C. | | | | |
|---|---|---|---|---|---|
| | 20 | 400 | 600 | 800 | 1000 |
| 22 | 1,4 | > 3 | > 3 | > 3 | > 3 |
| 23 | 1,1 | > 3 | > 3 | > 3 | > 3 |
| 24 | 0,93 | 2,1 | 1,7 | 2,1 | > 3 |
| 25 | 0,70 | 0,96 | 1,3 | 0,47 | > 3 |
| 26 | 0,51 | 0,76 | 0,54 | 0,46 | 0,92 |
| 27 | 0,44 | 0,38 | 0,37 | 0,26 | 0,45 |
| 28 | 0,34 | 0,41 | 0,36 | 0,28 | 0,35 |

*) 4 Megapyr braids from 0,4 mm.dia.wire

**Table 17:** Impact Strength of Reinforced Charpy Bars (Nickel-Chromium) at Elevated Temperatures

| Specimen No. | [••] *) Impact strength mkg./cm.$^2$ at $^o$C. | | | | |
|---|---|---|---|---|---|
| | 20 | 400 | 600 | 800 | 1000 |
| 22 | 1,8 | > 3 | > 3 | > 3 | > 3 |
| 23 | 1,4 | > 3 | 1,7 | > 3 | > 3 |
| 24 | 1,0 | 1,3 | 1,3 | 1,2 | > 3 |
| 25 | 0,80 | 1,1 | 1,2 | 1,1 | > 3 |
| 26 | 0,70 | 0,64 | 0,67 | 0,86 | > 3 |
| 27 | 0,51 | 0,48 | 0,47 | 0,39 | 1,0 |
| 28 | 0,40 | 0,34 | 0,5 | 0,29 | 0,48 |

*) 2 nickel-chromium wires 0,8 mm.Ø

**Table 18:** Impact Strength of Reinforced Charpy Bars (Nickel-Chromium) at Elevated Temperatures

| Specimen No. | *) Impact strength mkg./cm.$^2$ at $^{o}$C. | | | | |
|---|---|---|---|---|---|
| | 20 | 400 | 600 | 800 | 1000 |
| 22 | 1,5 | > 3 | > 3 | > 3 | > 3 |
| 23 | 1,2 | > 3 | 2,1 | > 3 | > 3 |
| 24 | 0,83 | 1,8 | 1,3 | 1,3 | > 3 |
| 25 | 0,74 | 1,7 | 1,4 | 0,90 | > 3 |
| 26 | 0,65 | 0,93 | 0,78 | 0,73 | 2,3 |
| 27 | 0,48 | 0,51 | 0,47 | 0,44 | 0,45 |
| 28 | 0,35 | 0,35 | 0,35 | 0,21 | 0,20 |

*) 4 nickel-chromium wires 0,8 mm.ø

Table 19: Impact Strength of Reinforced Charpy Bars (Nickel-Chromium) at Elevated Temperatures

| Specimen No. | ⊡ *) Impact strength mkg./cm.$^2$ at $^o$C. | | | | |
|---|---|---|---|---|---|
| | 20 | 400 | 600 | 800 | 1000 |
| 22 | 1,6 | > 3 | > 3 | > 3 | > 3 |
| 23 | 1,4 | > 3 | 1,5 | > 3 | > 3 |
| 24 | 0,90 | 2,1 | 1,4 | 1,3 | > 3 |
| 25 | 0,92 | 1,4 | 1,4 | 1,5 | > 3 |
| 26 | 0,69 | 0,64 | 0,87 | 0,80 | 2,0 |
| 27 | 0,51 | 0,52 | 0,35 | 0,36 | 0,65 |
| 28 | 0,38 | 0,53 | 0,34 | 0,27 | 0,53 |

*) 1 nickel-chromium wire 1,5 mm.Ø

**Table 20:.** Impact Strength of Reinforced Charpy Bars (Nickel-Chromium) at Elevated Temperatures

| Specimen No. | [• •] *) Impact strength mkg./cm.$^2$ at $^o$C. | | | | |
|---|---|---|---|---|---|
| | 20 | 400 | 600 | 800 | 1000 |
| 22 | 1,9 | > 3 | > 3 | > 3 | > 3 |
| 23 | 1,0 | > 3 | 1,76 | > 3 | > 3 |
| 24 | 1,0 | 1,4 | 1,2 | 1,0 | > 3 |
| 25 | 0,93 | 1,3 | 1,3 | 1,2 | > 3 |
| 26 | 0,67 | 0,75 | 0,84 | 0,52 | 1,2 |
| 27* | 0,51 | 0,54 | 0,57 | 0,43 | 0,77 |
| 28 | 0,46 | 0,54 | 0,42 | 0,33 | 0,53 |

*) 2 nickel-chromium wires 1,5 mm.Ø

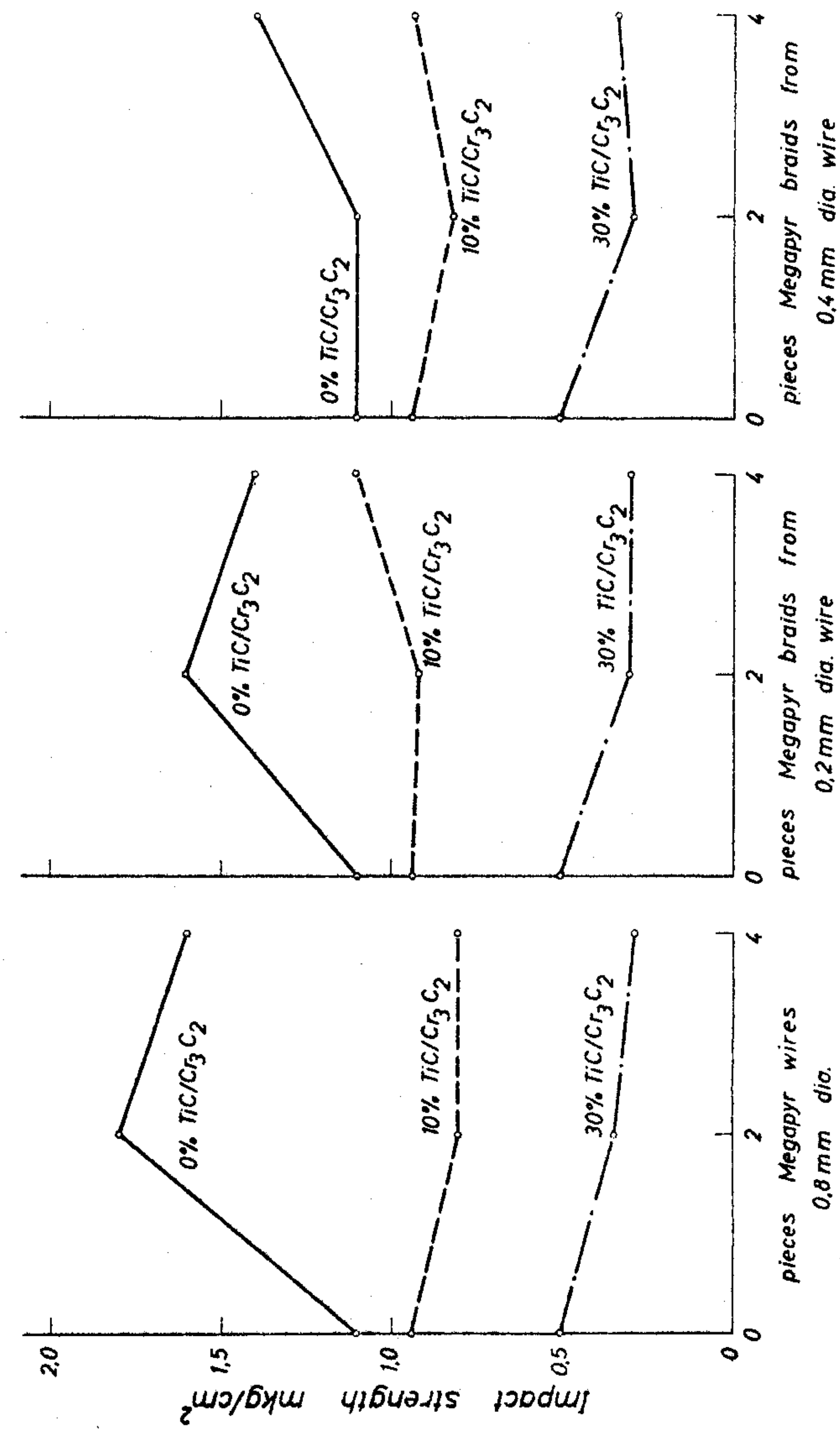


Fig. 15 Impact Strength of Reinforced Charpy Bars (Megapyr wires and braids) from Fe-Al-Mo-TiC/$Cr_3C_2$ Alloys

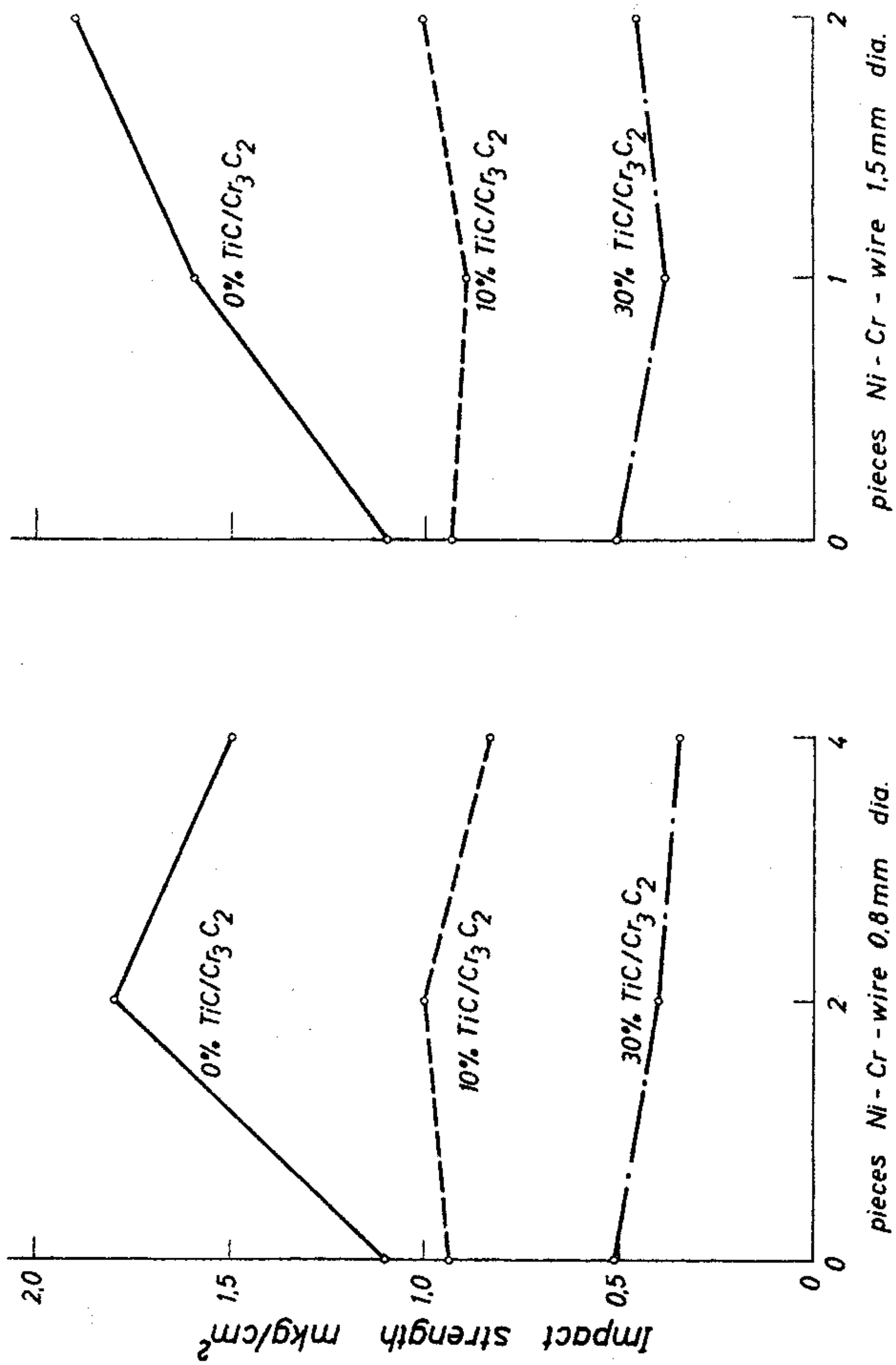


Fig. 16: Impact Strength of Reinforced Charpy Bars (nickel-chromium wires) from Fe-Al-Mo-TiC/$Cr_3C_2$ Alloys

PHOTOMICROGRAPH DOUBLE MOUNTING SHEET

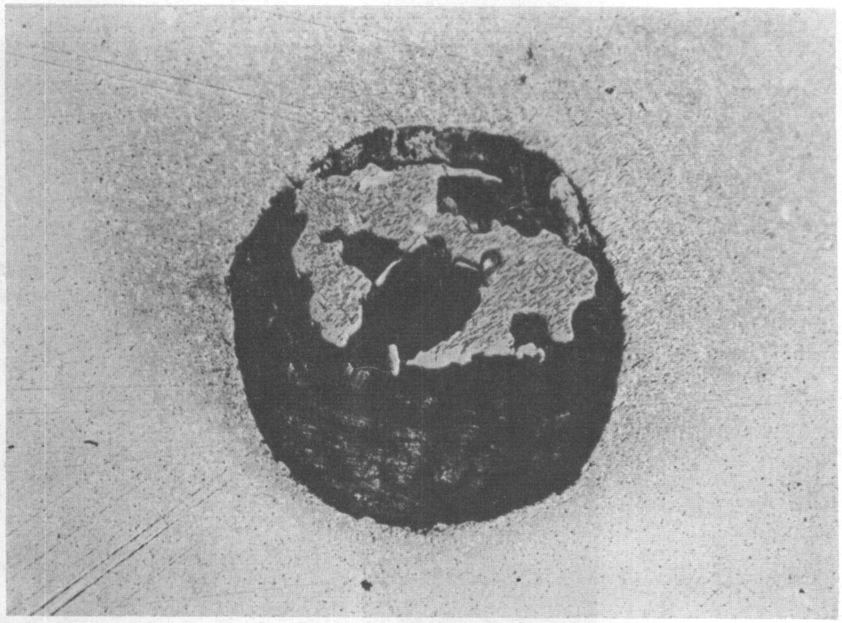

Fig. 17 Plate

Magn. 60X Diam Etch

Remarks:

Section through reinforced charpy bar. 0.8 mm dia. Megapyr wire. Composition 22 (without carbide)

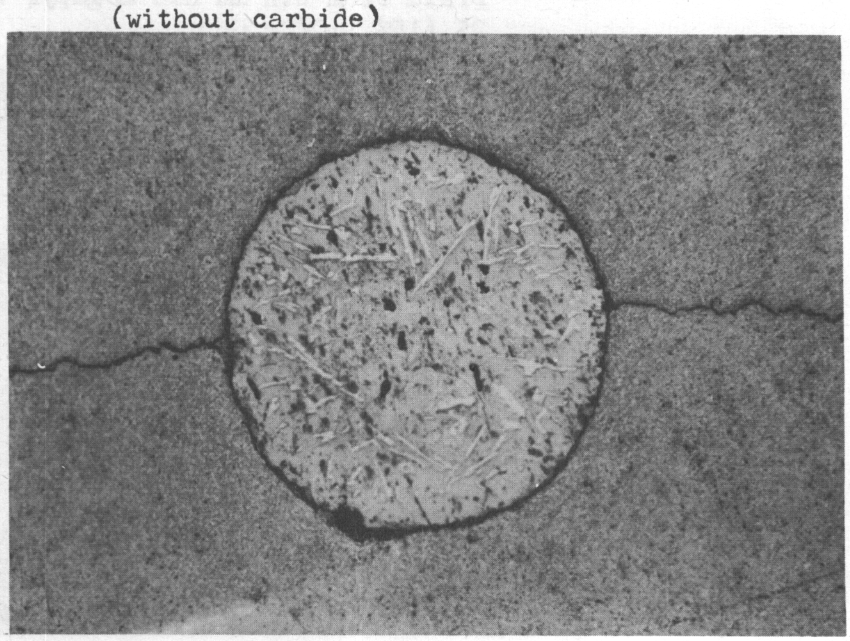

Fig. 18 Plate

Magn. 60X Diam Etch

Remarks:

Section through reinforced charpy bar. 0.8 mm. dia megapyr wire. Composition 28 (30% TiC/$Cr_3C_2$)

PHOTOMICROGRAPH DOUBLE MOUNTING SHEET

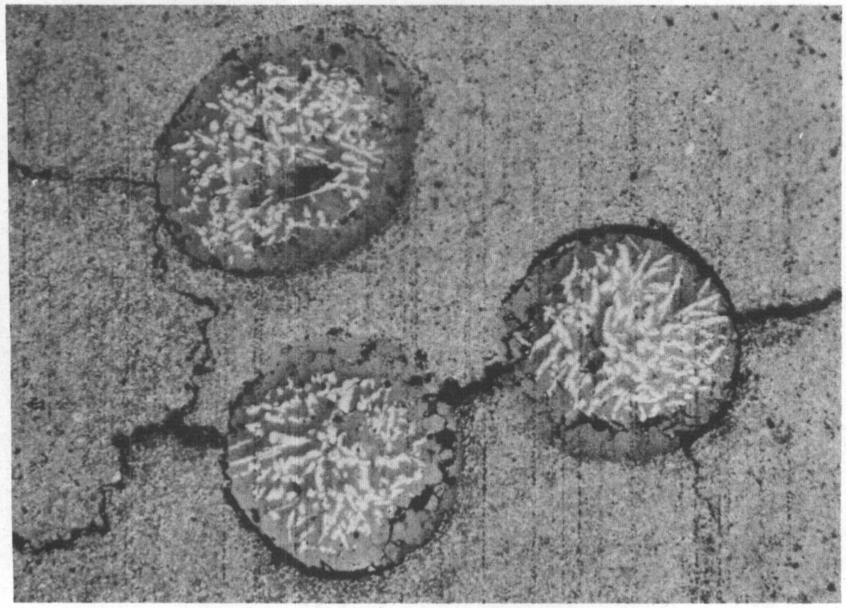

Fig.....19...... Plate..............

Magn..70X... Diam Etch...............

Remarks:

Section through reinforced charpy bar.
Braid from 0.4 mm dia megapyr wire. Composition
25 (15% TiC/Cr [illegible]

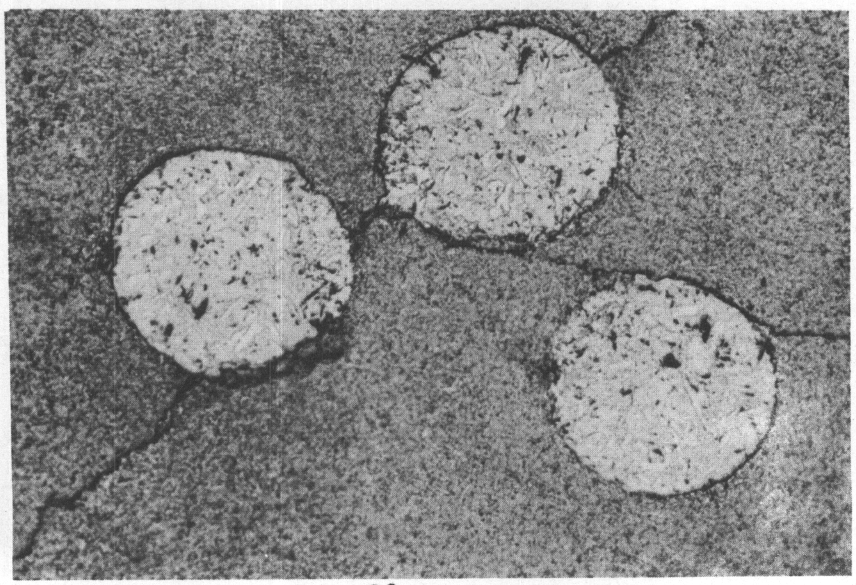

Fig.......20...... Plate............

Magn....70X.... Diam Etch..............

Remarks:

Section through reinforced charpy bar.
Braid from 0.4 mm dia. Megapyr wire.
Composition 28. (30% $TiC/Cr_3C_2$)

PHOTOMICROGRAPH DOUBLE MOUNTING SHEET

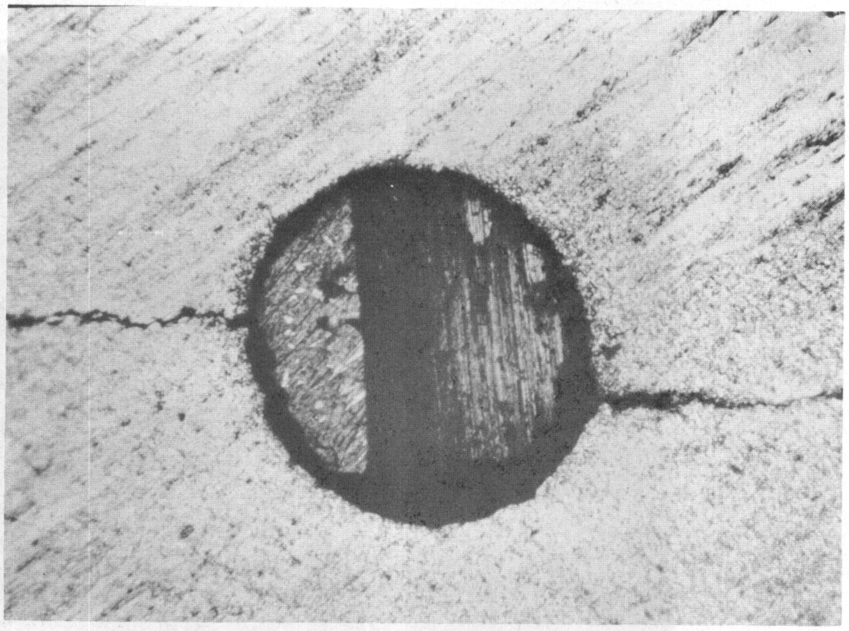

Fig. 21 Plate

Magn. 50X Diam Etch

Remarks:

Section through reinforced Charpy bar. 0.8 mm dia. nickel-chromium wire. Composition 25 (15% $TiC/Cr_3C_2$)

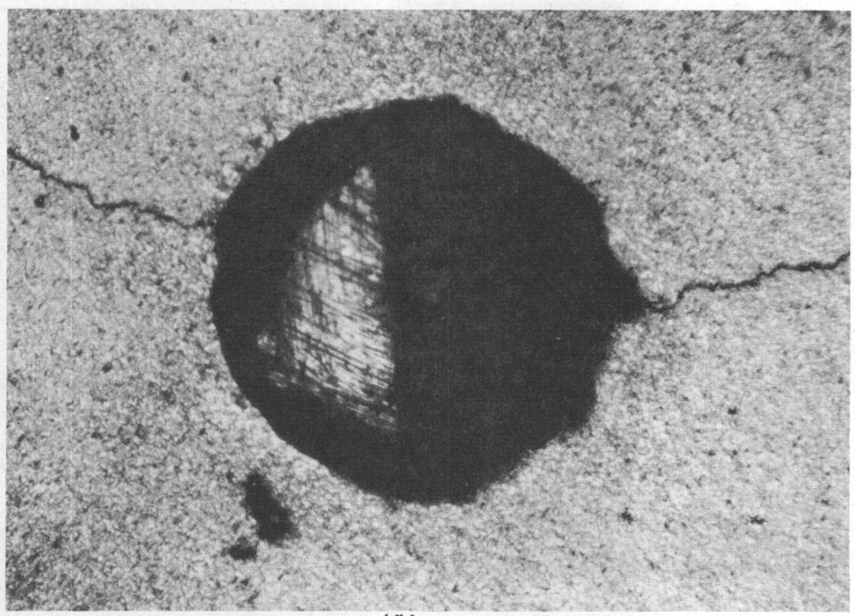

Fig. 22 Plate

Magn. 50X Diam Etch

Remarks:

Section through reinforced Charpy bar. 0.8 mm dia nickel chromium wire, Composition 28 (30% $TiC/Cr_3C_2$)

PHOTOMICROGRAPH DOUBLE MOUNTING SHEET

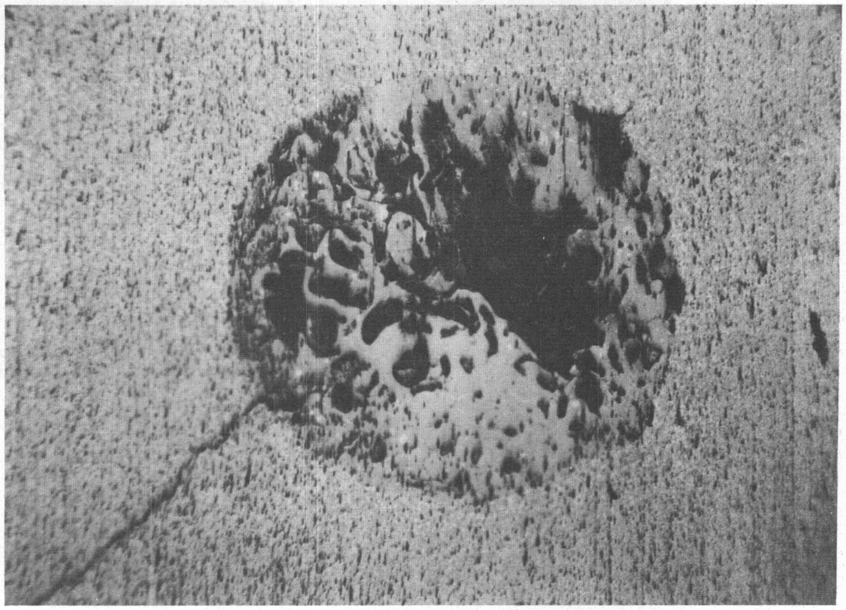

Fig.....23..... Plate..............

Magn...40X... Diam Etch...............

Remarks:

Section through reinforced Charpy bar. 1.5 mm dia. nickel-chromium wire. Composition 25 (15% $TiC/Cr_3C_2$)

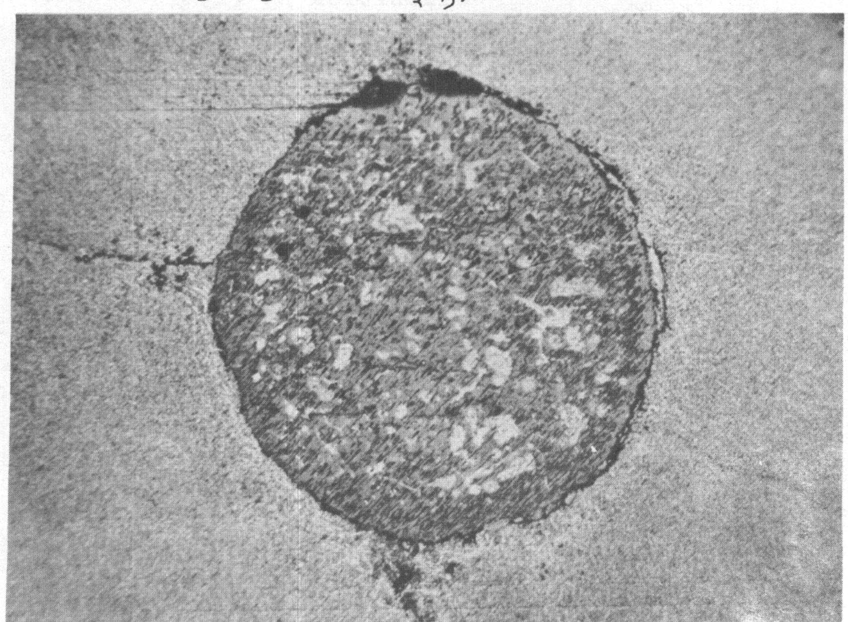

Fig.....24..... Plate............

Magn......40X. Diam Etch..............

Remarks:

Section through reinforced Charpy bar 1.5 mm dia. Nickel_Chromium wire. Composition 28 (30% $TiC/Cr_3C_2$)

Table 21: Composition Fe-Al-Ti-TiC/$Cr_3C_2$ 90/10-B

| Specimen No | Composition % | | | | | Approx. % | | | | |
|---|---|---|---|---|---|---|---|---|---|---|
| | Carbonyl-iron | Ferro-aluminum | Titanium-hydride | TiC/$Cr_3C_2$ | Ferro-boron | Fe | Al | Ti | TiC/$Cr_3C_2$ | B |
| 29 | 64 | 28 | 5 | -- | 3 | 80.7 | 14.1 | 4.7 | -- | 0.5 |
| 30 | 61 | 26.6 | 4.7 | 5 | 2.7 | 76.6 | 13.4 | 4.5 | 5 | 0.5 |
| 31 | 57.6 | 25.2 | 4.5 | 10 | 2.7 | 72.6 | 12.6 | 4.3 | 10 | 0.5 |
| 32 | 54.5 | 23.8 | 4.2 | 15 | 2.5 | 68.6 | 11.9 | 4.1 | 15 | 0.4 |
| 33 | 51.2 | 22.4 | 4.0 | 20 | 2.4 | 64.5 | 11.2 | 3.9 | 20 | 0.4 |
| 34 | 48.0 | 21.0 | 3.8 | 25 | 2.2 | 60.5 | 10.5 | 3.6 | 25 | 0.4 |
| 35 | 44.8 | 19.6 | 3.5 | 30 | 2.1 | 56.5 | 9.9 | 3.3 | 30 | 0.3 |

materials had, therefore, lower tensile strength (see Table 22). The non-scaling property of these alloys was very good (Tables 23 and 24). Fig. 25 shows some of the values of the hot hardness (Table 25), the hot tensile strength (Table 26) and the hot transverse rupture strength (Table 27). If we compare these values with alloys of molybdenum content, they show no remarkable facts and the values are only much lower when compared to the corresponding values at room temperature. The hot transverse rupture strength is clearly rising in the range of 500°C.

A reinforcement with molybdenum wires and braids exercises a negligible influence at both room and elevated temperatures. (Tables 28 to 32, and Fig. 26).

e. Alloys on the Base of NiAl and CoAl

It is well known from previous publications that the intermetallic compounds NiAl and CoAl show good properties at high temperatures. Both compounds were produced by exothermic reaction from their components and used after a fine milling.

The different series of alloys contained pure NiAl and CoAl respectively with additions of 0, 5, 10, 15, 20, 25, and 30% solid solution of $TiC/Cr_3C_2$ each (see Tables 33 and 34), further NiAl and CoAl with 5% Ni and 5% Co respectively and 0, 10, 20 and 30% solid solution $TiC/Cr_3C_2$ (Tables 35, 36) and finally mixtures of NiAl and CoAl in the ratio 3:1, 1:1, and 1:3 together with additions of solid solutions of carbides (Table 37). The manufacture of the samples was done as previously described both by hot pressing and by vacuum sintering at $10^{-2}$ Torr and 1250°C. or 1300°C. respectively during 2 hours. We also carried out tests with samples reinforced by molybdenum wire. The hardness and density (Tables 38, 39) of hot pressed samples show, according to Fig. 27, a considerable decrease in its density and an increase of the hardness if the addition of carbide is rising. A clear maximum is at a carbide content of 15%. The impact strength of conventionally sintered specimens at both room and higher temperature (Tables 40 and 41) was in general the same with all samples showing the values of only 0,05 to 0,1 mkg. per sq. cm. The materials are, therefore, very brittle. The surface of fracture was of a metallic lustre and of shell-like shape. As there was pratically no effect from the test temperature, we can presume a very high stress to rupture strength and a low creep.

An addition of nickel or cobalt, in order to get away from the stoichiometric composition of the intermetallic compound, brought certain small improvements of the properties (Tables 42, 43, 44 and 45). The same applies to mixtures of both compounds (Tables 46, 47).

The non-scaling property of the alloys is remarkable in nearly all cases and the scale layer has strong adherence even at high temperatures (Tables 48 to 56, Fig. 28 to 30) We obtained a very important increase in the impact strength if we reinforced the specimens with 4 molybdenum wires

**Table 22:** Physical Properties Fe-Al-Ti-TiC/$Cr_3C_2$ 90/10-B (wet milled 24 hours)

| Specimen No. | Density g./cm.$^3$ | | Shrinkage | Hardness $H_V$ | Tensile strength | Impact strength mkg./cm.$^2$ | |
|---|---|---|---|---|---|---|---|
| | Pressed | Sintered | % | kg./mm.$^2$ | kg./mm.$^2$ | *) | **) |
| 29 | 4,55 | 4,78 | 1,8 | 140 | 19,5 | 0,28 | 0,35 |
| 30 | 4,42 | 4,50 | 0,8 | 119 | 11,4 | 0,17 | 0,28 |
| 31 | 4,38 | 4,39 | 0,5 | 101 | 10,3 | 0,16 | 0,24 |
| 32 | 4,35 | 4,42 | 0,9 | 116 | 9,8 | 0,10 | 0,21 |
| 33 | 4,27 | 4,32 | 0,5 | 112 | 9,2 | 0,10 | 0,15 |
| 34 | 4,23 | 4,33 | 1,1 | 134 | 9,7 | 0,08 | 0,14 |
| 35 | 4,18 | 4,36 | 1,6 | 139 | 9,0 | 0,08 | 0,13 |

*) Flat test bars, approx. 5 x 10 mm. without notch
**) Charpy specimens, approx. 10 x 10 mm. without notch

**Table 23:** Scaling Properties Fe-Al-Ti-TiC/$Cr_3C_2$ 90/10-B at 800°C. (wet milled 24 hours)

| Specimen No. | Gain in weight (g./cm.$^2$) after hours: | | | | | |
|---|---|---|---|---|---|---|
| | 2 | 4 | 8 | 16 | 32 | 64 |
| 29 | 0,00540 | 0,00676 | 0,00835 | 0,01038 | 0,01417 | 0,02133 |
| 30 | 0,02559 | 0,02898 | 0,03230 | 0,03631 | 0,04367 | 0,05830 |
| 31 | 0,02920 | 0,03867 | 0,05039 | 0,05983 | 0,07282 | 0,08285 |
| 32 | 0,02433 | 0,02929 | 0,03389 | 0,03683 | 0,03877 | 0,04219 |
| 33 | 0,01821 | 0,01948 | 0,02019 | 0,02083 | 0,02247 | 0,02713 |
| 34 | 0,01222 | 0,01259 | 0,01298 | 0,01347 | 0,01489 | 0,01982 |
| 35 | 0,00657 | 0,00680 | 0,00711 | 0,00759 | 0,00870 | 0,01242 |

**Table 24: Scaling Properties Fe-Al-Ti-TiC/$Cr_3C_2$ 90/10-B at 900°C. (wet milled 24 hours)**

| Specimen No. | Gain in weight (g./cm.²) after hours: | | | | | |
|---|---|---|---|---|---|---|
| | 2 | 4 | 8 | 26 | 32 | 64 |
| 29 | 0,01503 | 0,01938 | 0,02239 | 0,02569 | 0,02840 | 0,03261 |
| 30 | 0,02693 | 0,04191 | 0,04852 | 0,05570 | 0,06245 | 0,07400 |
| 31 | 0,02042 | 0,03885 | 0,04472 | 0,04935 | 0,05238 | 0,05700 |
| 32 | 0,01412 | 0,01617 | 0,01794 | 0,02025 | 0,02309 | 0,02823 |
| 33 | 0,01191 | 0,01312 | 0,01559 | 0,08661 | 0,02226 | 0,02895 |
| 34 | 0,00721 | 0,00836 | 0,01068 | 0,01367 | 0,01818 | 0,02949 |
| 35 | 0,00579 | 0,00666 | 0,00801 | 0,01034 | 0,01354 | 0,02261 |

Table 25: Hot Hardness Fe-Al-Ti-TiC/$Cr_3C_2$ 90/10-B (wet milled 24 hours)

| Specimen No. | Hot hardness (kg./mm.$^2$) at $^oC$. 20 | 200 | 400 | 500 | 600 | 700 |
|---|---|---|---|---|---|---|
| 29 | 140 | 100 • | 93 | 55 | 59 | 35 |
| 30 | 119 | 102 | 93 | 75 | 51 | 25 |
| 31 | 101 | 104 | 87 | 70 | 48 | 18 |
| 32 | 116 | 113 | 91 | 70 | 61 | 35 |
| 33 | 112 | 106 | 85 | 83 | 51 | 23 |
| 34 | 134 | 112 | 105 | 95 | 68 | 39 |
| 35 | 139 | 144 | 149 | 136 | 81 | 50 |

**Table 26:.** Tensile Strength at Elevated Temperatures
Fe-Al-Ti-TiC/$Cr_3C_2$ 90/10-B (wet milled 24 hours)

| Specimen No. | Tensile strength (kg./mm.$^2$) at °C. | | | |
|---|---|---|---|---|
| | 20 | 500 | 700 | 900 |
| 29 | 19,5 | 16,1 | 13,2 | 4,3 |
| 30 | 11,4 | 10,6 | 9,5 | 4,4 |
| 31 | 10,3 | 6,1 | 8,5 | 2,8 |
| 32 | 9,8 | 7,7 | 7,7 | 2,7 |
| 33 | 9,2 | 8,2 | 6,0 | 3,0 |
| 34 | 9,7 | 4,1 | 6,3 | 2,5 |
| 35 | 9,0 | 4,3 | 8,7 | 2,6 |

Table 27: Transverse Rupture Strength at Elevated Temperatures Fe-Al-Ti-TiC/$Cr_3C_2$ 90/10-B (wet milled 24 hours)

| Specimen No. | Transverse rupture strength (kg./mm.$^2$) at $^o$C. | | | |
|---|---|---|---|---|
| | 20 | 500 | 700 | 900 |
| 29 | 48 | 60 | 41 | 11 |
| 30 | 41 | 46 | 27 | 8 |
| 31 | 31 | 41 | 22 | 8 |
| 32 | 34 | 39 | 23 | 8 |
| 33 | 20 | 29 | 23 | 8 |
| 34 | 18 | 24 | 22 | 10 |
| 35 | 26 | 29 | 22 | 11 |

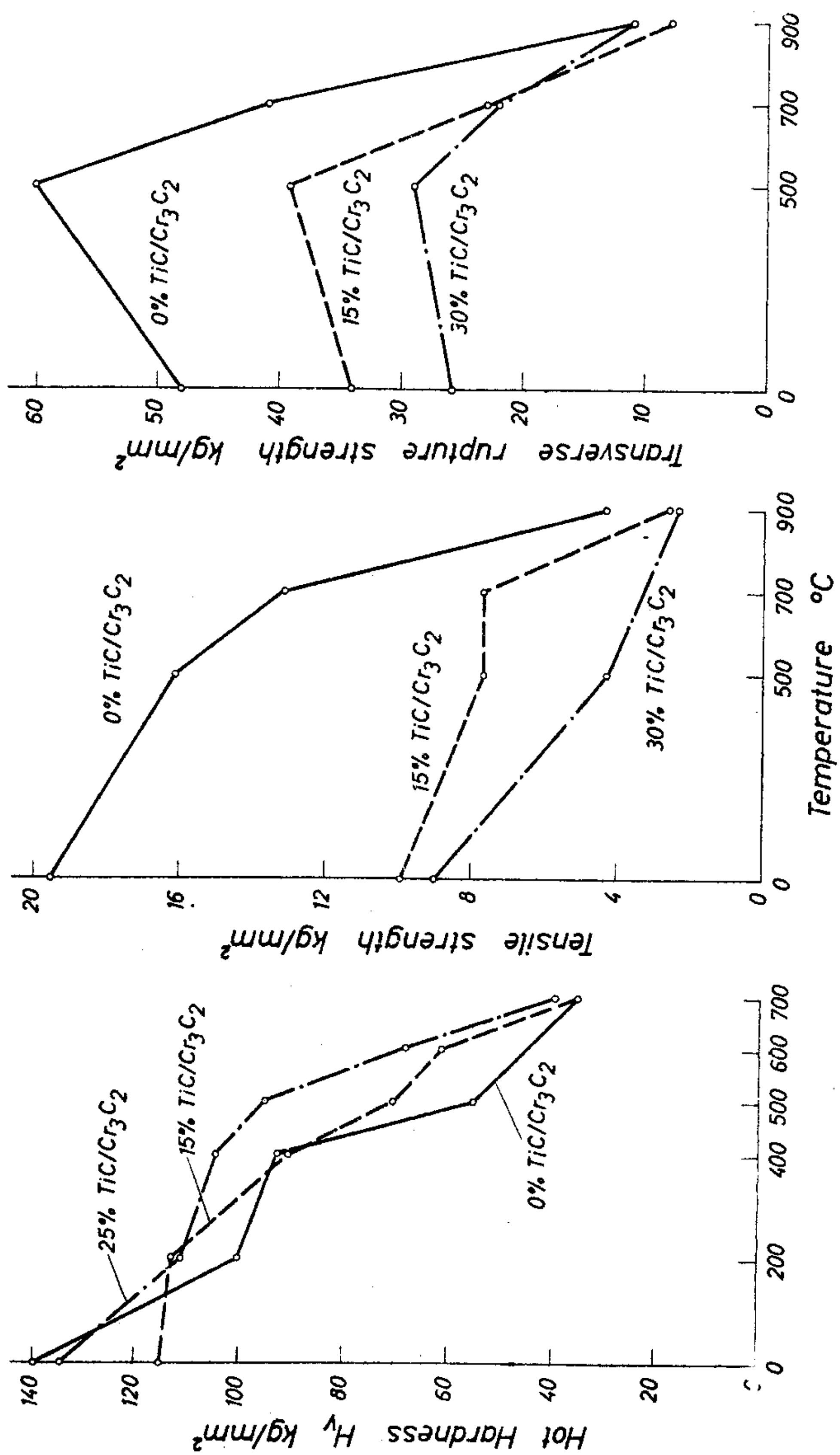


Fig. 25. Hardness, Tensile Strength and Transverse Rupture Strength at Elevated Temperatures of Fe-Al-Ti-$TiC/Cr_3C_2$ Alloys

**Table 28:** Impact Strength of Charpy Bars (Comp. 29 to 35) without Reinforcement at Elevated Temperatures

| Specimen No. | Impact strength mkg./cm.$^2$ at $^o$C. | | | | |
|---|---|---|---|---|---|
| | 20 | 400 | 600 | 800 | 1000 |
| 29 | 0,35 | 1,1 | n.d. | n.d. | n.d. |
| 30 | 0,28 | 0,29 | 0,40 | 0,32 | 0,42 |
| 31 | 0,24 | 0,26 | 0,30 | 0,14 | 0,19 |
| 32 | 0,21 | 0,24 | 0,18 | 0,18 | 0,16 |
| 33 | 0,15 | 0,16 | 0,14 | 0,10 | 0,11 |
| 34 | 0,14 | 0,15 | 0,12 | 0,10 | 0,07 |
| 35 | 0,13 | 0,16 | 0,12 | 0,10 | 0,09 |

**Table 29:** Impact Strength of Reinforced Charpy Bars (Comp. 29 to 35) at Elevated Temperatures

| Specimen No. | [• •]*) Impact strength mkg./cm.$^2$ at $^o$C. | | | | |
|---|---|---|---|---|---|
| | 20 | 400 | 600 | 800 | 1000 |
| 29 | 0,37 | n.d. | n.d. | n.d. | n.d. |
| 30 | 0,31 | 0,44 | 0,37 | 0,33 | 0,40 |
| 31 | 0,28 | 0,28 | 0,30 | 0,20 | 0,28 |
| 32 | 0,21 | 0,22 | 0,21 | 0,22 | 0,12 |
| 33 | 0,18 | 0,19 | 0,16 | 0,12 | 0,13 |
| 34 | 0,13 | 0,20 | 0,16 | 0,12 | 0,11 |
| 35 | 0,20 | 0,19 | 0,15 | 0,15 | 0,11 |

*) 2 molybdenum wires 0,8 mm.Ø

Table 30 Impact Strength of Reinforced Charpy Bars (Comp. 29 to 35) at Elevated Temperatures

| Specimen No. | ⁞ *) Impact strength mkg./cm.$^2$ at °C. | | | | |
|---|---|---|---|---|---|
| | 20 | 400 | 600 | 800 | 1000 |
| 29 | 0,37 | n.d. | n.d. | n.d. | n.d. |
| 30 | 0,29 | 0,37 | 0,45 | 0,37 | 0,32 |
| 31 | 0,25 | 0,40 | 0,33 | 0,21 | 0,31 |
| 32 | 0,29 | 0,34 | 0,24 | 0,20 | 0,21 |
| 33 | 0,32 | 0,26 | 0,23 | 0,15 | 0,16 |
| 34 | 0,27 | 0,28 | 0,22 | 0,16 | 0,15 |
| 35 | 0,16 | 0,25 | 0,21 | 0,19 | 0,16 |

*) 4 molybdenum wires 0,8 mm.Ø

**Table 31** Impact Strength of Reinforced Charpy Bars (Comp. 29 to 35) at Elevated Temperatures

| Specimen No. | xx *) Impact strength mkg./cm.$^2$ at °C. | | | | |
|---|---|---|---|---|---|
| | 20 | 400 | 600 | 800 | 1000 |
| 29 | 0,39 | n.d. | n.d. | n.d. | n.d. |
| 30 | 0,33 | 0,27 | 0,40 | 0,34 | 0,44 |
| 31 | 0,30 | 0,26 | 0,28 | 0,15 | 0,22 |
| 32 | 0,23 | 0,23 | 0,17 | 0,18 | 0,16 |
| 33 | 0,18 | 0,16 | 0,14 | 0,10 | 0,10 |
| 34 | 0,14 | 0,15 | 0,12 | 0,14 | 0,10 |
| 35 | 0,18 | 0,16 | 0,12 | 0,16 | 0,13 |

*) 2 molybdenum braids from 0,4 mm.dia. wire

**Table 32:** Impact Strength of Charpy Bars (Comp. 29 to 35) at Elevated Temperatures

| Specimen No. | ☒☒ *) Impact strength mkg./cm.$^2$ at °C. | | | | |
|---|---|---|---|---|---|
| | 20 | 400 | 600 | 800 | 1000 |
| 29 | 0,43 | n.d. | n.d. | n.d. | n.d. |
| 30 | 0,37 | 0,41 | 0,43 | 0,48 | 0,50 |
| 31 | 0,29 | 0,31 | 0,30 | 0,16 | 0,24 |
| 32 | 0,24 | 0,50 | 0,18 | 0,17 | 0,14 |
| 33 | 0,17 | 0,17 | 0,13 | 0,11 | 0,10 |
| 34 | 0,15 | 0,22 | 0,13 | 0,10 | 0,11 |
| 35 | 0,17 | 0,18 | 0,12 | 0,10 | 0,11 |

*) 4 molybdenum braids from 0,4 mm.dia. wire

Table 33 . Composition NiAl-TiC/$Cr_3C_2$ Alloys

| Specimen No. | Composition % | | | Approx. % | | | |
|---|---|---|---|---|---|---|---|
| | NiAl*) | TiC/$Cr_3C_2$ | Ferroboron | Ni | Al | TiC/$Cr_3C_2$ | B + Fe |
| 36 | 97 | - | 3 | 67,5 | 39,5 | - | 0,5 + 2,5 |
| 37 | 92,2 | 5 | 2,8 | 64 | 28,2 | 5 | 0,5 + 2,3 |
| 38 | 87,3 | 10 | 2,7 | 60,7 | 26,6 | 10 | 0,4 + 2,3 |
| 39 | 82,5 | 15 | 2,5 | 57,4 | 25,1 | 15 | 0,4 + 2,1 |
| 40 | 77,7 | 20 | 2,3 | 54 | 23,7 | 20 | 0,3 + 2,0 |
| 41 | 72,8 | 25 | 2,2 | 50,7 | 22,1 | 25 | 0,3 + 1,9 |
| 42 | 68 | 30 | 2 | 47,3 | 20,7 | 30 | 0,2 + 1,8 |

*) Composition 70% Ni
30% Al

Table 34 Composition CoAl-TiC/$Cr_3C_2$ Alloys

| Specimen No. | Composition % | | | Approx. % | | | |
|---|---|---|---|---|---|---|---|
| | CoAl *) | TiC/$Cr_3C_2$ | Ferroboron | Co | Al | TiC/$Cr_3C_2$ | B + Fe |
| 43 | 97 | - | 3 | 72,8 | 24,2 | - | 0,5 + 2,5 |
| 44 | 92,2 | 5 | 2,8 | 69,1 | 23,1 | 5 | 0,5 + 2,3 |
| 45 | 87,3 | 10 | 2,7 | 65,5 | 21,8 | 10 | 0,4 + 2,3 |
| 46 | 82,5 | 15 | 2,5 | 62 | 20,5 | 15 | 0,4 + 2,1 |
| 47 | 77,7 | 20 | 2,3 | 58,4 | 19,3 | 20 | 0,3 + 2,0 |
| 48 | 72,8 | 25 | 2,2 | 54,6 | 18,2 | 25 | 0,3 + 1,9 |
| 49 | 68 | 30 | 2 | 51 | 17 | 30 | 0,2 + 1,8 |

*) Composition: 75% Co
25% Al

**Table 35:** Composition NiAl-TiC/$Cr_3C_2$ Alloys

| Specimen No. | Composition % | | | | Approx. % | | | |
|---|---|---|---|---|---|---|---|---|
| | NiAl*) | TiC/$Cr_3C_2$ | Ferroboron | Carbonyl-nickel | Ni | Al | TiC/$Cr_3C_2$ | B + Fe |
| 50 | 97 | - | 3 | - | 66 | 31 | - | 0,5 + 2,5 |
| 51 | 87,2 | 10 | 2,8 | - | 59,4 | 27,8 | 10 | 0,5 + 2,3 |
| 52 | 77,6 | 20 | 2,4 | - | 52,7 | 24,9 | 20 | 0,4 + 2,0 |
| 53 | 68 | 30 | 2 | - | 46,3 | 21,7 | 30 | 0,2 + 1,8 |
| 54 | 92 | - | 3 | 5 | 67,5 | 29,5 | - | 0,5 + 2,5 |
| 55 | 83,2 | 10 | 2,8 | 4 | 60,6 | 26,6 | 10 | 0,5 + 2,3 |
| 56 | 74,6 | 20 | 2,4 | 3 | 53,7 | 23,9 | 20 | 0,4 + 2,0 |
| 57 | 66 | 30 | 2 | 2 | 46,9 | 21,1 | 30 | 0,2 + 1,8 |

*) Composition 68% Ni
32% Al

**Table 36:** Composition CoAl-TiC/$Cr_3C_2$ Alloys

| Specimen No. | Composition % | | | | Approx. % | | | |
|---|---|---|---|---|---|---|---|---|
| | CoAl*) | TiC/$Cr_3C_2$ | Ferroboron | Cobalt | Co | Al | TiC/$Cr_3C_2$ | B + Fe |
| 58 | 97 | - | 3 | - | 67,9 | 29,1 | - | 0,5 + 2,5 |
| 59 | 87,2 | 10 | 2,8 | - | 61 | 26,2 | 10 | 0,5 + 2,3 |
| 60 | 77,6 | 20 | 2,4 | - | 54,3 | 23,3 | 20 | 0,4 + 2,0 |
| 61 | 68 | 30 | 2 | - | 47,6 | 20,4 | 30 | 0,2 + 1,8 |
| 62 | 92 | - | 3 | 5 | 69,4 | 27,6 | - | 0,5 + 2,5 |
| 63 | 83,2 | 10 | 2,8 | 4 | 62,3 | 24,9 | 10 | 0,5 + 2,3 |
| 64 | 74,6 | 20 | 2,4 | 3 | 55,2 | 22,4 | 20 | 0,4 + 2,0 |
| 65 | 66 | 30 | 2 | 2 | 48,2 | 19,8 | 30 | 0,2 + 1,8 |

*) Composition 70% Co
30% Al

**Table 37:** Composition NiAl-CoAl-TiC/$Cr_3C_2$ Alloys

| Specimen No. | Composition % | | | | Approx. % | | | | |
|---|---|---|---|---|---|---|---|---|---|
| | NiAl*) | CoAl**) | TiC/$Cr_3C_2$ | Ferro-boron | Ni | Co | Al | TiC/$Cr_3C_2$ | B + Fe |
| 66 | 73 | 24 | - | 3 | 49,6 | 16,8 | 30,4 | - | 0,5 + 2,5 |
| 67 | 65 | 22 | 10 | 3 | 44,2 | 15,4 | 27,4 | 10 | 0,5 + 2,5 |
| 68 | 58,5 | 19 | 20 | 2,5 | 39,8 | 13,3 | 24,4 | 20 | 0,4 + 2,1 |
| 69 | 51 | 17 | 30 | 2 | 34;7 | 11,9 | 21,4 | 30 | 0,2 + 1,8 |
| 70 | 49 | 48 | - | 3 | 33,3 | 33,6 | 30,1 | - | 0,5 + 2,5 |
| 71 | 43 | 44 | 10 | 3 | 29,2 | 30,8 | 27,0 | 10 | 0,5 + 2,5 |
| 72 | 39,5 | 38 | 20 | 2,5 | 26,1 | 26,6 | 24,8 | 20 | 0,4 + 2,1 |
| 73 | 34 | 34 | 30 | 2 | 23,1 | 23,8 | 21,1 | 30 | 0,2 + 1,8 |
| 74 | 24 | 73 | - | 3 | 16,3 | 51,1 | 29,6 | - | 0,5 + 2,5 |
| 75 | 22 | 65 | 10 | 3 | 15 | 45,5 | 26,5 | 10 | 0,5 + 2,5 |
| 76 | 19 | 58,5 | 20 | 2,5 | 12,9 | 40,9 | 23,7 | 20 | 0,4 + 2,1 |
| 77 | 17 | 51 | 30 | 2 | 11,6 | 35,7 | 20,7 | 30 | 0,2 + 1,8 |

*) Composition 68% Ni
32% Al

**) Composition 70% Co
30% Al

**Table 38:.** Density and Hardness of Hot Pressed $NiAl-TiC/Cr_3C_2$ Alloys

| Specimen No. | Density g./cm.$^3$ | Hardness $H_V$ kg./mm.$^2$ |
|---|---|---|
| 36 | 5,95 | 150 - 160 |
| 37 | 5,70 | 310 - 350 |
| 38 | 5,65 | 310 - 350 |
| 39 | 5,50 | 380 - 410 |
| 40 | 5,10 | 700 - 780 |
| 41 | 4,88 | 320 - 350 |
| 42 | 4,82 | 420 - 520 |

**Table 39:** Density and Hardness of Hot Pressed CoAl-TiC/$Cr_3C_2$ Alloys

| Specimen No. | Density g./cm.$^3$ | Hardness $H_V$ kg./mm.$^2$ |
|---|---|---|
| 43 | 6,20 | 400 - 420 |
| 44 | 6,04 | 350 - 380 |
| 45 | 5,98 | 460 - 520 |
| 46 | 5,86 | 640 - 720 |
| 47 | 5,80 | 400 - 460 |
| 48 | 5,74 | 320 - 380 |
| 49 | 5,70 | 570 - 640 |

Table 40. Impact Strength of NiAl-TiC/$Cr_3C_2$ Alloys at Elevated Temperatures (Charpy Bars)

| Specimen No. | Impact strength mkg./cm.$^2$ at $^o$C. | | | | |
|---|---|---|---|---|---|
| | 20 | 400 | 600 | 800 | 1000 |
| 36 | - | 0,09 | 0,11 | 0,13 | 0,06 |
| 37 | 0,05 | 0,09 | 0,08 | 0,07 | 0,04 |
| 38 | 0,08 | 0,10 | 0,10 | 0,06 | 0,04 |
| 39 | 0,08 | 0,08 | 0,10 | 0,06 | 0,04 |
| 40 | 0,04 | 0,04 | 0,04 | 0,04 | 0,04 |
| 41 | 0,04 | 0,04 | 0,04 | 0,04 | 0,04 |
| 42 | 0,03 | 0,04 | 0,04 | 0,04 | 0,04 |

**Table 41:** Impact Strength of CoAl-TiC/$Cr_3C_2$ Alloys at Elevated Temperatures (Charpy Bars)

| Specimen No. | Impact strength mkg./cm.$^2$ at °C. | | | | |
|---|---|---|---|---|---|
| | 20 | 400 | 600 | 800 | 1000 |
| 43 | 0,07 | 0,06 | 0,05 | 0,05 | 0,06 |
| 44 | 0,06 | 0,05 | 0,05 | 0,06 | 0,03 |
| 45 | 0,05 | 0,05 | 0,05 | 0,17 | 0,16 |
| 46 | 0,05 | 0,05 | 0,05 | 0,20 | 0,07 |
| 47 | 0,05 | 0,05 | 0,06 | 0,35 | 0,14 |
| 48 | 0,05 | 0,06 | 0,06 | 0,08 | 0,05 |
| 49 | 0,06 | 0,05 | 0,06 | 0,12 | 0,15 |

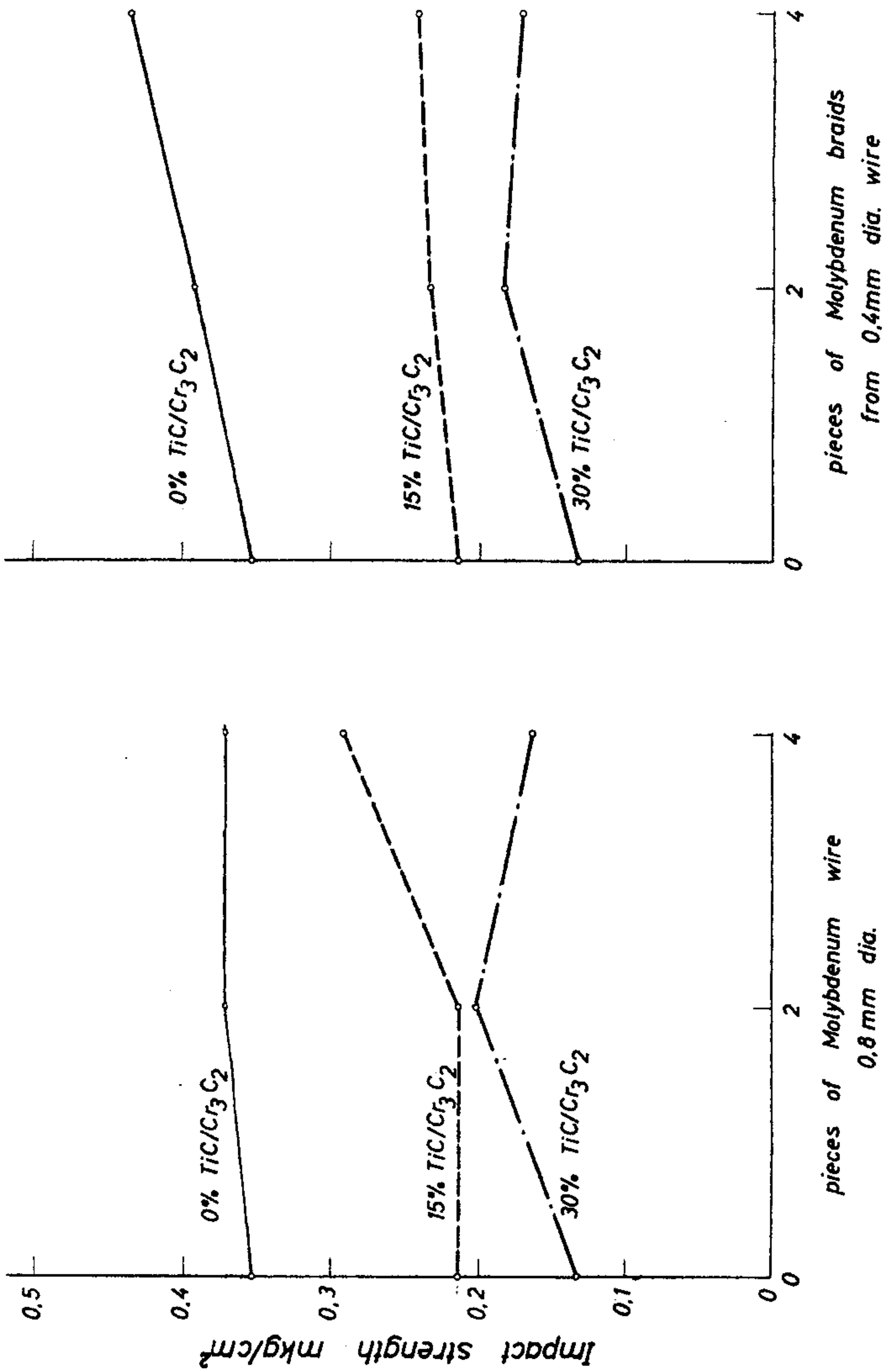


Fig. 26 : Impact Strength of Reinforced Charpy Bars of Fe-Al-Ti-TiC/$Cr_3C_2$ Alloys

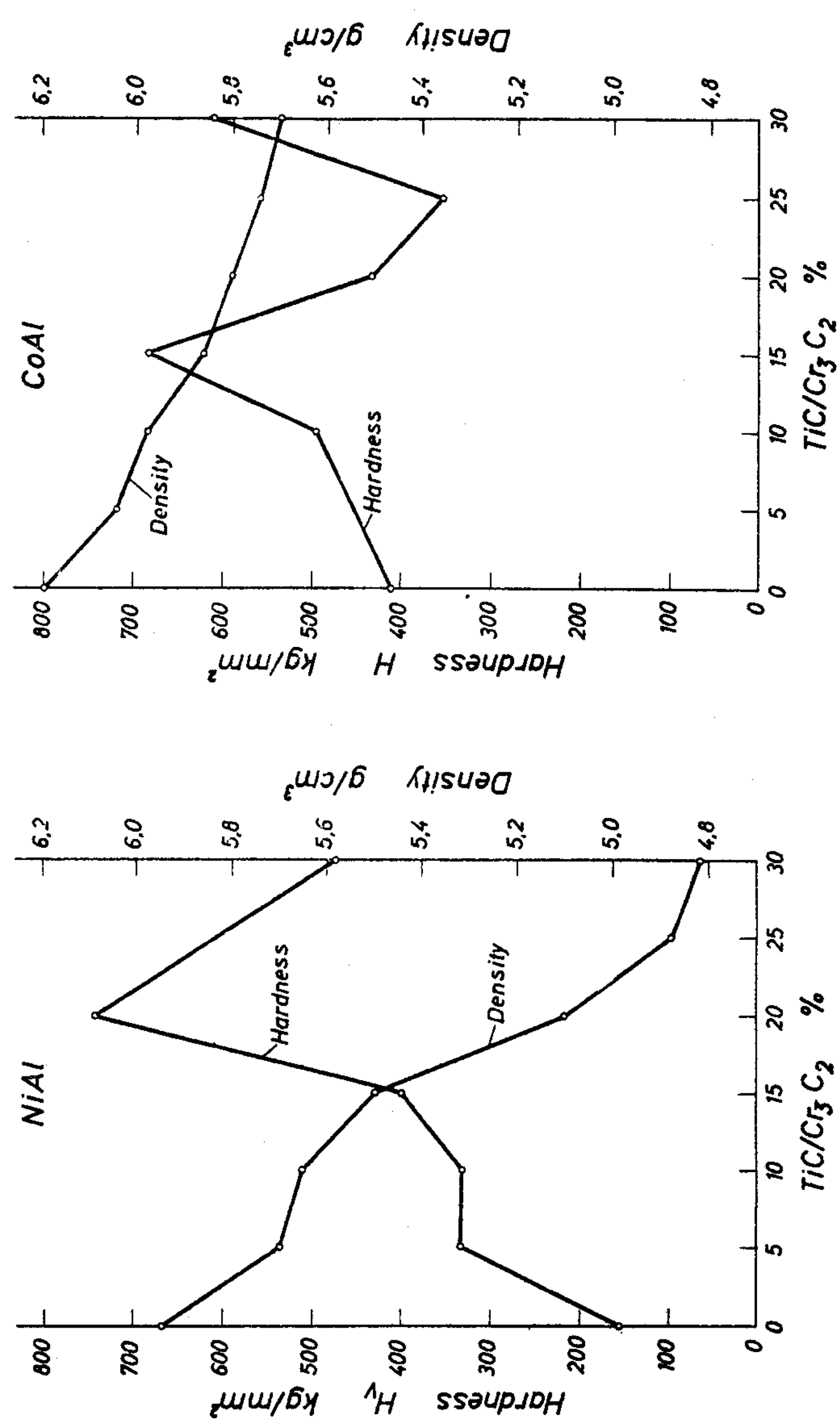


Fig. 27 : Density and Hardness of Hot Pressed NiAl-and CoAl-TiC/$Cr_3C_2$ Alloys, Respectively.

**Table 42:** Physical Properties of NiAl-TiC/$Cr_3C_2$ Alloys

| Specimen No. | Density g./cm.$^3$ | | Shrinkage % | Hardness $H_V$ kg./mm.$^2$ | Tensile strength kg./mm.$^2$ | Impact strength mkg./cm.$^2$ |
|---|---|---|---|---|---|---|
| | Pressed | Sintered | | | | |
| 50 | 4,04 | 5,80 | 11,5 | 340 - 360 | (5,9) | 0,06 |
| 51 | 3,94 | 4,02 | 1,5 | 90 - 95 | (3,2) | 0,05 |
| 52 | 3,89 | 4,03 | 2,0 | 110 - 120 | (4,3) | 0,05 |
| 53 | 3,87 | 4,03 | 2,2 | 110 - 120 | (2,9) | 0,04 |
| 54 | 4,13 | 5,96 | 11,9 | 360 - 380 | (11,1) | 0,07 |
| 55 | 4,07 | 4,10 | 1,3 | 110 - 130 | (4,7) | 0,07 |
| 56 | 3,95 | 4,11 | 2,1 | 100 - 120 | (5,0) | 0,06 |
| 57 | 3,91 | 4,12 | 2,7 | 120 - 140 | (3,6) | 0,05 |

**Table 43:** Physical Properties of CoAl-TiC/$Cr_3C_2$ Alloys

| Specimen No. | Density g./cm.$^3$ | | Shrinkage % | Hardness $H_V$ kg./mm.$^2$ | Tensile strength kg./mm.$^2$ | Impact strength mkg./cm.$^2$ |
|---|---|---|---|---|---|---|
| | Pressed | Sintered | | | | |
| 58 | 4,14 | 5,77 | 11,2 | 410 - 440 | (0,8) | 0,07 |
| 59 | 4,06 | 4,35 | 3,4 | 180 - 200 | (1,1) | 0,03 |
| 60 | 3,98 | 4,39 | 4,3 | 240 - 260 | (0,9) | 0,03 |
| 61 | 3,93 | 4,39 | 4,6 | 230 - 250 | (1,5) | 0,03 |
| 62 | 4,22 | 6,08 | 12,0 | 440 - 460 | (0,7) | 0,06 |
| 63 | 4,14 | 5,65 | 10,7 | 410 - 420 | (1,7) | 0,04 |
| 64 | 4,05 | 5,25 | 9,7 | 460 - 480 | (1,9) | 0,04 |
| 65 | 3,95 | 4,93 | 8,5 | 570 - 590 | (1,6) | 0,03 |

**Table 44:** Impact Strength NiAl-TiC/$Cr_3C_2$ Alloys at Elevated Temperatures (Charpy Bars)

| Specimen No. | Impact strength mkg./cm.$^2$ at $^oC$. | | | | |
|---|---|---|---|---|---|
| | 20 | 400 | 600 | 800 | 1000 |
| 50 | 0,11 | 0,15 | 0,15 | 0,17 | 0,15 |
| 51 | 0,06 | 0,08 | 0,10 | 0,10 | 0,09 |
| 52 | 0,06 | 0,07 | 0,09 | 0,08 | 0,05 |
| 53 | 0,04 | 0,06 | 0,07 | 0,06 | 0,05 |
| 54 | 0,10 | 0,14 | 0,13 | 0,14 | 0,13 |
| 55 | 0,08 | 0,13 | 0,12 | 0,09 | 0,05 |
| 56 | 0,07 | 0,10 | 0,09 | 0,08 | 0,05 |
| 57 | 0,04 | 0,07 | 0,07 | 0,06 | 0,05 |

Table 45: Impact Strength of CoAl-TiC/$Cr_3C_2$ Alloys at Elevated Temperatures (Charpy Bars)

| Specimen No. | Impact strength mkg./cm.$^2$ at $^oC$. | | | | |
|---|---|---|---|---|---|
| | 20 | 400 | 600 | 800 | 1000 |
| 58 | 0,10 | 0,09 | 0,10 | 0,09 | 0,08 |
| 59 | 0,05 | 0,04 | 0,08 | 0,08 | 0,08 |
| 60 | 0,04 | 0,03 | 0,16 | 0,08 | 0,07 |
| 61 | 0,04 | 0,04 | 0,07 | 0,04 | 0,06 |
| 62 | 0,06 | 0,07 | 0,11 | 0,09 | 0,13 |
| 63 | 0,10 | 0,10 | 0,11 | 0,11 | 0,08 |
| 64 | 0,06 | 0,09 | 0,10 | 0,10 | 0,08 |
| 65 | 0,06 | 0,09 | 0,10 | 0,10 | 0,09 |

**Table 46:** Physical Properties of NiAl-CoAl-TiC/$Cr_3C_2$ Alloys

| Specimen No. | Density g./cm.$^3$ | | Shrinkage % | Hardness $H_V$ kg./mm.$^2$ | Tensile strength kg./mm.$^2$ | Impact strength mkg./cm.$^2$ |
|---|---|---|---|---|---|---|
| | Pressed | Sintered | | | | |
| 66 | 4,03 | 5,66 | 10,9 | 320 - 340 | (3,5) | 0,09 |
| 67 | 3,96 | 4,10 | 1,1 | 90 - 95 | (1,2) | 0,04 |
| 68 | 3,97 | 4,12 | 1,1 | 90 - 95 | (1,3) | 0,04 |
| 69 | 3,95 | 4,10 | 1,4 | 100 - 110 | (1,5) | 0,04 |
| 70 | 4,18 | 5,35 | 7,3 | 330 - 340 | (1,0) | 0,03 |
| 71 | 4,14 | 5,66 | 9,2 | 410 - 420 | (0,5) | 0,03 |
| 72 | 4,01 | 4,17 | 1,4 | 120 - 140 | (0,3) | 0,02 |
| 73 | 3,80 | 4,14 | 2,7 | 160 - 170 | (0,7) | 0,02 |
| 74 | 4,06 | 4,15 | 1,1 | 110 - 120 | (0,5) | 0,03 |
| 75 | 4,04 | 4,29 | 2,2 | 140 - 150 | (0,6) | 0,03 |
| 76 | 3,97 | 4,34 | 3,2 | 170 - 180 | (0,6) | 0,02 |
| 77 | 3,88 | 4,31 | 3,7 | 200 - 220 | (1,4) | 0,02 |

**Table 47:** Impact Strength of NiAl-CoAl-TiC/$Cr_3C_2$ Alloys at Elevated Temperatures (Charpy Bars)

| Specimen No. | Impact strength mkg./cm.$^2$ at °C. | | | | |
|---|---|---|---|---|---|
| | 20 | 400 | 600 | 800 | 1000 |
| 66 | 0,09 | 0,08 | 0,09 | 0,09 | 0,12 |
| 67 | 0,04 | 0,06 | 0,07 | 0,07 | 0,06 |
| 68 | 0,04 | 0,04 | 0,05 | 0,04 | 0,04 |
| 69 | 0,04 | 0,04 | 0,04 | 0,04 | 0,04 |
| 70 | 0,05 | 0,07 | 0,06 | 0,08 | 0,06 |
| 71 | 0,05 | 0,05 | 0,07 | 0,04 | 0,10 |
| 72 | 0,04 | 0,04 | 0,04 | 0,05 | 0,04 |
| 73 | 0,04 | 0,04 | 0,06 | 0,04 | 0,06 |
| 74 | 0,04 | 0,04 | 0,04 | 0,06 | 0,05 |
| 75 | 0,04 | 0,04 | 0,04 | 0,08 | 0,07 |
| 76 | 0,04 | 0,04 | 0,04 | 0,07 | 0,05 |
| 77 | 0,04 | 0,04 | 0,07 | 0,04 | 0,05 |

**Table 48:** Scaling Properties NiAl-TiC/$Cr_3C_2$ 90/10 Alloys at 800°C.

| Specimen | Gain in weight (g/cm.²) after hours | | | | | |
|---|---|---|---|---|---|---|
| No. | 2 | 4 | 8 | 16 | 32 | 64 |
| 50 | 0.00004 | 0,00010 | 0,00016 | 0,00023 | 0,00027 | 0,00035 |
| 51 | 0,01370 | 0,02854 | 0,04453 | 0,05750 | 0,07011 | 0,08813 |
| 52 | 0,01959 | 0,04139 | 0,05834 | 0,07590 | 0,08931 | 0,10296 |
| 53 | 0,00268 | 0,00951 | 0,01384 | 0,01971 | 0,02151 | 0,02308 |
| 54 | 0,00006 | 0,00012 | 0,00015 | 0,00019 | 0,00025 | 0,00037 |
| 55 | 0,01227 | 0,02687 | 0,03184 | 0,05963 | 0,07701 | 0,09760 |
| 56 | 0,01231 | 0,02726 | 0,04090 | 0,05848 | 0,06954 | 0,07607 |
| 57 | 0,00465 | 0,00848 | 0,01323 | 0,01732 | 0,01896 | 0,02110 |

**Table 49:** Scaling Properties NiAl-TiC/$Cr_3C_2$ 90/10 Alloys at 900°C.

| Specimen No. | Gain in weight (g/cm.$^2$) after hours 2 | 4 | 8 | 16 | 32 | 64 |
|---|---|---|---|---|---|---|
| 50 | 0,00045 | 0,00047 | 0,00048 | 0,00049 | 0,00052 | 0,00055 |
| 51 | 0,06825 | 0,08575 | 0,09939 | 0,11760 | 0,12860 | 0,13280 |
| 52 | 0,02745 | 0,03016 | 0,03202 | 0,03377 | 0,03577 | 0,03863 |
| 53 | 0,01083 | 0,01202 | 0,01384 | 0,01700 | 0,02146 | 0,02577 |
| 54 | 0,00024 | 0,00027 | 0,00030 | 0,00031 | 0,00037 | 0,00040 |
| 55 | 0,06441 | 0,08056 | 0,09750 | 0,11490 | 0,13240 | 0,14070 |
| 56 | 0,02772 | 0,03029 | 0,03199 | 0,03328 | 0,03482 | 0,03750 |
| 57 | 0,01058 | 0,01150 | 0,01249 | 0,01383 | 0,01550 | 0,01786 |

**Table 50a** Scaling Properties NiAl-TiC/$Cr_3C_2$ 90/10 Alloys at 1000°C.

| Specimen No. | Gain in weight (g./cm.²) after hours | | | | | |
|---|---|---|---|---|---|---|
| | 2 | 4 | 8 | 16 | 32 | 64 |
| 50 | 0,00023 | 0,00030 | 0,00030 | 0,00033 | 0,00040 | 0,00044 |
| 51 | 0,07185 | 0,08371 | 0,09864 | 0,11610 | 0,14150 | 0,15830 |
| 52 | 0,01383 | 0,01525 | 0,01787 | 0,02123 | 0,02993 | 0,03750 |
| 53 | 0,01219 | 0,01559 | 0,02090 | 0,02878 | 0,04103 | 0,06593 |
| 54 | 0,00021 | 0,00025 | 0,00027 | 0,00027 | 0,00032 | 0,00038 |
| 55 | 0,07807 | 0,09055 | 0,10080 | 0,11180 | 0,12800 | 0,14100 |
| 56 | 0,14000 | 0,01528 | 0,01738 | 0,01992 | 0,02827 | 0,04093 |
| 57 | 0,00982 | 0,01198 | 0,01654 | 0,02238 | 0,02711 | 0,04981 |

**Table** 51 Scaling Properties CoAl-TiC/$Cr_3C_2$ 90/10 Alloys at 800°C.

| Specimen No. | Gain in weight (g./cm.²) after hours | | | | | |
|---|---|---|---|---|---|---|
| | 2 | 4 | 8 | 16 | 32 | 64 |
| 58 | 0,00004 | 0,00014 | 0,00020 | 0,00027 | 0,00036 | 0,00047 |
| 59 | 0,01204 | 0,02285 | 0,03592 | 0,05537 | 0,06554 | 0,08370 |
| 60 | 0,00831 | 0,01372 | 0,02063 | 0,02847 | 0,02941 | 0,03097 |
| 61 | 0,00488 | 0,00783 | 0,01147 | 0,01676 | 0,01784 | 0,01935 |
| 62 | 0,00008 | 0,00017 | 0,00022 | 0,00032 | 0,00055 | 0,00063 |
| 63 | 0,00009 | 0,00022 | 0,00035 | 0,00047 | 0,00056 | 0,00066 |
| 64 | 0,00034 | 0,00055 | 0,00099 | 0,00141 | 0,00161 | 0,00186 |
| 65 | 0,00030 | 0,00057 | 0,00097 | 0,00140 | 0,00187 | 0,00280 |

Table 52: Scaling Properties CoAl-TiC/$Cr_3C_2$ 90/10 Alloys at 900°C.

| Specimen No. | Gain in weight (g./cm.$^2$) after hours 2 | 4 | 8 | 16 | 32 | 64 |
|---|---|---|---|---|---|---|
| 58 | 0,00035 | 0,00044 | 0,00050 | 0,00051 | 0,00053 | 0,00065 |
| 59 | 0,04351 | 0,05326 | 0,06103 | 0,06540 | 0,06856 | 0,07099 |
| 60 | 0,01421 | 0,01551 | 0,01708 | 0,01909 | 0,02192 | 0,02469 |
| 61 | 0,00956 | 0,01059 | 0,01198 | 0,01368 | 0,01645 | 0,01888 |
| 62 | 0,00024 | 0,00029 | 0,00030 | 0,00033 | 0,00040 | 0,00046 |
| 63 | 0,00077 | 0,00082 | 0,00088 | 0,00094 | 0,00098 | 0,00118 |
| 64 | 0,00114 | 0,00141 | 0,00166 | 0,00174 | 0,00243 | 0,00284 |
| 65 | 0,00240 | 0,00296 | 0,00368 | 0,00435 | 0,00566 | 0,00682 |

**Table 53:** Scaling Properties of CoAl-TiC/$Cr_3C_2$ 90/10 Alloys at 1000°C.

| Specimen No. | Gain in weight (g./cm.$^2$) after hours | | | | | |
|---|---|---|---|---|---|---|
| | 2 | 4 | 8 | 16 | 32 | 64 |
| 58 | 0,00044 | 0,00057 | 0,00067 | 0,00073 | 0,00083 | 0,00095 |
| 59 | 0,02186 | 0,02933 | 0,04014 | 0,04937 | 0,07083 | 0,01334 |
| 60 | 0,01342 | 0,01604 | 0,02181 | 0,02920 | 0,05638 | 0,06352 |
| 61 | 0,00975 | 0,01147 | 0,01615 | 0,03032 | 0,06762 | 0,01055 |
| 62 | 0,00014 | 0,00024 | 0,00030 | 0,00050 | 0,00055 | 0,00039 |
| 63 | 0,00096 | 0,00130 | 0,00158 | 0,00195 | 0,00249 | 0,00288 |
| 64 | 0,00184 | 0,00233 | 0,00322 | 0,00417 | 0,00617 | 0,00809 |
| 65 | 0,00198 | 0,00276 | 0,00435 | 0,00613 | 0,00930 | 0,01207 |

Table 54: Scaling Properties of NiAl-CoAl-TiC/$Cr_3C_2$ Alloys at 800°C.

| Specimen No. | Gain in weight (g./cm.$^2$) after hours | | | | | |
|---|---|---|---|---|---|---|
| | 2 | 4 | 8 | 16 | 32 | 64 |
| 66 | 0,00009 | 0,00014 | 0,00024 | 0,00028 | 0,00038 | 0,00052 |
| 67 | 0,00388 | 0,00436 | 0,00916 | 0,01224 | 0,01469 | 0,01547 |
| 68 | 0,00450 | 0,00559 | 0,00752 | 0,00811 | 0,01123 | 0,01253 |
| 69 | 0,00292 | 0,00335 | 0,00361 | 0,00367 | 0,00404 | 0,00440 |
| 70 | 0,00164 | 0,00184 | 0,00261 | 0,00287 | 0,00508 | 0,00629 |
| 71 | 0,00170 | 0,00198 | 0,00211 | 0,00237 | 0,00244 | 0,00248 |
| 72 | 0,00461 | 0,00565 | 0,00741 | 0,00793 | 0,01101 | 0,01277 |
| 73 | 0,00217 | 0,00229 | 0,00245 | 0,00255 | 0,00284 | 0,00316 |
| 74 | 0,00438 | 0,00452 | 0,00552 | 0,00593 | 0,00976 | 0,01147 |
| 75 | 0,00428 | 0,00445 | 0,00528 | 0,00547 | 0,00617 | 0,00812 |
| 76 | 0,00428 | 0,00518 | 0,00651 | 0,00701 | 0,00810 | 0,00843 |
| 77 | 0,00168 | 0,00176 | 0,00187 | 0,00191 | 0,00212 | 0,00232 |

**Table 55:** Scaling Properties of NiAl-CoAl-TiC/$Cr_3C_2$ Alloys at 900°C.

| Specimen No, | Gain in weight (g./cm.$^2$) after hours | | | | | |
|---|---|---|---|---|---|---|
| | 2 | 4 | 8 | 16 | 32 | 64 |
| 66 | 0,00029 | 0,00035 | 0,00042 | 0,00047 | 0,00066 | 0,00072 |
| 67 | 0,00657 | 0,00865 | 0,01089 | 0,01182 | 0,01257 | 0,01401 |
| 68 | 0,02000 | 0,02405 | 0,02936 | 0,03619 | 0,04614 | 0,06300 |
| 69 | 0,01338 | 0,01682 | 0,02096 | 0,02675 | 0,03202 | 0,04618 |
| 70 | 0,00330 | 0,00459 | 0,00615 | 0,00694 | 0,00816 | 0,01125 |
| 71 | 0,00700 | 0,00810 | 0,00842 | 0,00986 | 0,00101 | 0,01134 |
| 72 | 0,01711 | 0,01889 | 0,02127 | 0,02396 | 0,02631 | 0,03075 |
| 73 | 0,01144 | 0,01321 | 0,01543 | 0,01841 | 0,01917 | 0,02810 |
| 74 | 0,00710 | 0,00955 | 0,01187 | 0,01244 | 0,01313 | 0,01492 |
| 75 | 0,00661 | 0,00880 | 0,01100 | 0,01191 | 0,01285 | 0,01483 |
| 76 | 0,01154 | 0,01258 | 0,01377 | 0,01614 | 0,01694 | 0,02080 |
| 77 | 0,00857 | 0,00940 | 0,01065 | 0,01206 | 0,01233 | 0,01505 |

**Table** 56. Scaling Properties of NiAl-CoAl-TiC/$Cr_3C_2$ Alloys at 1000°C.

| Specimen No. | Gain in weight (g./cm.$^2$) after hours | | | | | |
|---|---|---|---|---|---|---|
| | 2 | 4 | 8 | 16 | 32 | 64 |
| 66 | 0,00051 | 0,00054 | 0,00058 | 0,00060 | 0,00064 | 0,00073 |
| 67 | 0,06060 | 0,11230 | 0,12700 | 0,13630 | 0,14194 | 0,15100 |
| 68 | 0,02390 | 0,02860 | 0,03890 | 0,05240 | 0,07510 | 0,10704 |
| 69 | 0,01724 | 0,02160 | 0,02972 | 0,03542 | 0,05206 | 0,07576 |
| 70 | 0,00382 | 0,00492 | 0,00662 | 0,00726 | 0,00876 | 0,09236 |
| 71 | 0,00817 | 0,00912 | 0,01631 | 0,01722 | 0,02644 | 0,03410 |
| 72 | 0,01852 | 0,02136 | 0,02632 | 0,03344 | 0,05132 | 0,07751 |
| 73 | 0,01232 | 0,01486 | 0,01928 | 0,02253 | 0,02286 | 0,04952 |
| 74 | 0,00925 | 0,01068 | 0,01242 | 0,01398 | 0,01627 | 0,02389 |
| 75 | 0,00842 | 0,09267 | 0,01196 | 0,01302 | 0,01426 | 0,01772 |
| 76 | 0,01342 | 0,01444 | 0,01622 | 0,01857 | 0,02387 | 0,03002 |
| 77 | 0,01043 | 0,01189 | 0,01448 | 0,01749 | 0,02174 | 0,02685 |

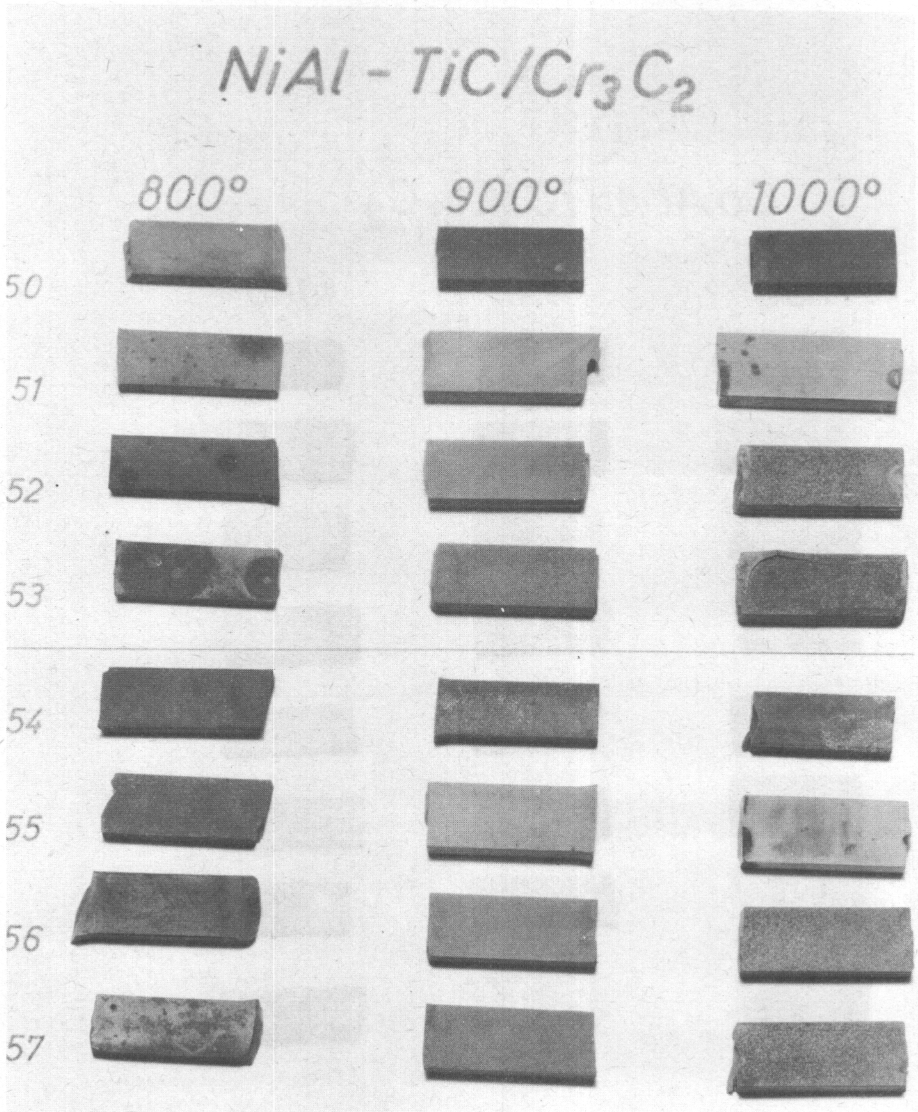


**Fig. 28:** Appearance of the Scale Test Specimens of $NiAl-TiC/Cr_3C_2$ Alloys
800°C. 64 hrs.
900°C. 64 hrs.
1000°C. 61 hrs.

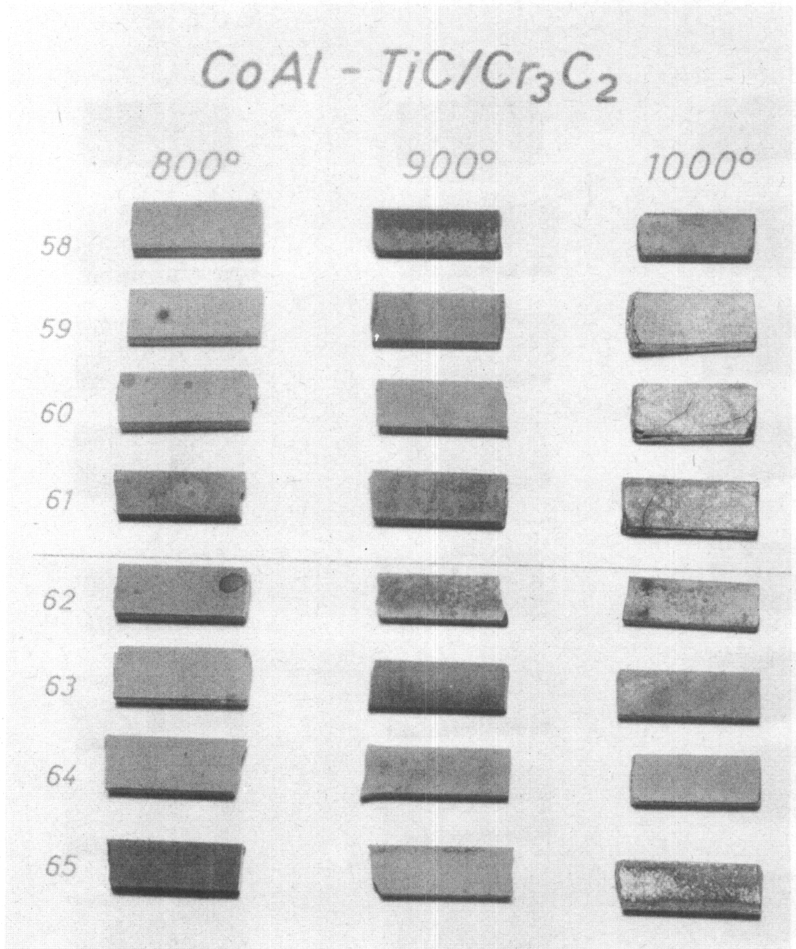


Fig. 29: Appearance of the Scale Test Specimens of $CoAl-TiC/Cr_3C_2$ Alloys
800°C. 64 hrs.
900°C. 64 hrs.
1000°C. 61 hrs.

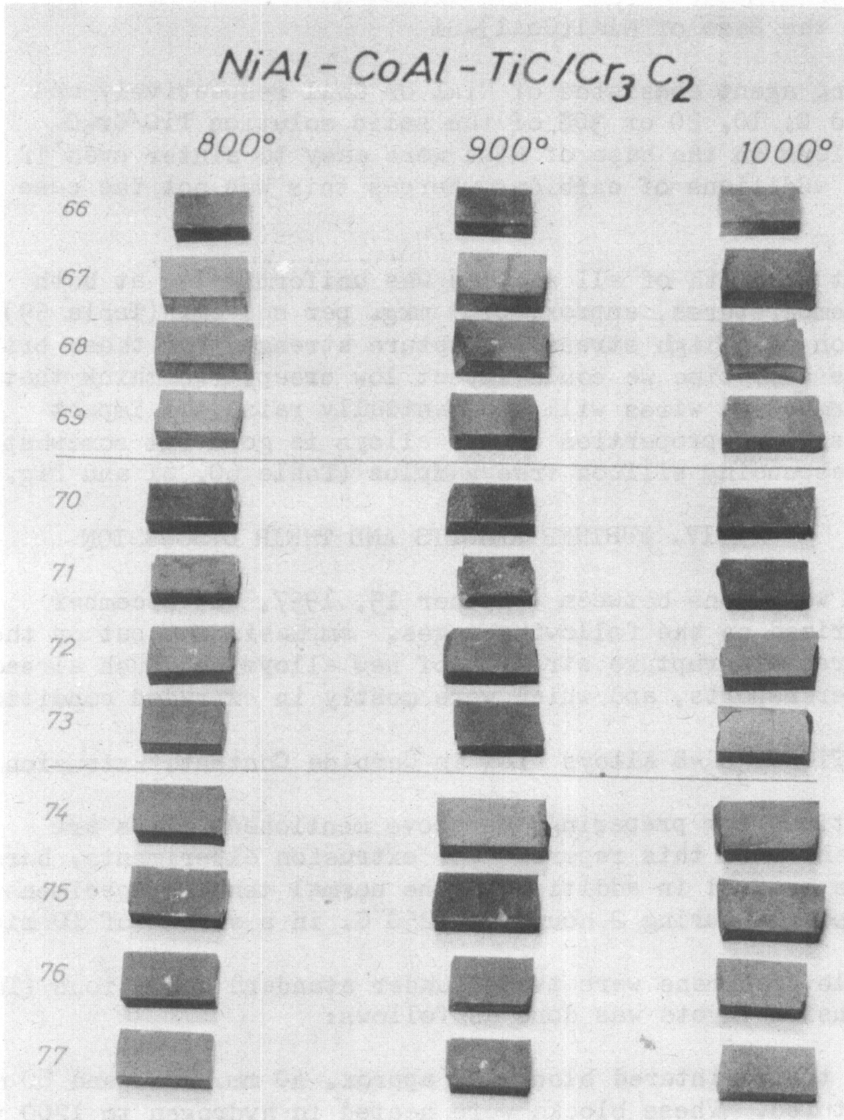


**Fig. 30:** Appearance of the Scale Test Specimens of $NiAl-CoAl-TiC/Cr_3C_2$ Alloys
800°C. 64 hrs.
900°C. 64 hrs.
1000°C. 64 hrs.

0,8 mm dia. and the hot impact strength evidences this fact especially with samples of carbide content (Table 59 and Fig. 31). The bond, however, between molybdenum wire and embedding alloy was not too good (Fig. 32 to 35), but the samples, which were first brittle, showed better impact strength especially at elevated temperatures.

f. Alloys on the Base of NiAl(CoAl)-Si

The binding agent consisted of NiAl or CoAl respectively and 5% silicon; we added 0, 10, 20 or 30% of the solid solution $TiC/Cr_3C_2$ (Table 58). The alloys on the base of NiAl were easy to sinter even if they contained high additions of carbides whereas this was not the case with CoAl alloys.

The impact strength of all samples was uniformly low at both room and elevated temperatures, approx. 0,05 mkg. per sq. cm. (Table 59). This is an indication of a high stress to rupture strength for these brittle materials and at the same time we could expect low creep. We think that a reinforcement by embedded wires will substantially raise the impact strength. The non-scaling properties of the alloys is good but somewhat worse than the corresponding silicon free samples (Table 60, 61 and Fig. 36)

IV. FURTHER RESULTS AND THEIR DISCUSSION

The results of work done between December 15, 1957, and December 31, 1958, are summarized on the following pages. Emphasis was put on the investigation of stress-to-rupture strength of new alloys and such already dealt with in earlier reports, and which were mostly in extruded condition.

a. Fe-Al-Mo-$TiC/Cr_3C_2$-B Alloys Low in Carbide Content, Extrusion Technique

The conditions for preparing the above mentioned alloys are described on pp. 5 and 6 of this report. For extrusion experiments, bars 40 X 40 X 80 mm were pressed in addition to the normal tensile specimens. Sintering was carried out during 2 hours at 1250°C. in a vacuum of 10 microns.

The tensile specimens were tested under standard conditions (Table 62). The working of extrusion ingots was done as follows:

For these tests sintered blocks of approx. 40 mm. dia. and 80 mm. height were manufactured. These blocks were heated in hydrogen to 1200 to 1300°C. in a muffle furnace with molybdenum heating elements. They subsequently were quickly put into the extrusion press and were extruded to round bars of approx. 9 mm. dia. and a length of approx. 1 meter. As the deformation pressure as well as the temperatures, especially with the material with high content of $TiC-Cr_3C_2$ and $Al_2O_3$, went up to very high figures, we used special dies made of refractory and scale resistant cemonted carbide grades. Though a part of the extruded rods showed cracks or fissures as well as saw teeth, especially if their temperature was not of an appropriate value and if the relatively porous specimens were kept too long in the hydrogen

**Table 57:.** Impact Strength of Reinforced Charpy Bars (Comp. 54-57 and 62-65) at Elevated Temperatures

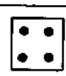

| Specimen No. | *) Impact strength mkg./cm.$^2$ at $^o$C. | | | | |
|---|---|---|---|---|---|
| | 20 | 400 | 600 | 800 | 1000 |
| 54 | 0,13 | 0,25 | 0,26 | 0,24 | 0,21 |
| 55 | 0,08 | 0,48 | 1,4 | 1,4 | 0,89 |
| 56 | 0,07 | 0,97 | 1,2 | 1,0 | 0,92 |
| 57 | 0,05 | 1,0 | 1,7 | 0,98 | 1,3 |
| 62 | 0,04 | 0,08 | 0,47 | 0,07 | 0,08 |
| 63 | 0,05 | 0,38 | 0,22 | 0,17 | 0,92 |
| 64 | 0,05 | 0,98 | 0,97 | 0,30 | 0,26 |
| 65 | 0,06 | 0,56 | 1,78 | 0,99 | 0,18 |

*) 4 molybdenum wires, 0,8 mm ø

| AF 61(514)-1144<br>Techn.Note | Metallwerk Plansee Ges.m.b.H.<br>Reutte/Tirol | |
|---|---|---|

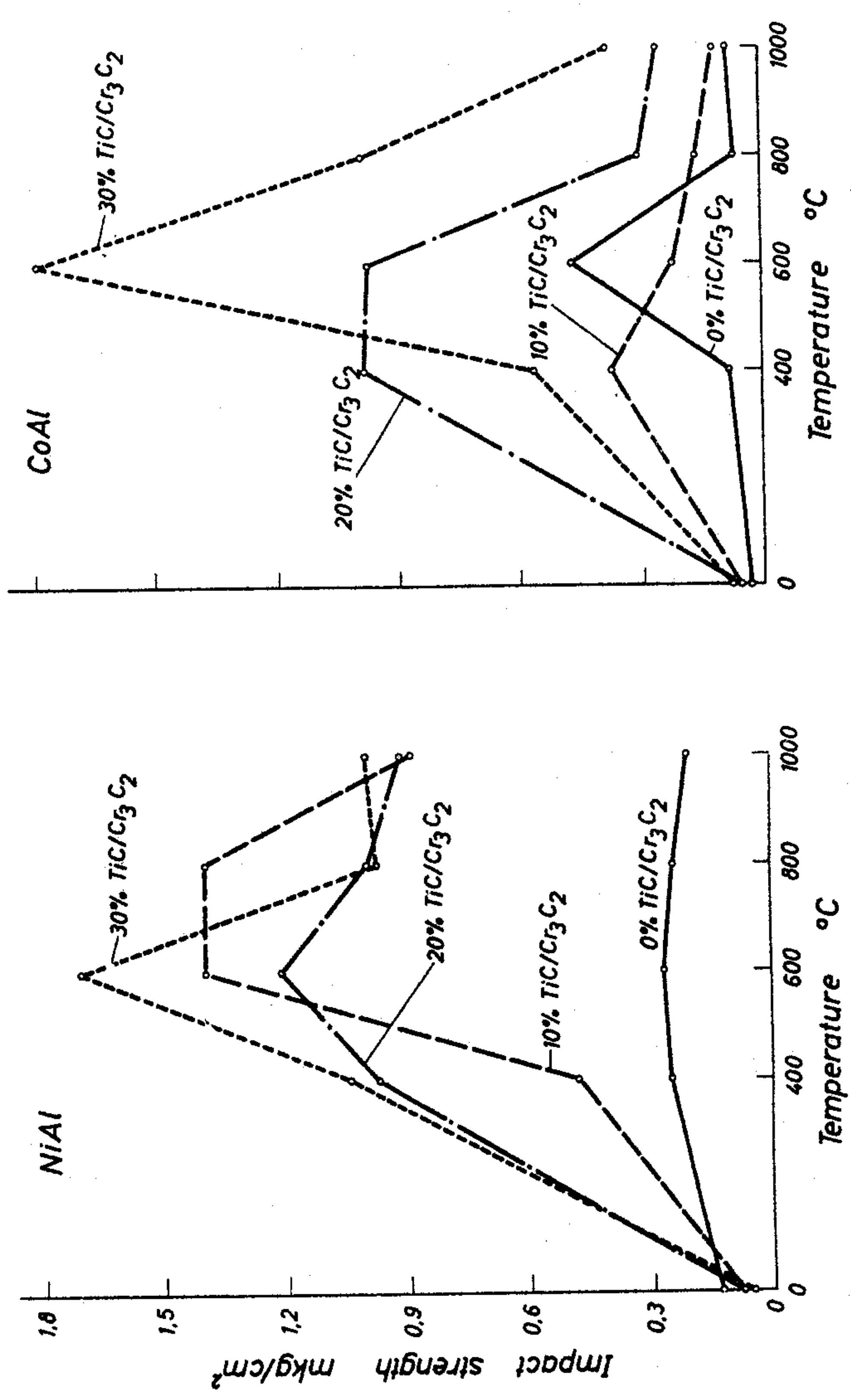


Fig. 31: Impact Strength at Elevated Temperatures of Reinforced NiAl(CoAl)-TiC/$Cr_3C_2$ Alloys (4 molybdenum wires 0,8 mm dia.)

PHOTOMICROGRAPH DOUBLE MOUNTING SHEET

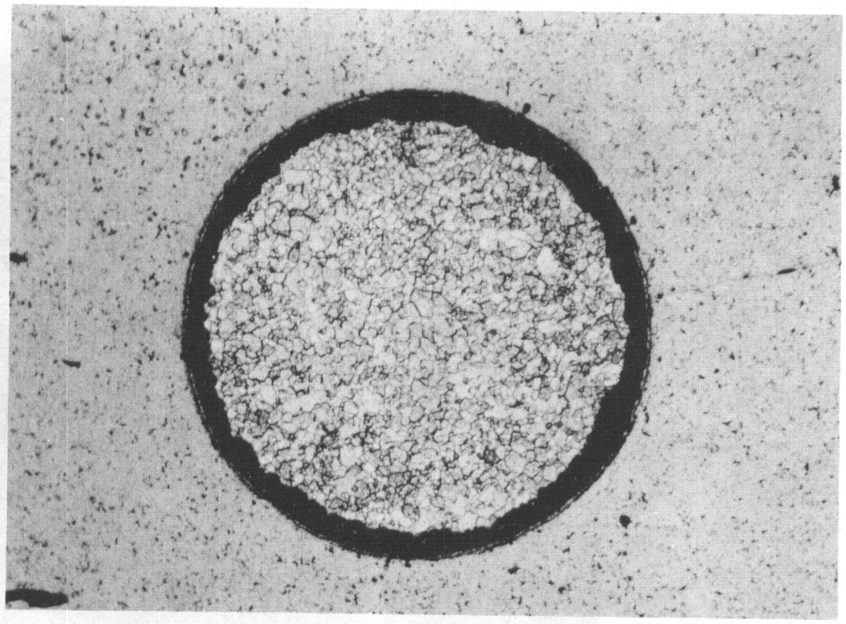

**Fig**...32.......... **Plate**..............

**Magn**..75X...... **Diam Etch**...............

**Remarks:**

Section through reinforced charpy bar. 0.8 mm dia molybdenum wire. Composition 54 (NiAl)

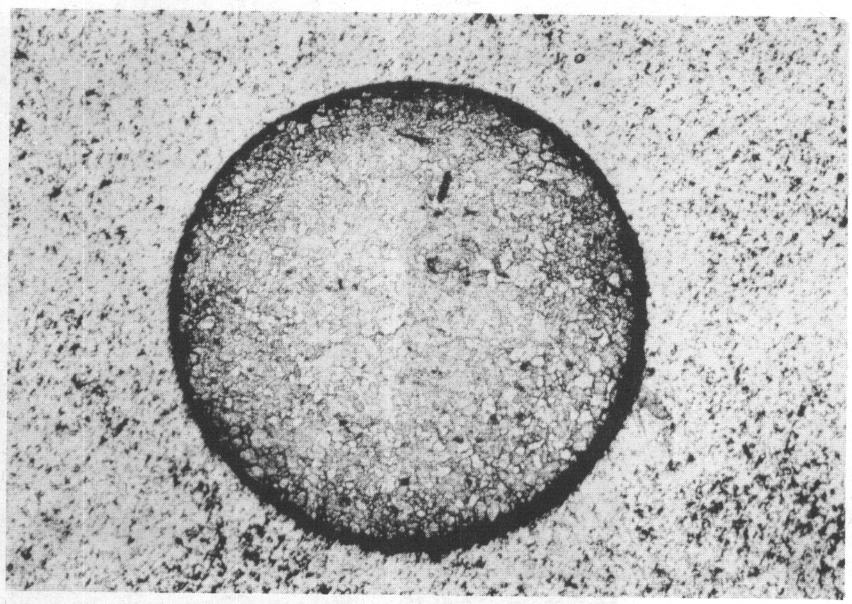

**Fig**...33.......... **Plate**............

**Magn**...75X.... **Diam Etch**.............

**Remarks:**

Section through reinforced charpy bar 0.8 mm dia. molybdenum wire. Composition 55 ($NiAl$-10$TiC/Cr_3C_2$)

PHOTOMICROGRAPH DOUBLE MOUNTING SHEET

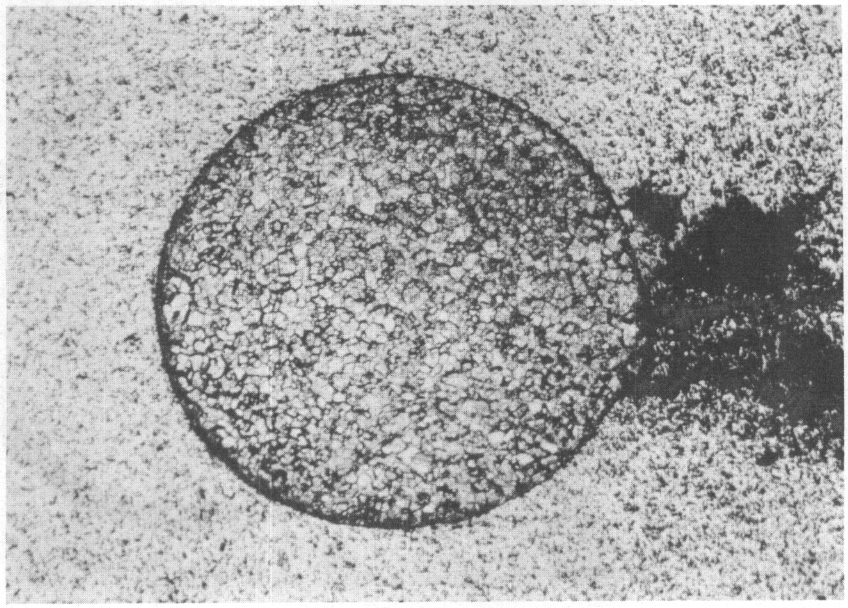

Fig...34......... Plate..............

Magn..75X..... Diam Etch...............
Remarks:

Section through reinforced Charpy bar
0.8 mm dia molybdenum wire. Composition
56 (NiAl-20 TiC/$Cr_3C_2$)

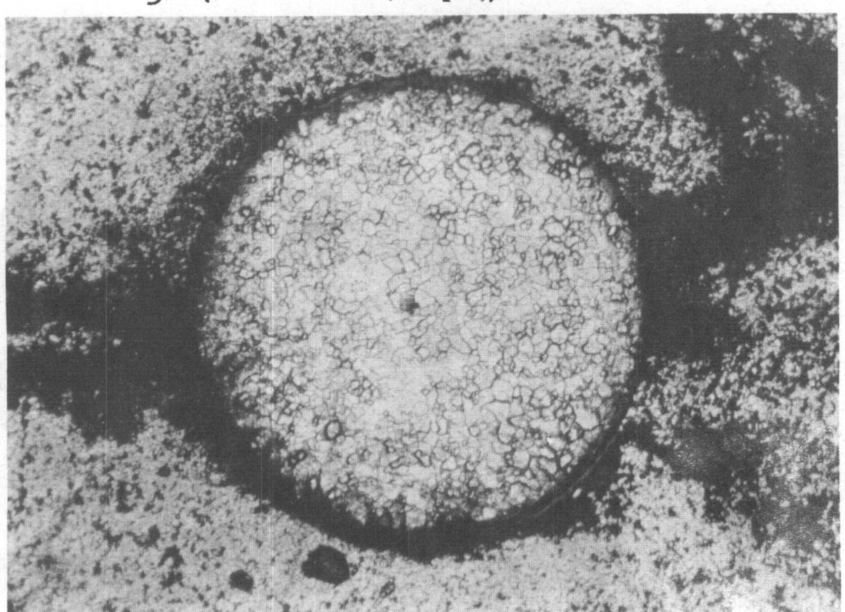

Fig....35.......... Plate............

Magn....75X...... Diam Etch.............
Remarks:

Section through reinforced Charpy bar.
0.8 mm dia. Molybdenum wire. Composition
57 (NiAl-30TiC/$Cr_3C_2$)

**Table 58:** Composition of NiAl(CoAl)-Si-TiC/$Cr_3C_2$ Alloys

| Specimen No. | Composition % | | | | | Approx.% | | | | | |
|---|---|---|---|---|---|---|---|---|---|---|---|
| | NiAl *) | CoAl **) | TiC/$Cr_3C_2$ | Si **) | Ferro-boron | Ni | Co | Al | TiC/$Cr_3C_2$ | Si | B + Fe |
| 78 | 92 | - | - | 5 | 3 | 62,6 | - | 29,4 | - | 5 | 0,5 +2,5 |
| 79 | 82,2 | - | 10 | 5 | 2,8 | 55,9 | - | 26,3 | 10 | 5 | 0,5 +2,3 |
| 80 | 72,6 | - | 20 | 5 | 2,4 | 49,4 | - | 23,2 | 20 | 5 | 0,4 +2,0 |
| 81 | 63 | - | 30 | 5 | 2 | 42,2 | - | 20,8 | 30 | 5 | 0,2 +1,8 |
| 82 | - | 92 | - | 5 | 3 | - | 64,4 | 27,6 | - | 5 | 0,5 2,5 |
| 83 | - | 82,2 | 10 | 5 | 2,8 | - | 57,6 | 24,6 | 10 | 5 | 0,5 +2,3 |
| 84 | - | 72,6 | 20 | 5 | 2,4 | - | 50,8 | 21,8 | 20 | 5 | 0,4 +2,0 |
| 85 | - | 63 | 30 | 5 | 2 | - | 44,1 | 18,9 | 30 | 5 | 0,2 +1,8 |

*) Composition 68% Ni, 32% Al
**) Composition 70% Co, 30% Al
***) Silicon powder < 0,06 mm, 99,6% Si

Table 59: Impact Strength of NiAl(CoAl)-Si-TiC/$Cr_3C_2$ Alloys at Elevated Temperatures (Charpy Bars)

| Specimen No. | Impact strength mkg./cm.$^2$ at $^oC$. | | | | |
|---|---|---|---|---|---|
| | 20 | 400 | 600 | 800 | 1000 |
| 78 | 0,05 | 0,05 | 0,05 | 0,04 | 0,06 |
| 79 | 0,04 | 0,04 | 0,04 | 0,04 | 0,04 |
| 80 | 0,04 | 0,04 | 0,04 | 0,05 | 0,04 |
| 81 | 0,04 | 0,04 | 0,04 | 0,05 | 0,06 |
| 82 | 0,04 | 0,03 | 0,04 | 0,04 | 0,05 |
| 83 | 0,04 | 0,04 | 0,03 | 0,04 | 0,04 |
| 84 | 0,04 | 0,04 | 0,04 | 0,04 | 0,04 |
| 85 | 0,04 | 0,03 | 0,04 | 0,04 | 0,04 |

Table 60: Scaling Properties of NiAl(CoAl)-Si-TiC/$Cr_3C_2$ Alloys at 800°C.

| Specimen No. | Gain in weight (g/cm.$^2$) after hours | | | | | |
|---|---|---|---|---|---|---|
| | 2 | 4 | 8 | 16 | 32 | 64 |
| 78 | 0,00010 | 0,00012 | 0,00082 | 0,00092 | 0,00093 | 0,00095 |
| 79 | 0,02836 | 0,03050 | 0,06216 | 0,07393 | 0,07398 | 0,07412 |
| 80 | 0,02890 | 0,03255 | 0,04059 | 0,04420 | 0,04651 | 0,04895 |
| 81 | 0,01419 | 0,01478 | 0,01919 | 0,02329 | 0,02354 | 0,02388 |
| 82 | 0,00011 | 0,00014 | 0,00035 | 0,00047 | 0,00050 | 0,00054 |
| 83 | 0,04229 | 0,04532 | 0,10246 | 0,12582 | 0,12621 | 0,12651 |
| 84 | 0,05152 | 0,05528 | 0,06743 | 0,08563 | 0,09432 | 0,10606 |
| 85 | 0,05934 | 0,06479 | 0,10010 | 0,12271 | 0,12899 | 0,13049 |

Table 61: Scaling Properties of NiAl(CoAl)-Si-TiC/$Cr_3C_2$ Alloys at 900°C.

| Specimen No. | Gain in weight (g/cm.$^2$) after hours | | | | | |
|---|---|---|---|---|---|---|
| | 2 | 4 | 8 | 16 | 32 | 64 |
| 78 | 0,00023 | 0,00032 | 0,00038 | 0,00055 | 0,00060 | 0,00083 |
| 79 | 0,04371 | 0,05096 | 0,05817 | 0,07818 | 0,07530 | 0,07823 |
| 80 | 0,02889 | 0,03678 | 0,04727 | 0,04921 | 0,05101 | 0,05309 |
| 81 | 0,01832 | 0,01902 | 0,01965 | 0,02427 | 0,02624 | 0,02820 |
| 82 | 0,00018 | 0,00025 | 0,00037 | 0,00055 | 0,00057 | 0,00063 |
| 83 | 0,07825 | 0,09406 | 0,10897 | 0,12637 | 0,13430 | 0,13968 |
| 84 | 0,06594 | 0,07217 | 0,07632 | 0,08429 | 0,09943 | 0,12836 |
| 85 | 0,06316 | 0,06873 | 0,11417 | 0,12482 | 0,13831 | 0,14456 |

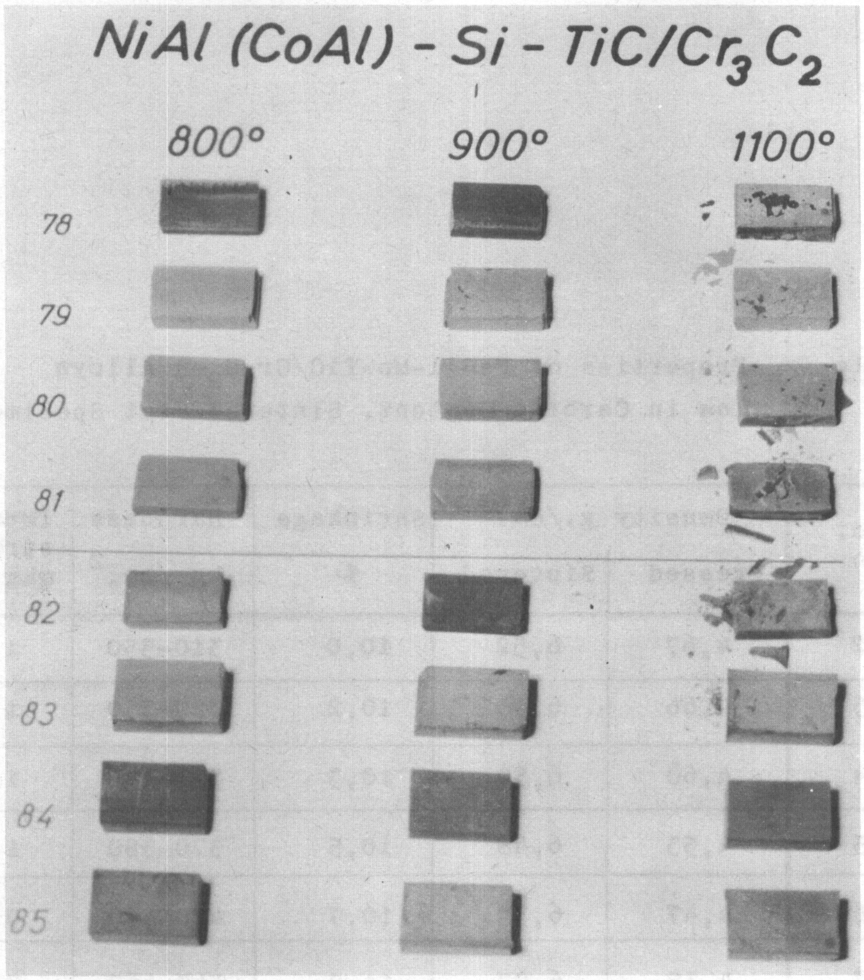


Fig. 36: Appearance of the Scale Test Specimens of NiAl(CoAl)-Si-TiC/$Cr_3C_2$ Alloys

800°C. 64 hrs.
900°C. 64 hrs.
1100°C. 4 hrs.

Table 62: Properties of Fe-Al-Mo-TiC/$Cr_3C_2$-B Alloys low in Carbide Content. Sintered Flat Specimens

| Spec. No. | Density g./cm.$^3$ | | Shrinkage | Hardness | Impact strength |
|---|---|---|---|---|---|
| | Pressed | Sintered | % | kg./mm.$^2$ | mkg./cm.$^2$ |
| 82 | 4,67 | 6,52 | 10,0 | 310-350 | 1,2 |
| 83 | 4,66 | 6,50 | 10,2 | 320-350 | 1,4 |
| 84 | 4,60 | 6,50 | 10,3 | 330-370 | 1,1 |
| 85 | 4,53 | 6,48 | 10,5 | 370-380 | 1,0 |
| 86 | 4,47 | 6,39 | 10,7 | 420-430 | 0,52 |
| 87 | 4,35 | 6,22 | 11,0 | 440-460 | 0,53 |

furnace, we however found that a high percentage of the rods was good and in unobjectionable condition. We cut the extruded rods into lengths of 90 mm, and did the stress relieving by annealing the pieces at 900°C. in vacuum for 1 hour. We used the pieces for tensile specimens to investigate the stress-to-rupture strength.

After evaluating density, hardness and impact strength, stress-to-rupture specimens were prepared (Fig. 37), in addition to ground and bored flat specimens (Fig. 38) and their stress-to-rupture behavior was examined.

The physical properties of the sintered as well as of the extruded samples are shown in Fig. 39. Specimens with a low porosity - the density decreases with increasing carbide content - show a definitely lower impact strength as compared with sintered material.

Fig. 40 shows the stress-to-rupture curves of extruded material for 500°C. (Table 63). With rising carbide content higher values of stress-to-rupture strength are attained. When comparing these values with those of only sintered specimens showing slight porosity, one should expect exceptionally higher strength from the highly densified extruded samples. This is, however, not the case and this fact indicates that a certain amount of pores may positively influence the strength-to-rupture behavior as does the axial orientation of the slip restraining intergranular substance, initiated by extrusion. In this case it is no longer able to increase the stress-to-rupture strength as would be true for its random distribution in a creep resistant matrix. The influence of amount and grain size of the intergranular substance will be discussed in the paragraph on electron microscopic examinations.

b. Fe-Al(14)-Mo-$Al_2O_3$-B Alloys, Extrusion Technique

The addition of TiC/$Cr_3C_2$ to the base alloy has proved favorable and the extrusion technique has been found as a means to prepare these materials with high density. It was decided to raise the stress-to-rupture strength of the Fe-Al-Mo base alloy by the addition of 0.5, 1.2, and 5 weight % $Al_2O_3$. The alumina used was a calcinated powder of very small grain size. Preparation of specimens was carried out as described. The blooms for extrusion were welded into boxes made of 0.5 mm. iron sheet, thus facilitating extrusion of the bars and attaining excellently worked rods even with high alumina additions. The thin iron layers of the extruded rods were worked off previous to homogenizing.

The properties of extruded alloys as compared to sintered ones at room temperature are graphically shown in Fig. 41. (Table 64 and 65).

The density-curve for extruded alloys represents the density of almost pore-free samples. The lower density after sintering influences the impact strength exceedingly more than the hardness. Extruded alloys show higher impact strength than the materials with TiC/$Cr_3C_2$ additions when considering the contents as volume - %. Stress-to-rupture strength is not substantially increased by $Al_2O_3$ additions (Fig. 42. Table 66).

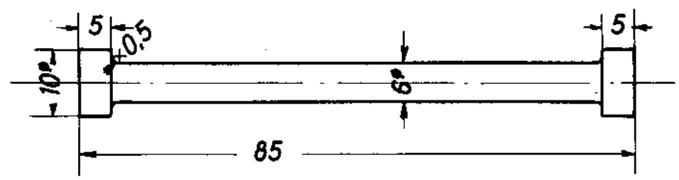


Fig. 37: Round Specimens from Extruded Rods for Stress-to-Rupture and Creep Tests (Dimensions in mm.)

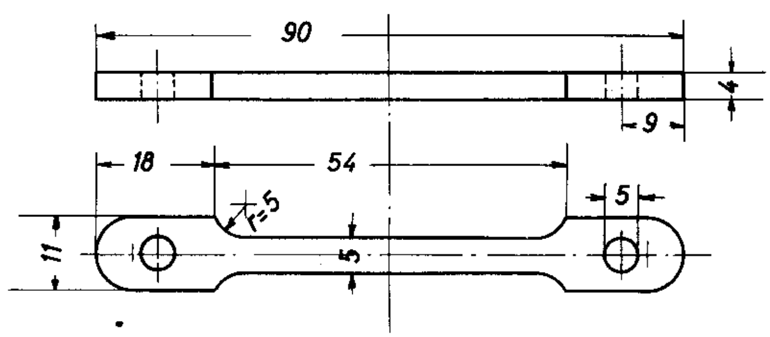


Fig. 38: Flat Specimens for Stress-to-Rupture Tests (Dimensions in mm.)

| AF 61(514) 1144 Techn.Note | Metallwerk Plansee A.G. Reutte/Tirol | |
|---|---|---|

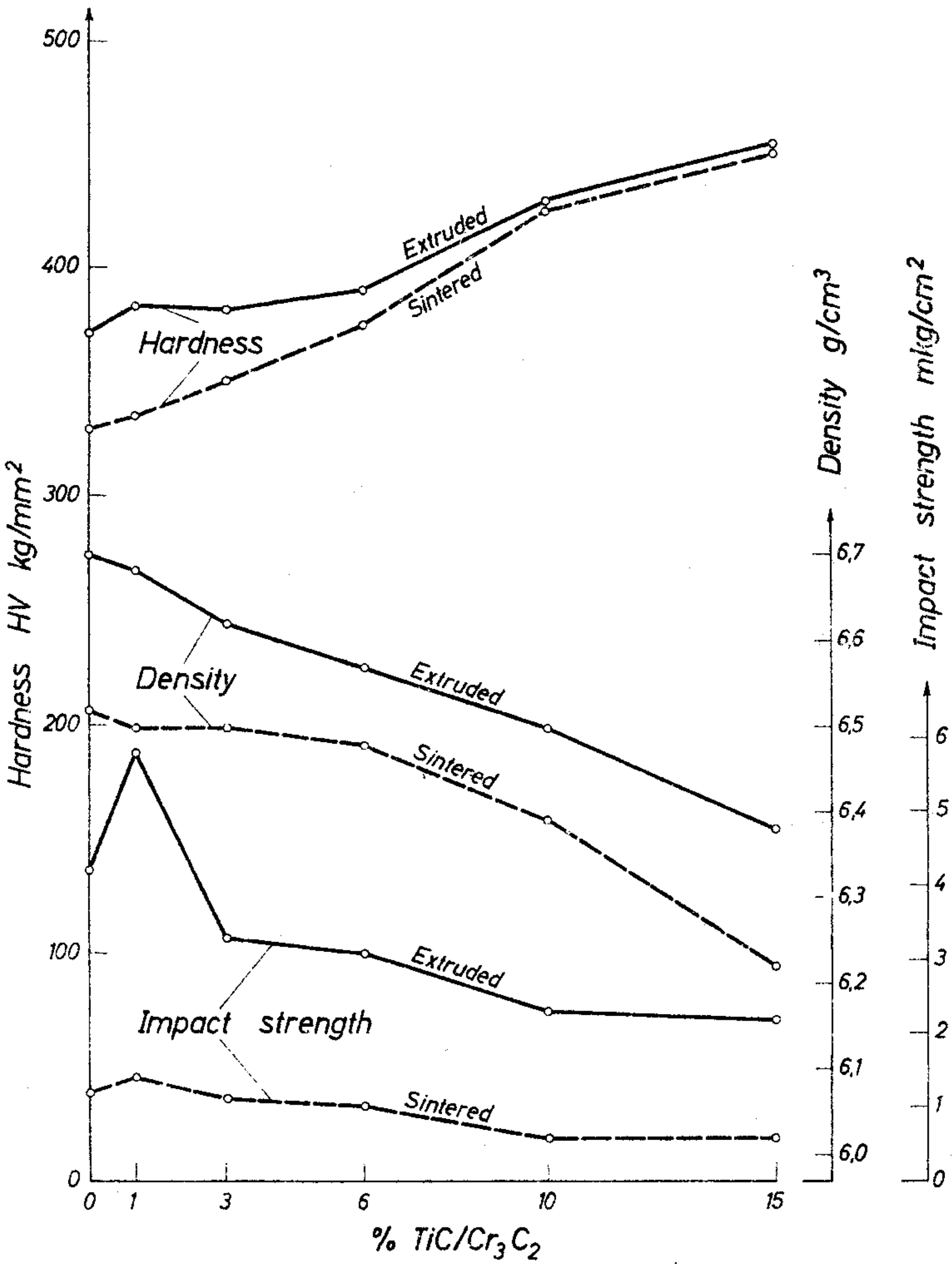


Fig. 39: Physical Properties of Fe-Al-Mo-TiC/$Cr_3C_2$-B Alloys, Low in Carbide Content. **Sintered and Extruded Specimens**

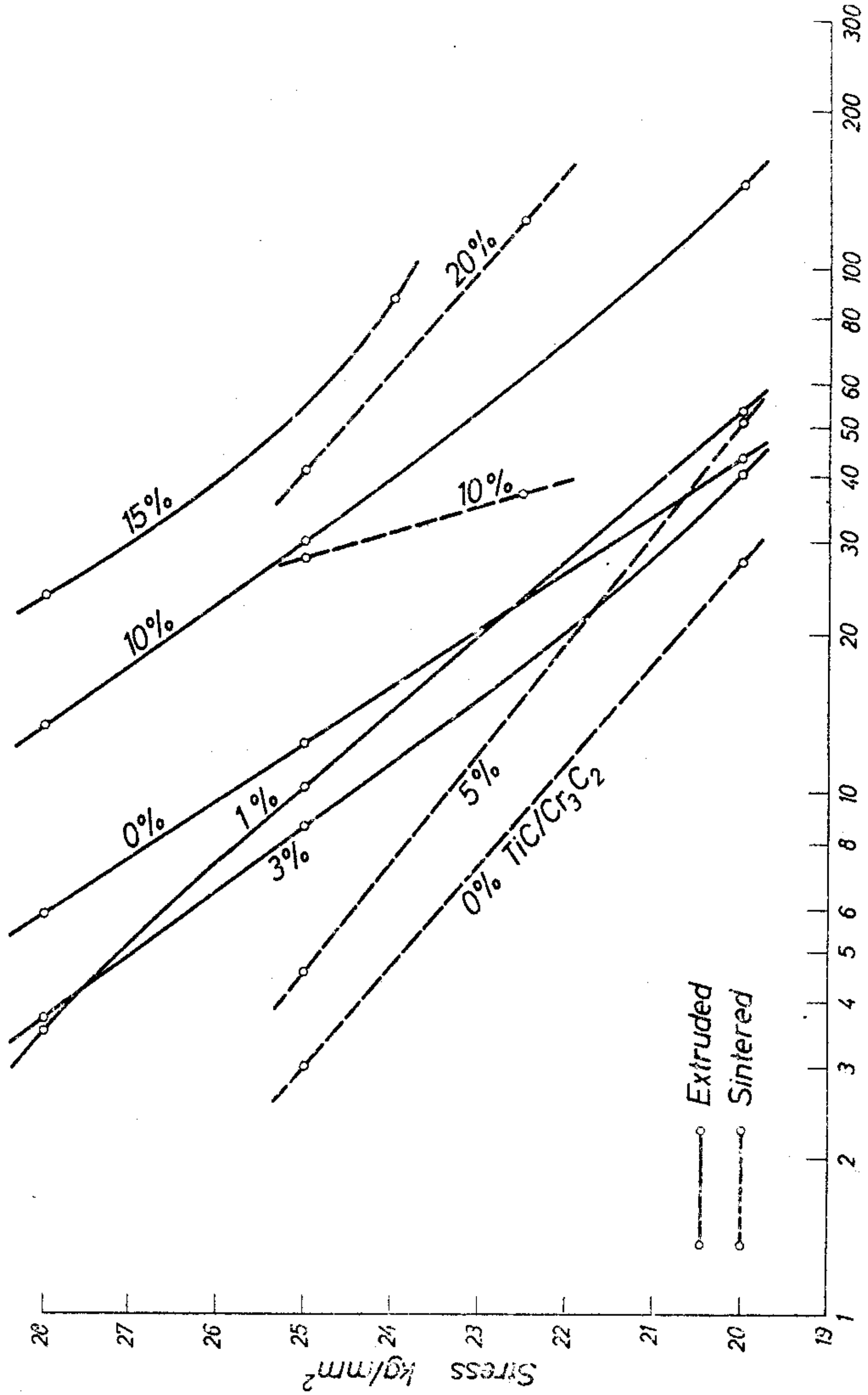


Fig. 40: Stress-to-Rupture Strength of Fe-Al-Mo-TiC/$Cr_3C_2$-B Alloys at 500°C. Comparison of only Sintered and Extruded Specimens

Table 63: Stress-to-Rupture Strength of Fe-Al-Mo-TiC/$Cr_3C_2$-B Alloys Low in Carbide Content. Round Extruded Specimens.

| Stress at 500°C kg./mm.$^2$ | Rupture Time in hrs. at Specimen No. | | | | | |
|---|---|---|---|---|---|---|
| | 82 | 83 | 84 | 85 | 86 | 87 |
| 20 | 43 | 53 | 40 | 58 | 147 | - |
| 24 | -- | -- | -- | -- | -- | 86 |
| 25 | 12,4 | 10,2 | 8,7 | 11,9 | 30,2 | -- |
| 28 | 5.7 | 3.5 | 3.7 | 2,7 | 13.3 | 23.7 |
| 31 | -- | -- | -- | -- | -- | 12 |

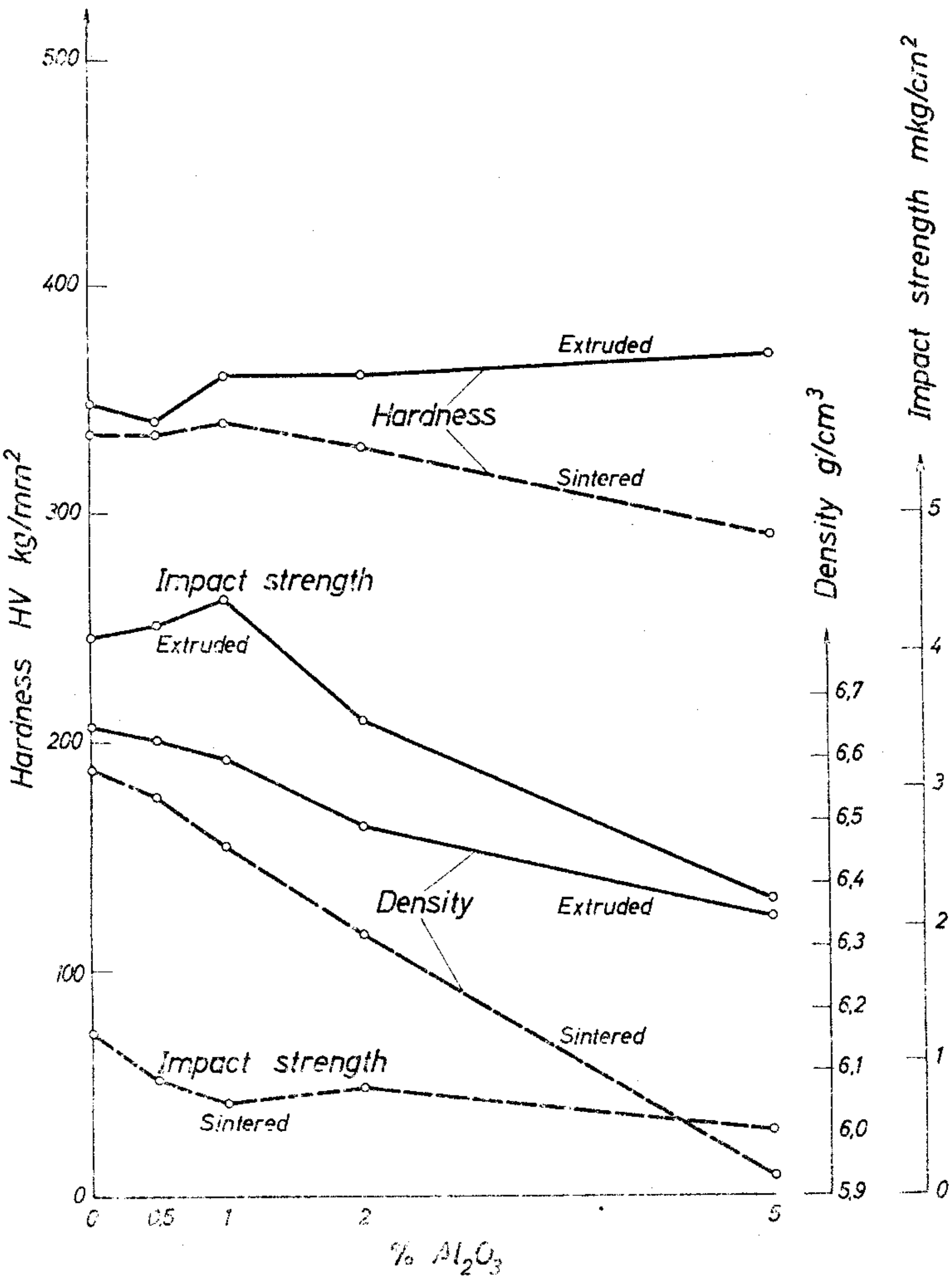


Fig. 41: Physical Properties of Fe-Al(14)-Mo-$Al_2O_3$-B Alloys, Sintered and Extruded Specimens

**Table 64:** Properties of Fe-Al-Mo-$Al_2O_3$-B Alloys at Room Temperature, Flat Sintered Specimens

| Spec. No. | Density g/cm.$^3$ Pressed | Density g/cm.$^3$ Sintered | Shrinkage % | Hardness kg./mm.$^2$ | Impact strength mkg./cm.$^2$ x) | Impact strength mkg./cm.$^2$ xx) |
|---|---|---|---|---|---|---|
| 88 | 4,58 | 6,58 | 10,6 | 320-350 | 1,1 | 1,3 |
| 89 | 4,60 | 6,54 | 10,1 | 330-340 | 0,88 | 0,82 |
| 90 | 4,57 | 6,46 | 9,8 | 330-350 | 0,67 | 0,72 |
| 91 | 4,56 | 6,32 | 9,4 | 320-340 | 0,71 | 0,88 |
| 92 | 4,52 | 5,93 | 9,6 | 280-300 | 0,37 | 0,65 |

x) Flat test bars, approx. 4 x 8 mm, without notch
xx) Charpy specimens approx. 8 x 8 mm, without notch

Table 65: Properties of Fe-Al-Mo-$Al_2O_3$-B Alloys. Specimens from Hot Extruded Rods.

| Spec. No. | Density g./cm.$^3$ Sintered | Extruded | Hardness kg./mm.$^2$ | Impact strength$^{x)}$ mkg./cm.$^2$ | Micro-structure |
|---|---|---|---|---|---|
| 88 | 6,58 | 6,65 | 348 | 4,1 | see fig.59 |
| 89 | 6,54 | 6,63 | 339-348 | 4,2 | " " 60 |
| 90 | 6,46 | 6,60 | 357-366 | 4,4 | " " 61 |
| 91 | 6,32 | 6,49 | 357-366 | 3,5 | " " 62 |
| 92 | 5,93 | 6,35 | 366-375 | 2,2 | |

x) Round specimens, 9 mm dia., without notch, distance 40 mm.

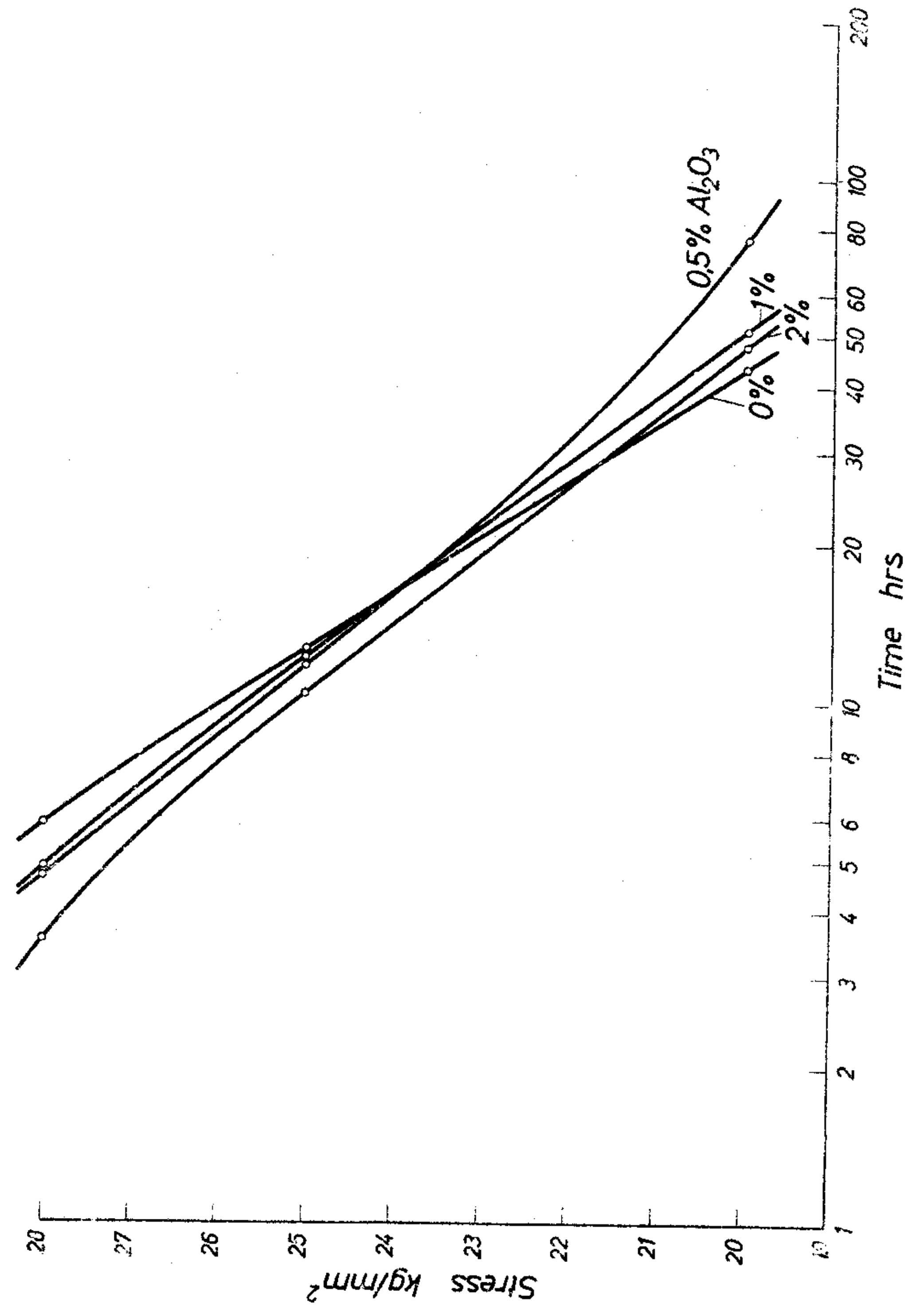


Fig. 42: Stress-to-Rupture Strength of Fe-Al-Mo-$Al_2O_3$-B Alloys at 500°C.
Extruded Specimens

Table 66: Stress-to-Rupture Strength of $Fe-Al-Mo-Al_2O_3-B$ Alloys. Round Extruded Specimens.

| Stress at 500°C. $kg./mm.^2$ | Rupture Time in hrs. at Specimen No. | | | | |
|---|---|---|---|---|---|
| | 88 | 89 | 90 | 91 | 92 |
| 20 | 43 | 77 | 51 | 48 | -- |
| 24 | -- | -- | -- | -- | -- |
| 25 | 12,4 | 11,7 | 12,1 | 10,2 | -- |
| 28 | 5,7 | 4,6 | 4,8 | 3,5 | -- |
| 31 | -- | -- | -- | -- | -- |

c. Ni-Cr (80/20)-$Al_2O_3$-B-Alloys

The good workability of sintered dispersion hardened materials by extrusion suggested the examination of other classical hot-strength alloys such as Ni-Cr (80/20) and Fe-Al-Cr (Megapyr) with additions of alumina in the sintered and extruded highly dense state.

Powder mixtures of carbonyl nickel and electrolytic chromium powder (grain size $<$ 0,06 mm.) with 0,5, 1, 2, and 5% $Al_2O_3$ and pressed to bars 40 X 40 X 80 mm. were sintered during 4 hours at 1200°C. in a vacuum of 10 microns. These bars were extruded after having been clad in iron boxes. The worked rods were then annealed. The mechanical properties of extruded samples at room temperature are graphically drawn in Fig. 43 (Table 67). The density decreases in linear proportion with rising alumina content. The hardness changes only slightly. The impact strength of unnotched samples was above 10 mkg./cm.$^2$. These samples could not be destroyed.

The stress-to-rupture values (Fig. 44 and Table 68), are considerably higher than for the previously examined materials. This means that the base alloy shows a good creep strength in spite of its low hardness and high ductility. Up to 1% $Al_2O_3$ addition, the stress-to-rupture strength increases; it is lowered by higher contents of alumina, probably through notch effect.

d. Fe-Cr-Al-$Al_2O_3$-B Alloys, Extrusion Technique

Powder mixtures of base alloy, corresponding to the Megapyr composition, with about 68% Fe, 27% Cr and 4% Al, and with 0,5, 1, 2 and 5% $Al_2O_3$ were sintered. The sintering conditions were the same as for Ni-Cr (see under c). The physical properties of only sintered specimens as compared to extruded alloys are graphically shown in Fig. 45 (see Tables 69 and 70). The sintered alloys have a considerably lower density than the extruded material which results in a lower hardness and an exceedingly lower impact strength. The impact strength of extruded samples with alumina content up to 3% was above 10 mkg./cm.$^2$. The stress-to-rupture curves of the extruded alloys are shown in Fig. 46 (Table 71). In comparison with other alloys, the stress-to-rupture values for 500°C. are low, although the curves are rather flat. With increasing alumina content the stress-to-rupture values are also increased.

e. Fe-Al(18)-Mo-$Al_2O_3$-B Alloys, Extrusion Technique.

The good extrudability exhibited by Fe-Al-Mo alloys containing 14% Al has stimulated the production of such alloys with Al contents up to 18 to 20% and with additions of 0,5, 1, 2, and 5% $Al_2O_3$ by extrusion. Their properties were then examined. The aluminum was added in form of a Fe-Al pre-alloy 50/50.

Fig. 47 shows the mechanical properties of such alloys in the sintered and extruded state (Tables 72 and 73). The densification through extrusion becomes primarily perceptible in the improved impact strength and not so much in a higher hardness of alloys. Compared with alloys containing only 14% Al, the impact strength is much higher even with $Al_2O_3$ additions up to 2%.

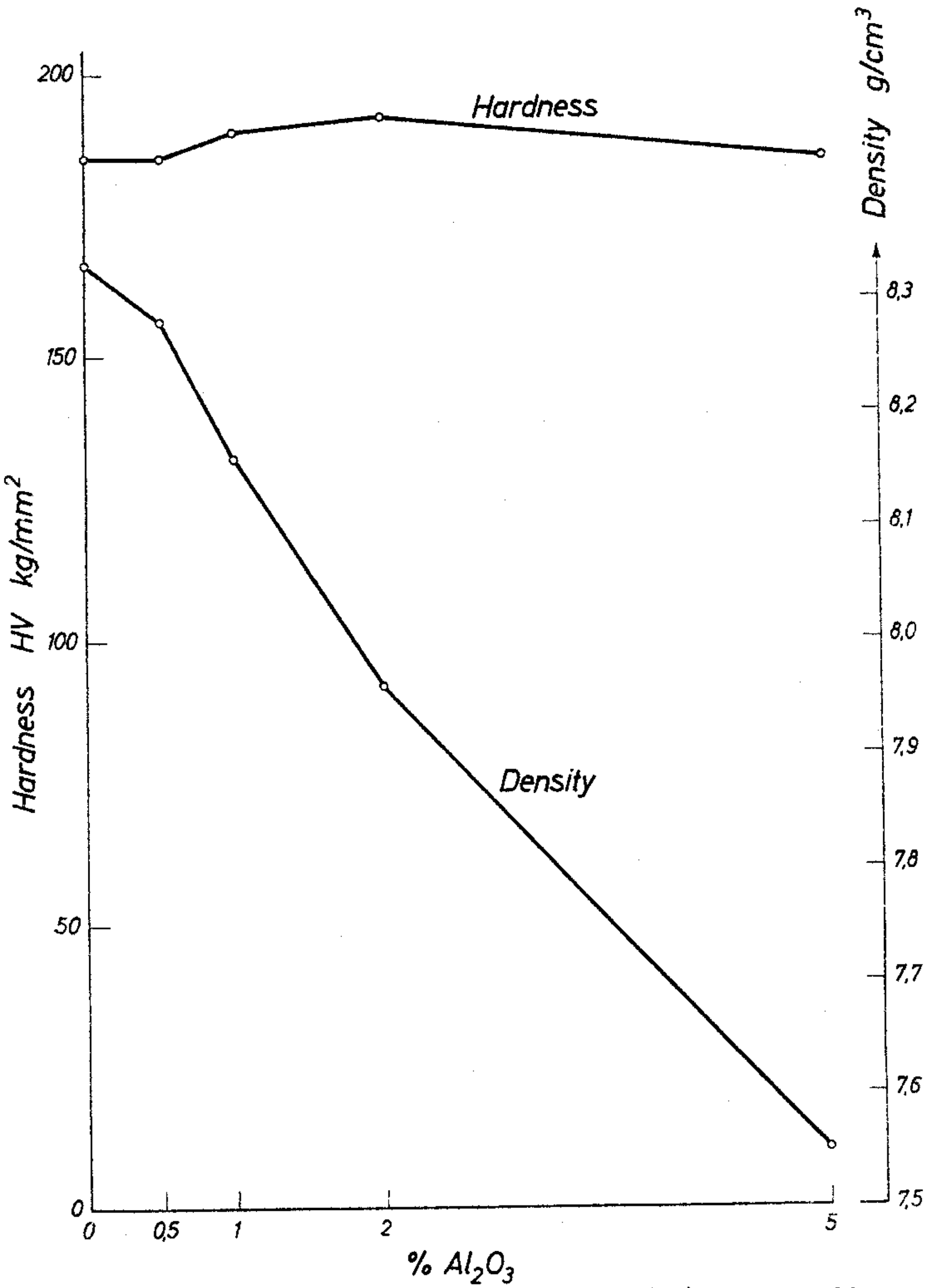


Fig. 43 Physical Properties of Ni-Cr(80/20)-$Al_2O_3$B Alloys, Extruded Specimens

Table 67: Properties of Ni-Cr (80/20)-$Al_2O_3$-B Alloys at Room Temperature
Specimens from Hot Extruded Rods

| Specimen No. | Density g./cm.$^3$ Sintered | Density g./cm.$^3$ Extruded | Hardness kg./mm.$^2$ | Impact Strength *) mkg./cm.$^2$ |
|---|---|---|---|---|
| 93 | 8,10 | 8,33 | 180-190 | > 10 |
| 94 | 7,90 | 8,28 | 180-190 | > 10 |
| 95 | 7,78 | 8,16 | 185-195 | > 10 |
| 96 | 7,12 | 7,96 | 190-195 | > 10 |
| 97 | 6,97 | 7,55 | 180-190 | 9,7 |

*) Round specimens, 9 mm.dia.approx., without notch. Distance 40 mm.

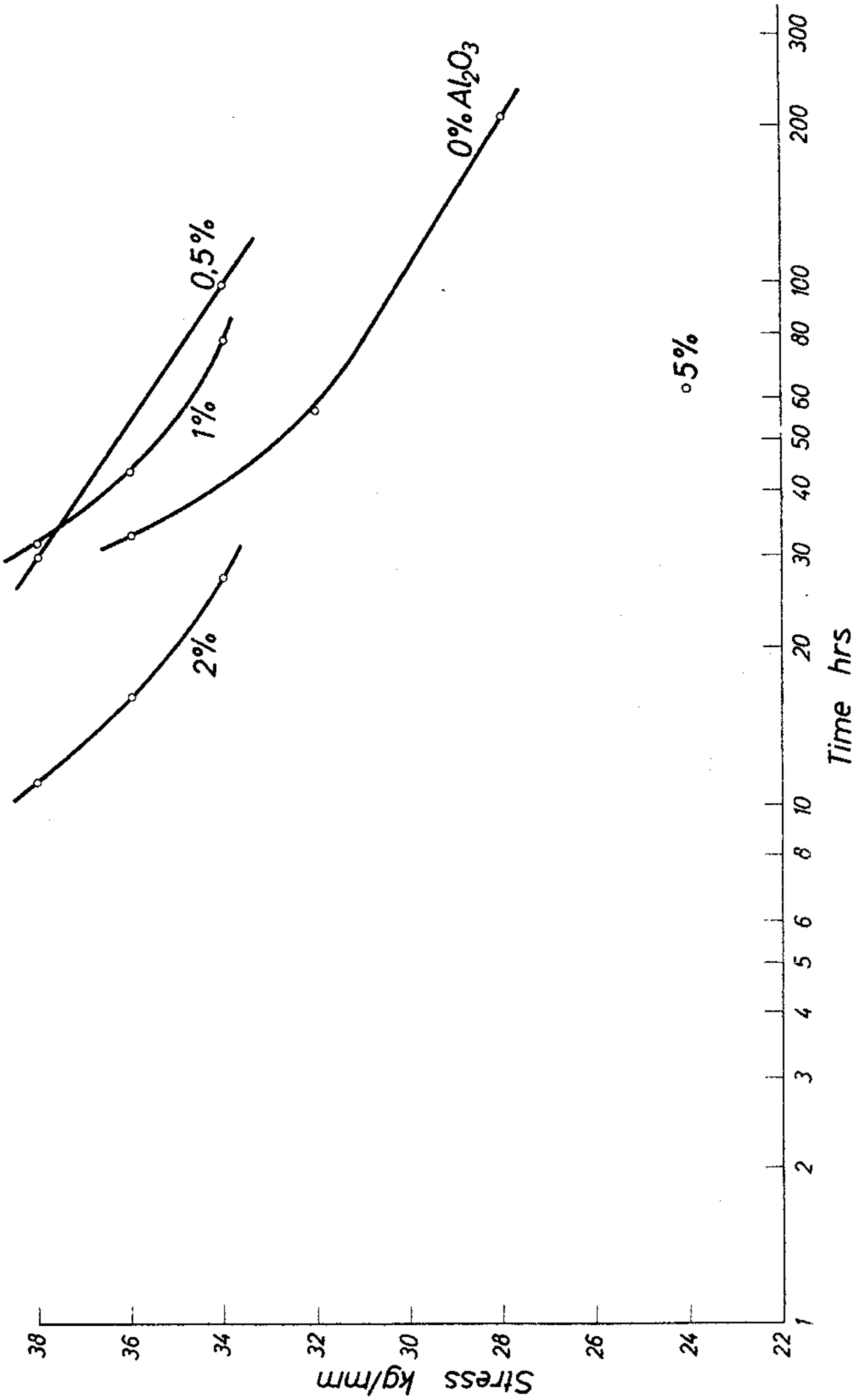


Fig. 44: Stress-to-Rupture Strength of Ni-Cr(80/20)-$Al_2O_3$-B Alloys at 500°C. Extruded Specimens

Table 68.: Stress-to-Rupture Strength of Ni-Cr(80/20)-$Al_2O_3$-B Alloys at 500°C. Extruded Specimens

| Stress at 500°C. kg./mm.$^2$ | Rupture Time in hrs. at Specimen No. 93 | 94 | 95 | 96 | 97 |
|---|---|---|---|---|---|
| 24 | -- | -- | -- | -- | 62 |
| 28 | 210 | -- | -- | -- | -- |
| 32 | 56 | -- | -- | -- | -- |
| 34 | -- | 99 | 77 | 27 | -- |
| 36 | 33 | -- | 43 | 16 | -- |
| 38 | -- | 30 | 32 | 11 | -- |

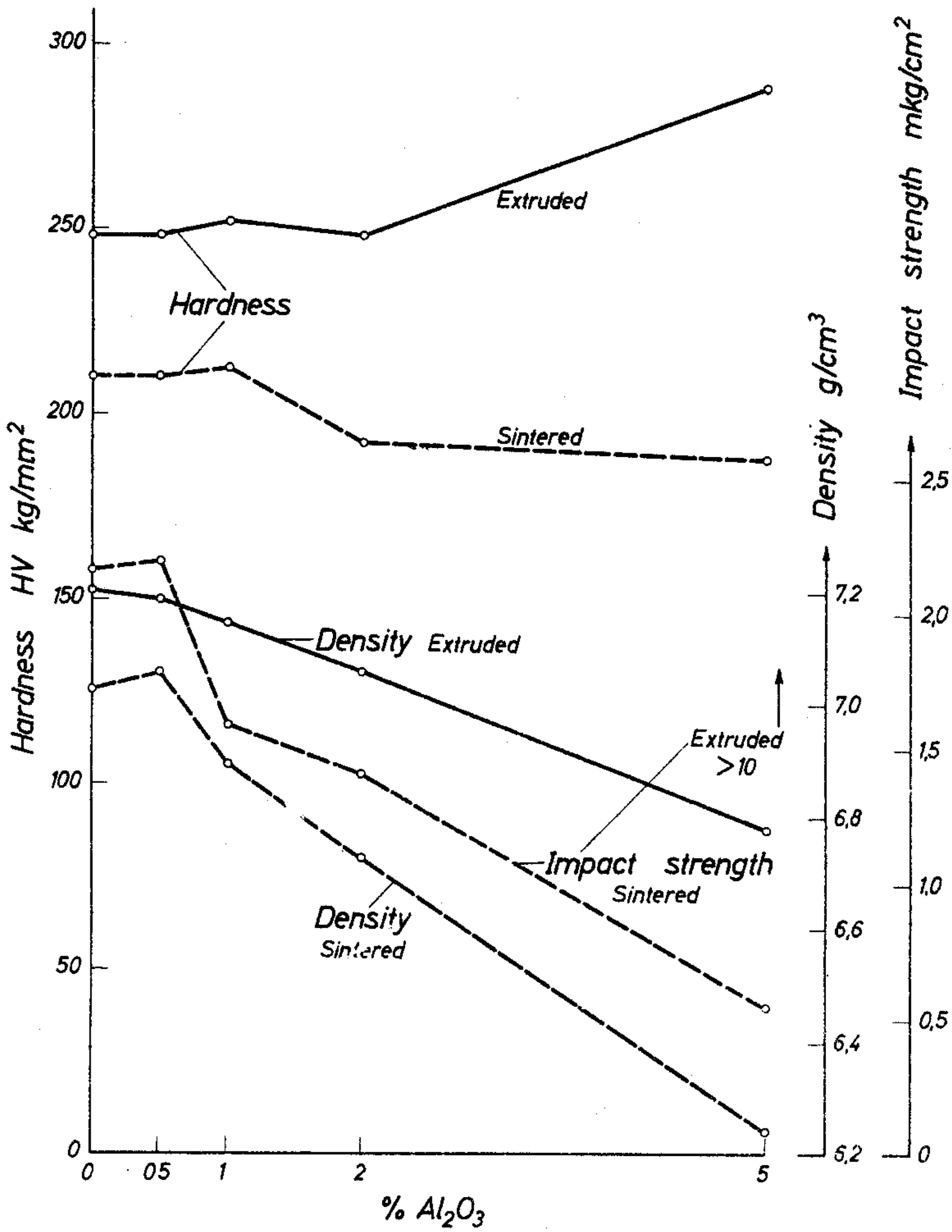


Fig. 45: Physical Properties of Fe-Cr-Al-$Al_2O_3$-B Alloys. Extruded and Sintered Specimens

**Table 69:** Properties of Fe-Cr-Al-$Al_2O_3$-B Alloys at Room Temperature. Flat Sintered Specimens.

| Specimen No. | Density g./cm.$^3$ Pressed | Density g./cm.$^3$ Sintered | Shrinkage % | Hardness kg./mm.$^2$ | Impact Strength mkg./cm.$^2$ |
|---|---|---|---|---|---|
| 98 | 5,36 | 7,03 | 10 | 210-230 | 2,6 |
| 99 | 5,35 | 7,06 | 8,9 | 210-230 | 2,2 |
| 100 | 5,33 | 6,90 | 8,5 | 220-230 | 1,6 |
| 101 | 5,29 | 6,73 | 7,6 | 180-190 | 1,4 |
| 102 | 5,18 | 6,24 | 6,1 | 170-180 | 0,56 |

**Table 70:** Properties of $Fe-Cr-Al-Al_2O_3-B$ Alloys
at Room Temperature.
Specimens from Hot Extruded Rods.

| Specimen No. | Density g./cm.$^3$ | | Hardness kg./mm.$^2$ | Impact Strength*) mkg./cm.$^2$ |
|---|---|---|---|---|
| | Sintered | Extruded | | |
| 98 | 7,03 | 7,21 | 240-250 | > 10 |
| 99 | 7,06 | 7,19 | 240-250 | > 10 |
| 100 | 6,90 | 7,15 | 250-260 | > 10 |
| 101 | 6,73 | 7,06 | 240-250 | > 10 |
| 102 | 6,24 | 6,78 | 270-280 | 6,7 |

*) Round Specimens, 9 mm.dia.approx., without notch.
Distance 40 mm.

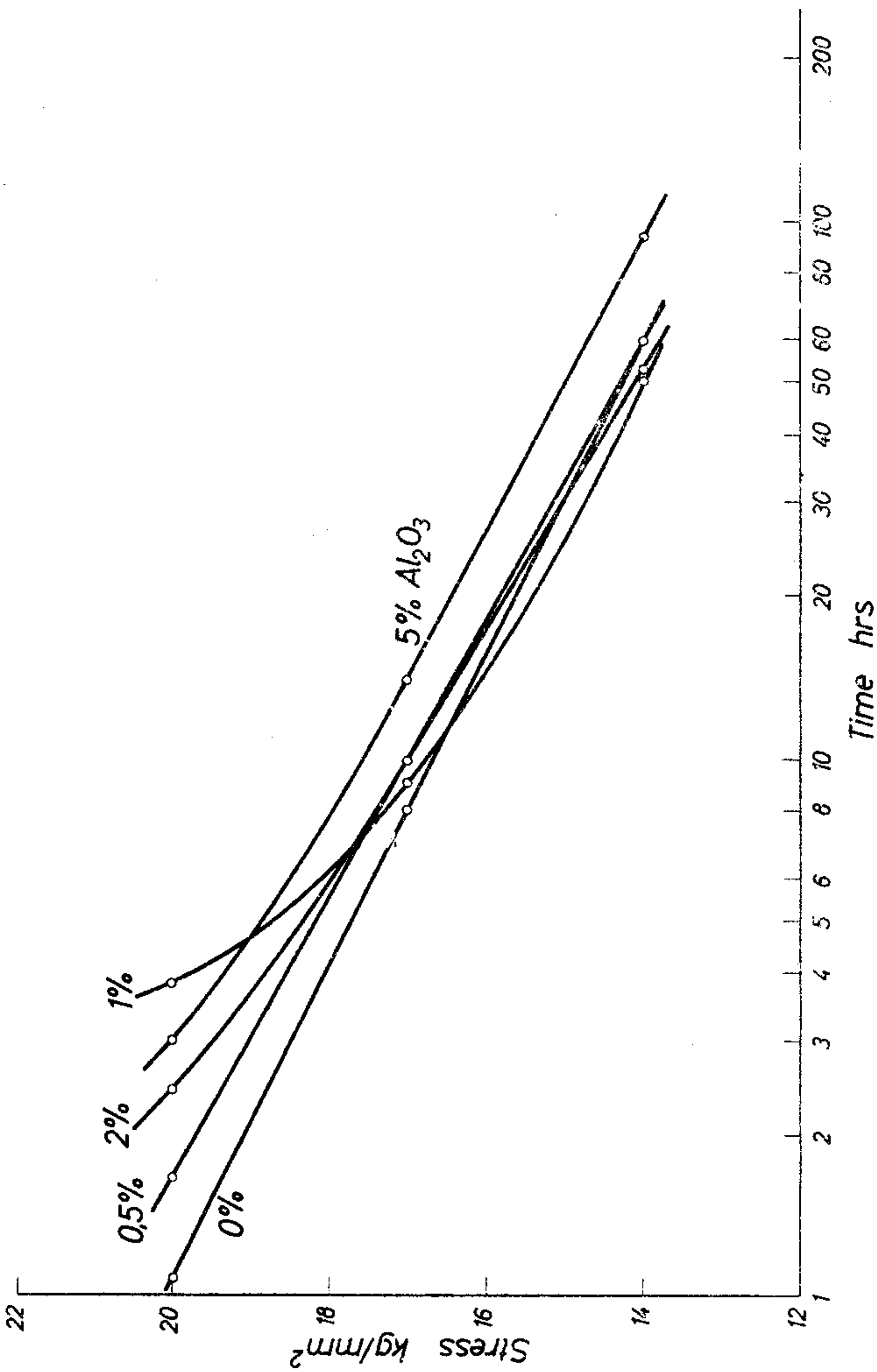


**Fig. 46:** Stress-to-Rupture Strength of Fe-Cr-Al-$Al_2O_3$-B Alloys at 500°C. Extruded Specimens

Table 71: Stress-to-Rupture Strength of Fe-Cr-Al-$Al_2O_3$-B Alloys at 500°C. Extruded Specimens.

| Stress at 500°C. kg./mm.$^2$ | Rupture time in hrs. at specimen no. | | | | |
|---|---|---|---|---|---|
| | 98 | 99 | 100 | 101 | 102 |
| 14 | 59 | 60 | 50 | 52 | 94 |
| 17 | 8 | 10 | 9 | 10 | 14 |
| 20 | ~1 | 1,6 | 3,8 | 2,4 | 3,0 |

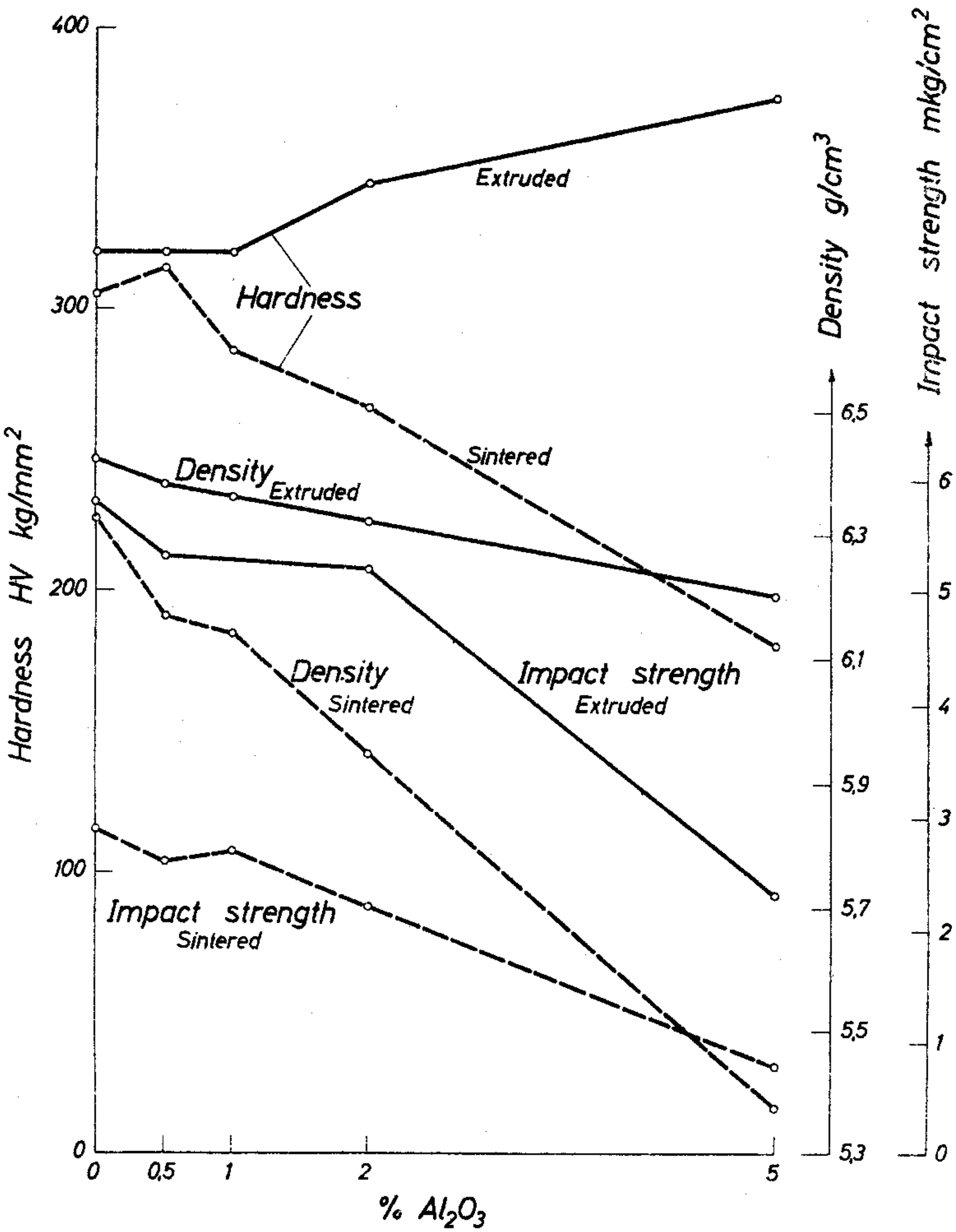


Fig. 47: Physical Properties of Fe-Al(18)-Mo-$Al_2O_3$-B Alloys, Extruded and Sintered Specimens.

**Table 72:** Properties of Fe-Al(18)-Mo-$Al_2O_3$-B Alloys at Room Temperature.
Flat Sintered Specimens

| Spec. No. | Density g./cm.$^3$ | | Shrinkage % | Hardness kg./mm.$^2$ | Impact strength mkg./cm.$^2$ |
|---|---|---|---|---|---|
| | Pressed | Sintered | | | |
| 108 | 4,31 | 6,33 | 11,5 | 300-310 | 2,9 |
| 109 | 4,37 | 6,17 | 10,2 | 310-320 | 2,6 |
| 110 | 4,33 | 6,14 | 10,3 | 280-290 | 2,7 |
| 111 | 4,32 | 5,95 | 9,5 | 260-270 | 2,2 |
| 112 | 4,25 | 5,37 | 4,8 | 170-190 | 0,8 |

**Table 73:** Properties of Fe-Al(18)-Mo-$Al_2O_3$-B Alloys at Specimens from Extruded Rods

| Spec. No. | Density g./cm.$^3$ Sintered | Density g./cm.$^3$ Extruded | Hardness kg./mm.$^2$ | Impact strength$^{x)}$ mkg./cm.$^2$ |
|---|---|---|---|---|
| 108 | 6,33 | 6,42 | 320 | 5,8 |
| 109 | 6,17 | 6,38 | 320 | 5,3 |
| 110 | 6,14 | 6,36 | 320 | 6,9 |
| 111 | 5,95 | 6,32 | 340 | 5,2 |
| 112 | 5,37 | 6,20 | 370 | 2,3 |

x) Round specimens, 9 mm dia., without notch, distance 40 mm.

From the stress-to-rupture curves of extruded specimens (Fig. 48) (Table 74) it can be seen that, compared with the Fe-Al(14)-Mo alloy, the values have increased quite markedly. With increasing alumina content these values are further increasing.

f. Fe-Al(20)-Mo-$Al_2O_3$-B Alloys, Extrusion Technique

Fig. 49 (Tables 75 and 76) shows the mechanical properties for sintered and extruded samples. The latter show a distinct drop of their impact strength compared with alloys having only 18% Al. Sintered alloys show higher impact strength because of the higher amount of liquid phase during sintering producing higher shrinkage.

The curves in Fig. 50 (Table 77) show an increase of stress-to-rupture strength with increasing Al and $Al_2O_3$ content respectively. The curves are rather steep now which indicates that the metallic matrix shows little creep resistance and that the non-metallic inclusions do not greatly influence this property.

## V. ELECTRON MICROSCOPIC INVESTIGATION

Since the dissolving power of the light microscope is not sufficient to reveal creep restricting fine particles, electron microscopic methods were used for the examination. A number of specimens with increasing $TiC/Cr_3C_2$ and $Al_2O_3$ additions respectively, embedded in the Fe-Al(14)-Mo base alloy, were chosen for examination of fractures. (Figs. 51-58.)

Fractures of the samples were coated with carbon while rotating the specimens around two axis. The carbon layer was then detached with aqua regia, washed several times and electron microscopically examined. Particles $> 0.01\mu$ which are insoluble in aqua regia, stick to the carbon layer in their original position and appear mostly as black and opaque dots. By means of comparing the amount of substance added, which is insoluble in the metallic matrix, with the amount and size of particles appearing in the fractograph, conclusions may be drawn as to the effect of these particles on the creep behavior.

Figs. 59 and 60 show fractographs of a Fe-Al(14)-Mo alloy with 1% and 10% $TiC/Cr_3C_2$ mixed crystal respectively. Fig. 61 represents the same base alloy with 2% alumina.

The pictures show clearly the monophasic matrix (Fe-Al-Mo alloy) and in this matrix the carbide or $Al_2O_3$ (also $FeAl_2$) particles as dark rounded grains. Their size differs widely between 0,1 and 1 micron. There are also agglomerated heaps of particles to be seen.

The electron micrographs show clearly that mechanical milling of creep inhibiting components does not result in their satisfactory distribution. Stress-to-rupture strength of such materials will increase but only with a severe drop of impact strength. It should be strived for a finer and

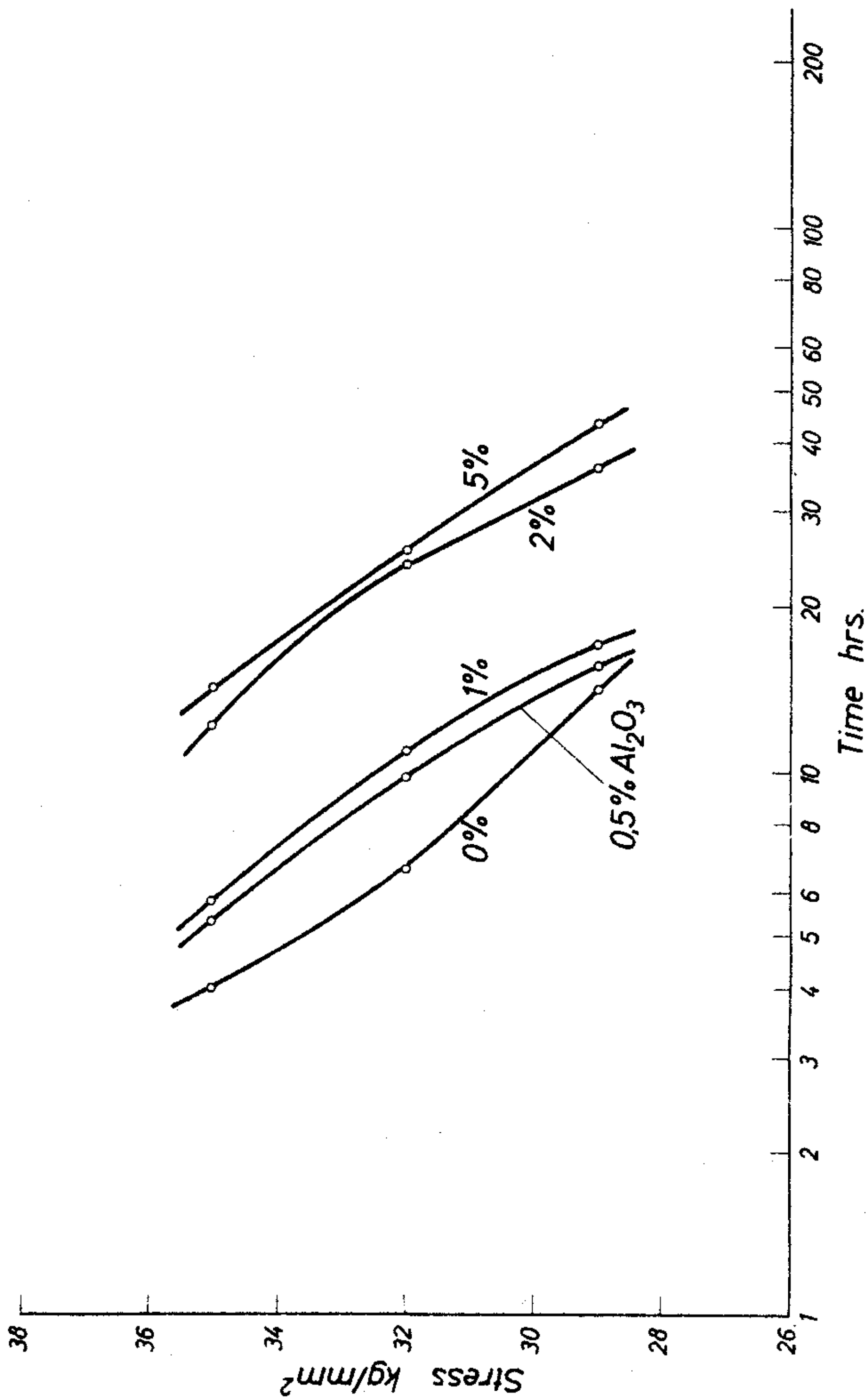


**Fig. 48:** Stress-to-Rupture Strength of Fe-Al(18)-Mo-$Al_2O_3$-B Alloys at 500°C. Extruded Specimens.

Table 74: Stress-to-Rupture Strength of Fe-Al(18)-Mo-$Al_2O_3$-B Alloys at 500°C. Extruded Specimens.

| Stress at 500°C. kg./mm.$^2$ | Rupture time in hrs. at specimen no. | | | | |
|---|---|---|---|---|---|
| | 108 | 109 | 110 | 111 | 112 |
| 29 | 14,3 | 15,5 | 17 | 35,5 | 43 |
| 32 | 6,6 | 10,8 | 9,8 | 25 | 23 |
| 35 | 4 | 5,3 | 5,7 | 12 | 13,8 |

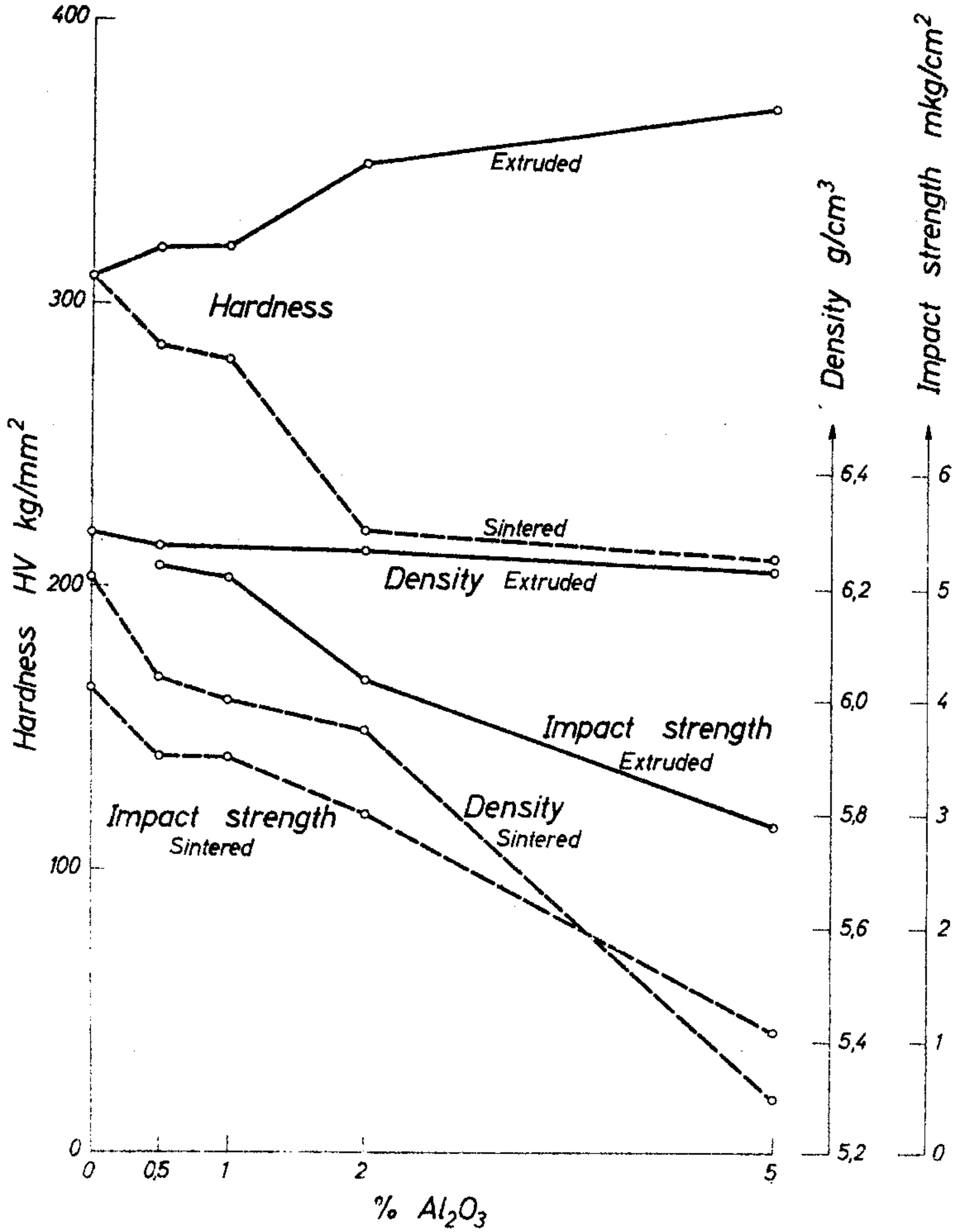


Fig. 49: Physical Properties of Fe-Al(20)-Mo-$Al_2O_3$-B Alloys, Extruded and Sintered Specimens.

**Table 75:**

**Properties of Fe-Al(20)-Mo-$Al_2O_3$-B Alloys at Room Temperature. Flat Specimens.**

| Spec. No. | Density g./cm.$^3$ | | Shrinkage | Hardness | Impact strength |
|---|---|---|---|---|---|
| | Pressed | Sintered | % | kg./mm.$^2$ | mkg./cm.$^2$ |
| 113 | 4,31 | 6,22 | 11,6 | 300-320 | 4,1 |
| 114 | 4,24 | 6,04 | 11,2 | 270-300 | 3,5 |
| 115 | 4,26 | 6,00 | 10,2 | 270-290 | 3,5 |
| 116 | 4,16 | 5,95 | 10,2 | 220-240 | 3,0 |
| 117 | 4,18 | 5,30 | 7,3 | 200-210 | 1,1 |

Table 76: Properties of Fe-Al(20)-Mo-$Al_2O_3$-B Alloys at Specimens from Extruded Rods

| Spec. No. | Density g./cm.$^3$ Sintered | Density g./cm.$^3$ Extruded | Hardness kg./mm.$^2$ | Impact strength x) mkg./cm.$^2$ |
|---|---|---|---|---|
| 113 | 6,22 | 6,30 | 310 | 4,2 |
| 114 | 6,04 | 6,28 | 320 | 5,2 |
| 115 | 6,00 | 6,31 | 320 | 5,1 |
| 116 | 5,95 | 6,28 | 340 | 4,2 |
| 117 | 5,30 | 6,25 | 370 | 2,9 |

x) Round specimens, 9 mm. dia., without notch, distance 40 mm.

| AF 61(514)-1144 Techn.Note | Metallwerk Plansee A.G. Reutte/Tirol | |
|---|---|---|

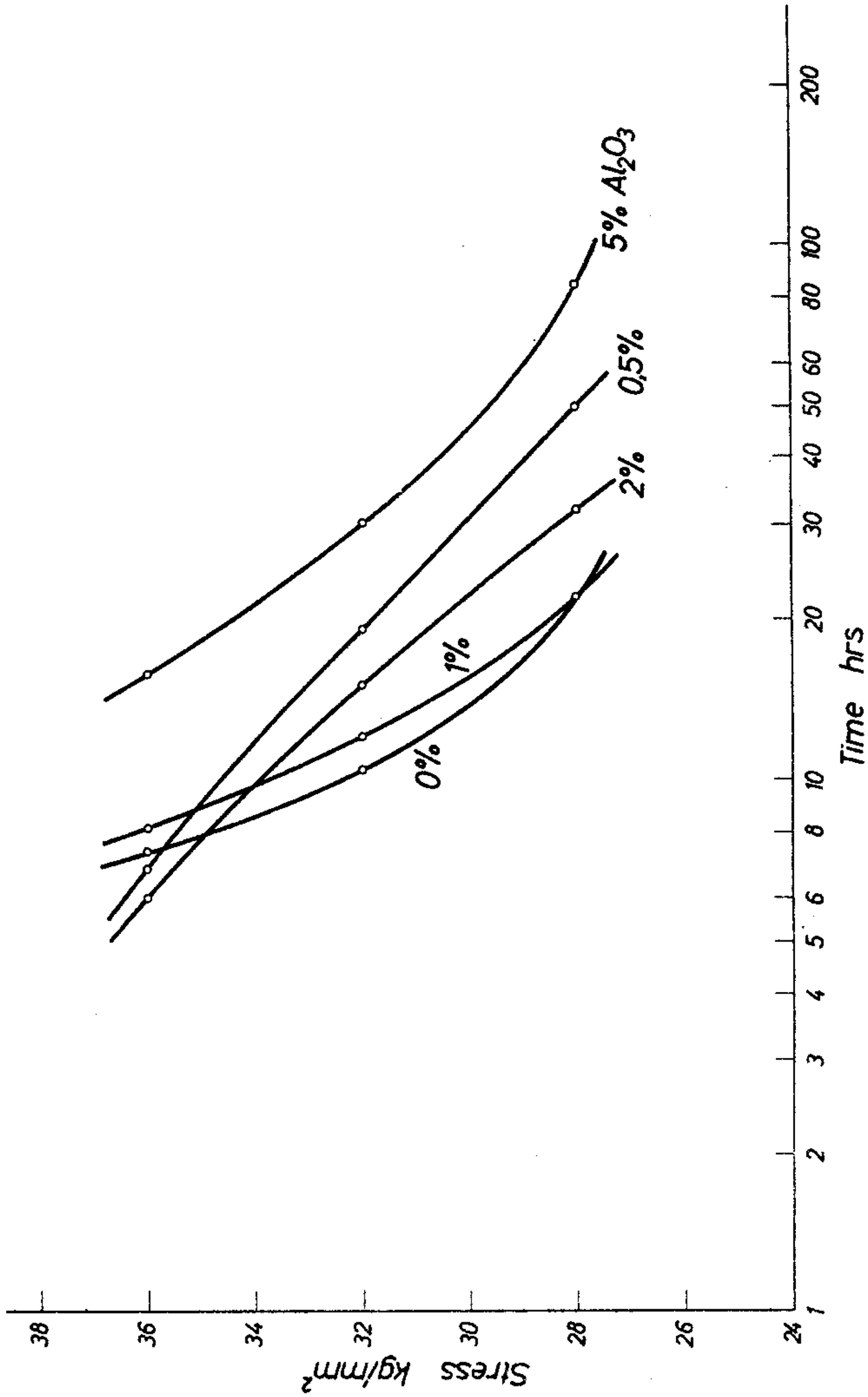


Fig. 50: Stress-to-Rupture Strength of Fe-Al(20)-Mo-$Al_2O_3$-B Alloys at 500° C. Extruded Specimens.

Table 77: Stress-to-Rupture Strength of Fe-Al(20)-Mo-$Al_2O_3$-B Alloys at 500°C. Extruded Specimens.

| Stress at 500°C. kg./mm.$^2$ | Rupture time in hrs. at specimen no. | | | | |
|---|---|---|---|---|---|
| | 113 | 114 | 115 | 116 | 117 |
| 28 | 22 | 20 | 22 | -- | 16 |
| 32 | 10,6 | 9 | 12 | 15 | 30 |
| 36 | 7,3 | 6,8 | -- | 6 | 80 |

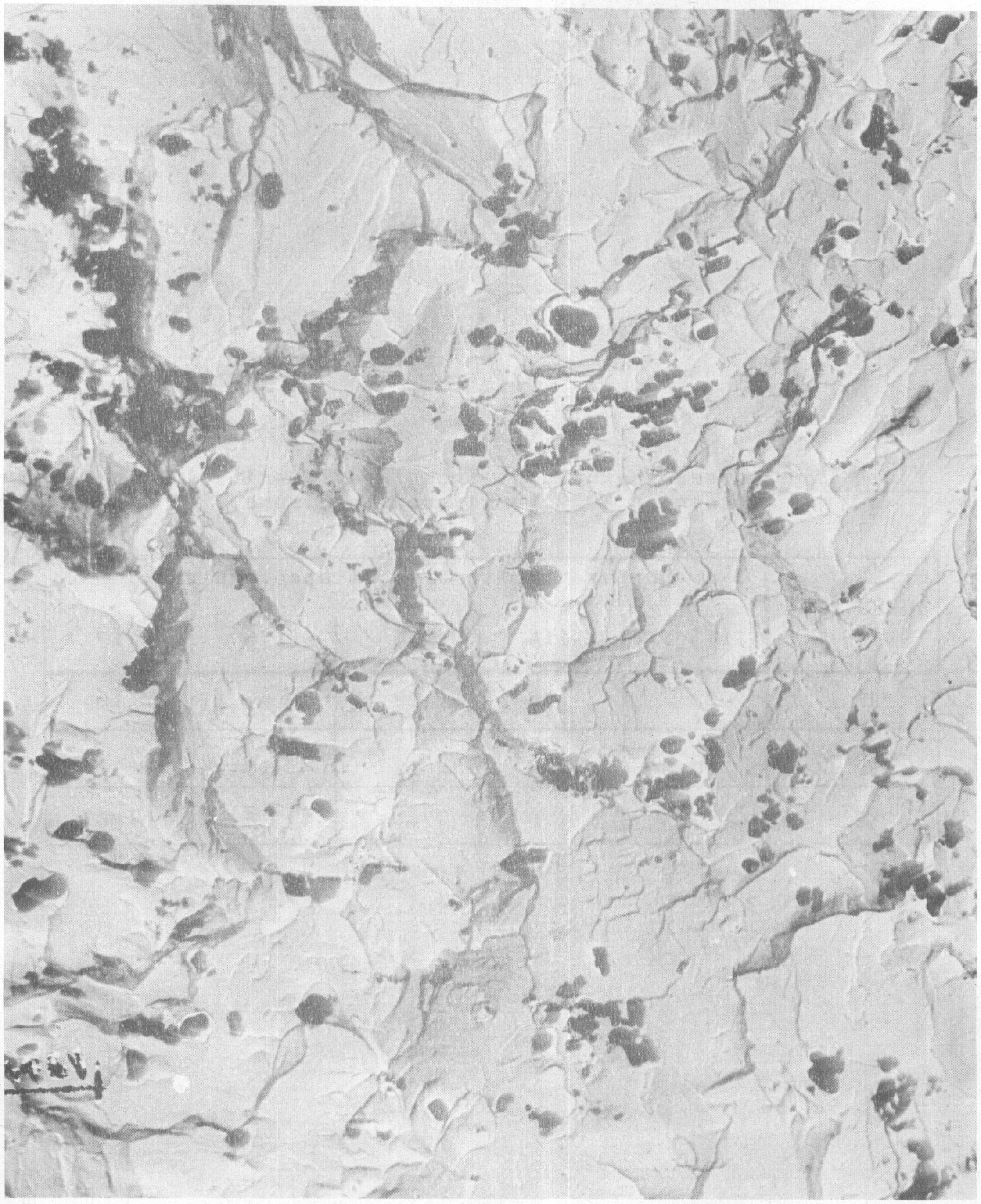

Fig. 51: Micro-Fractography.
Alloy 82 (80,5 Fe, 14 Al, 5 Mo, 0,5 B)
Electron microscopic x5000.

| | | |
|---|---|---|
| AF 61(514)-1144<br>6th QTSR,<br>Appendix | Metallwerk Plansee A.G.<br>Reutte/Tirol | |

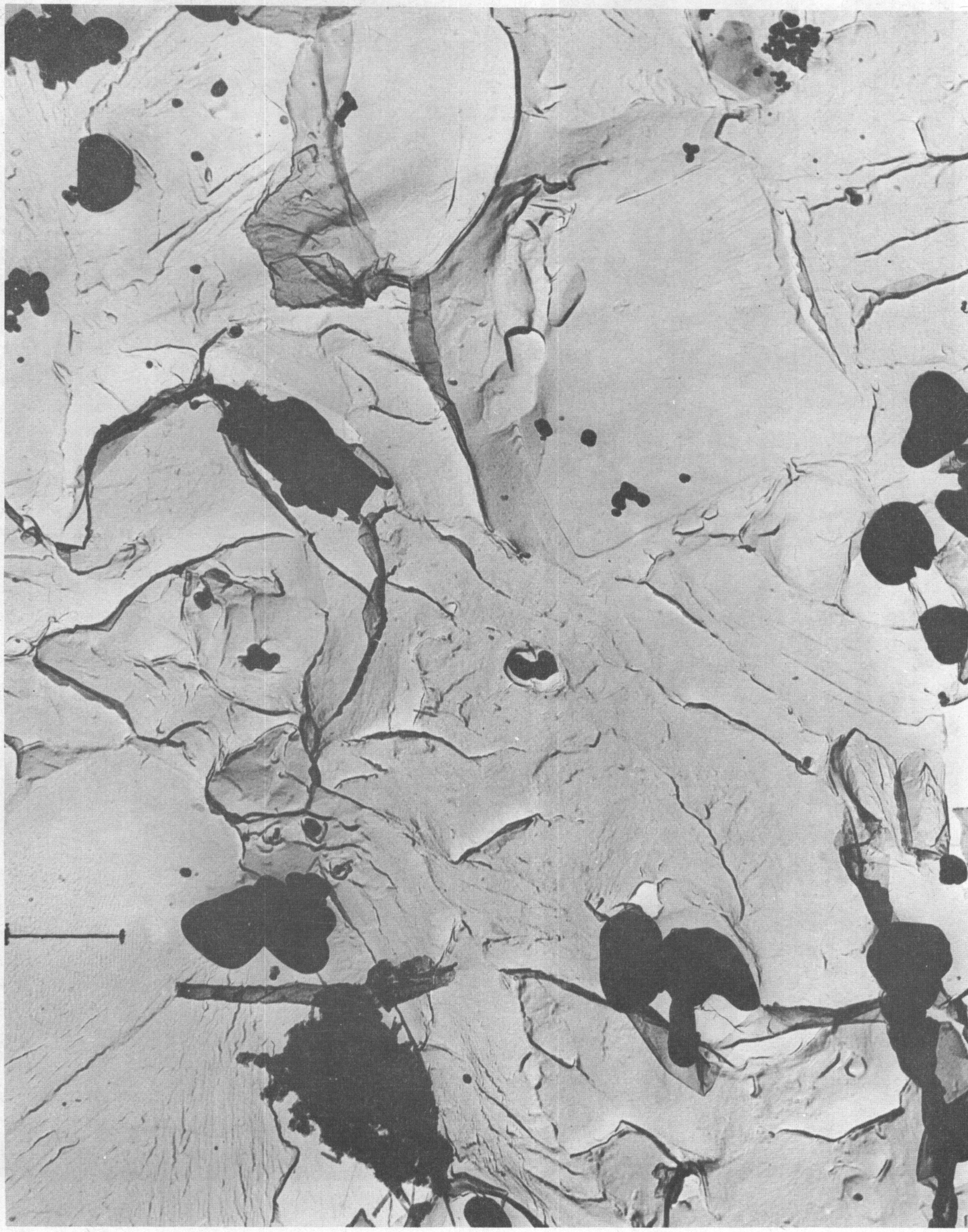

**Fig. 52:** Micro-Fractography.
Alloy 83 (79,8 Fe, 13,8 Al, 4,9 Mo, 1 TiC/$Cr_3C_2$, 0,5B)
Electron microscopic x 20.000.

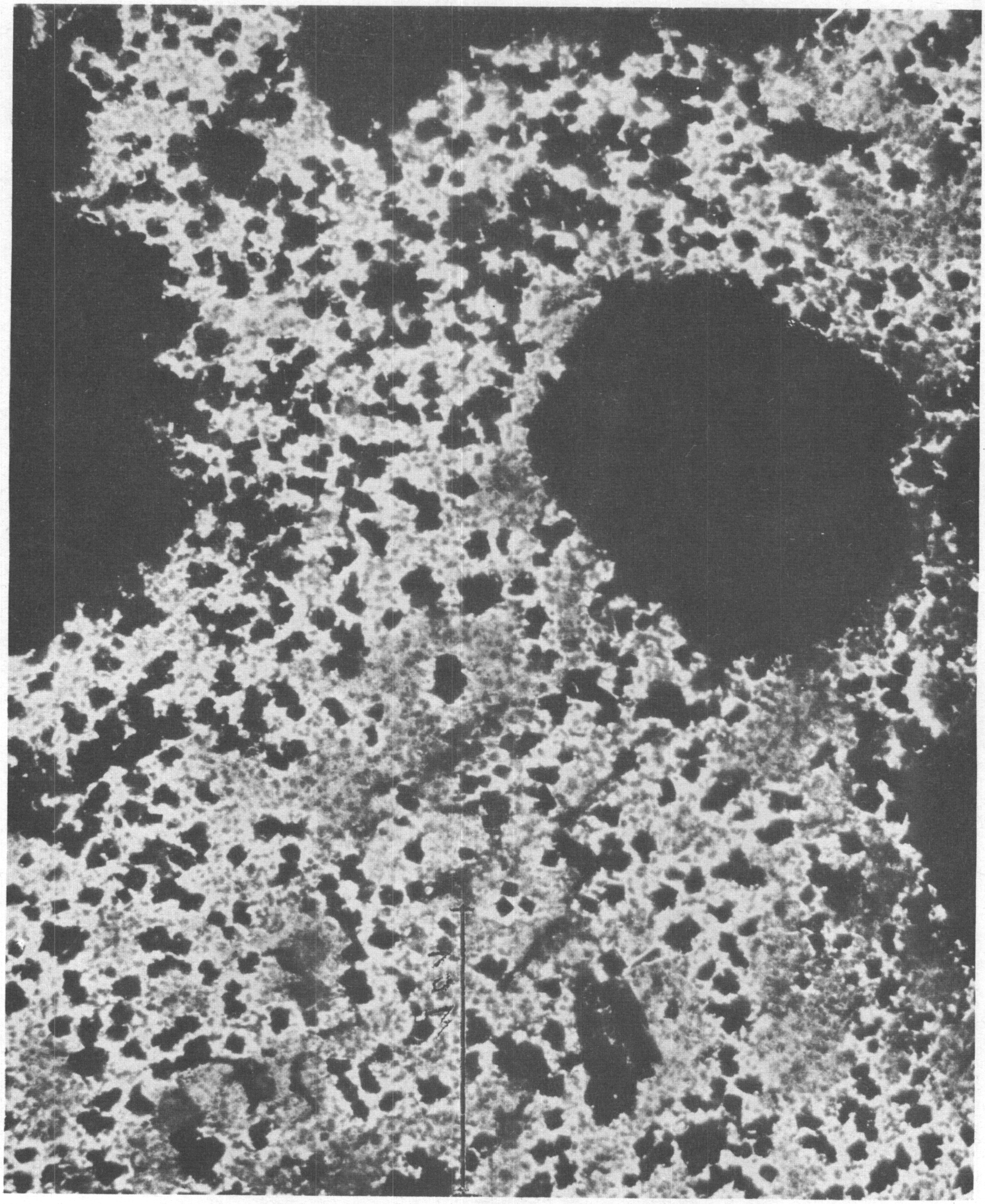

**Fig. 53:** Micro-Fractography.
Alloy 84 (77,4 Fe, 13,3 Al, 4,8 Mo, 3 TiC/$Cr_3C_2$, 0,5 B)
Electron microscopic x5000.

| | | |
|---|---|---|
| AF 61(514)-1144<br>6th QTSR,<br>Appendix | Metallwerk Plansee A.G.<br>Reutte/Tirol | |

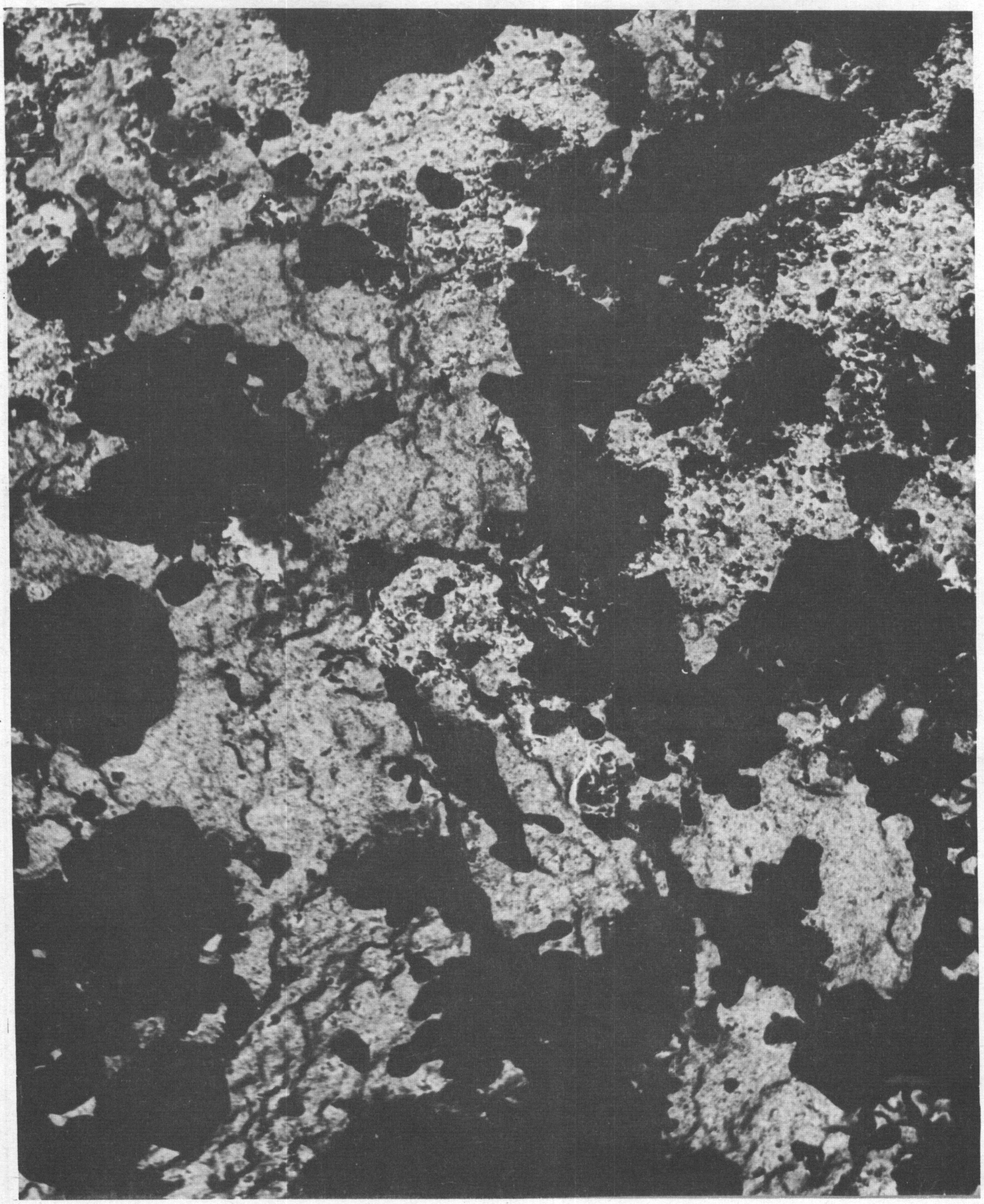

Fig. 54: Micro-Fractography.
Alloy 85 (75,7 Fe, 13,1 Al, 4,7 Mo, 6 TiC/$Cr_3C_2$, 0,5 B)
Electron microscopic x5000.

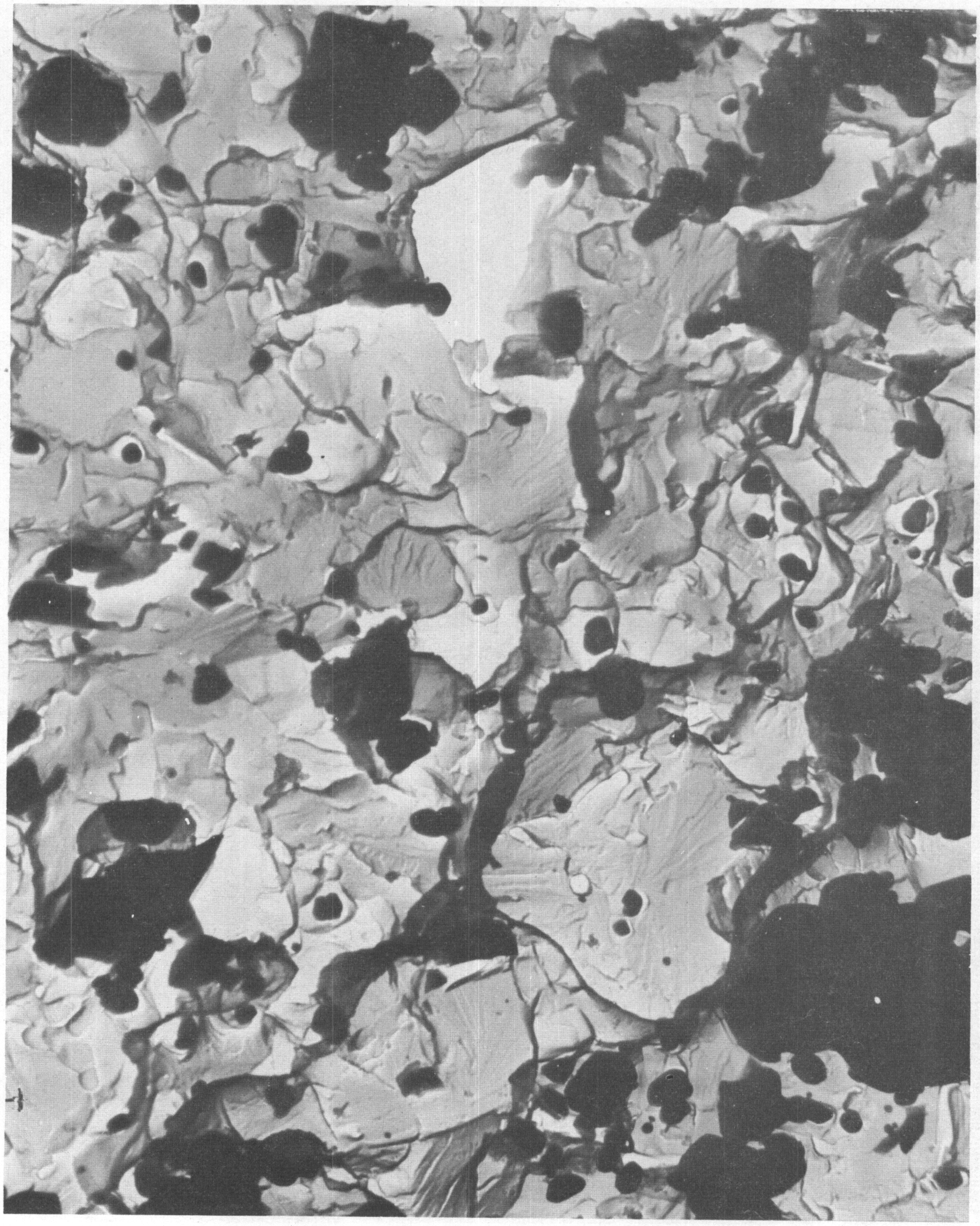

**Fig. 55:** Micro-Fractography.
Alloy 86 (72,4 Fe, 12,6 Al, 4,5 Mo, 10 TiC/$Cr_3C_2$, 0,5B)
Electron microscopic x5000.

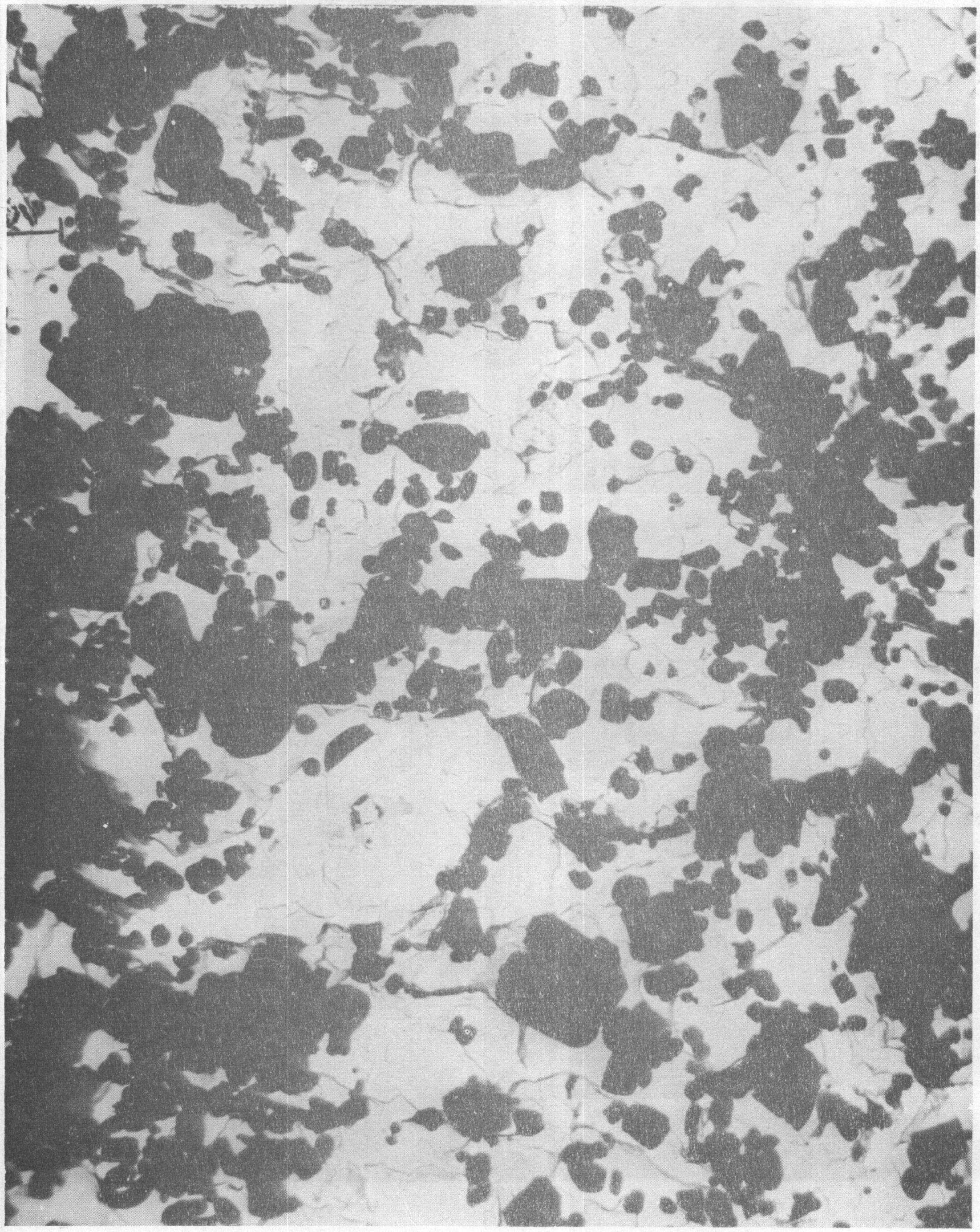

**Fig. 56:** Micro-Fractography.
Alloy 87 (68,5 Fe, 11,9 Al, 4,2 Mo, 15 $TiC/Cr_3C_2$, 0,4 B)
Electron microscopic x5000.

| AF 61(514)-1144 6th QTSR, Appendix | Metallwerk Plansee A.G. Reutte/Tirol | |
|---|---|---|

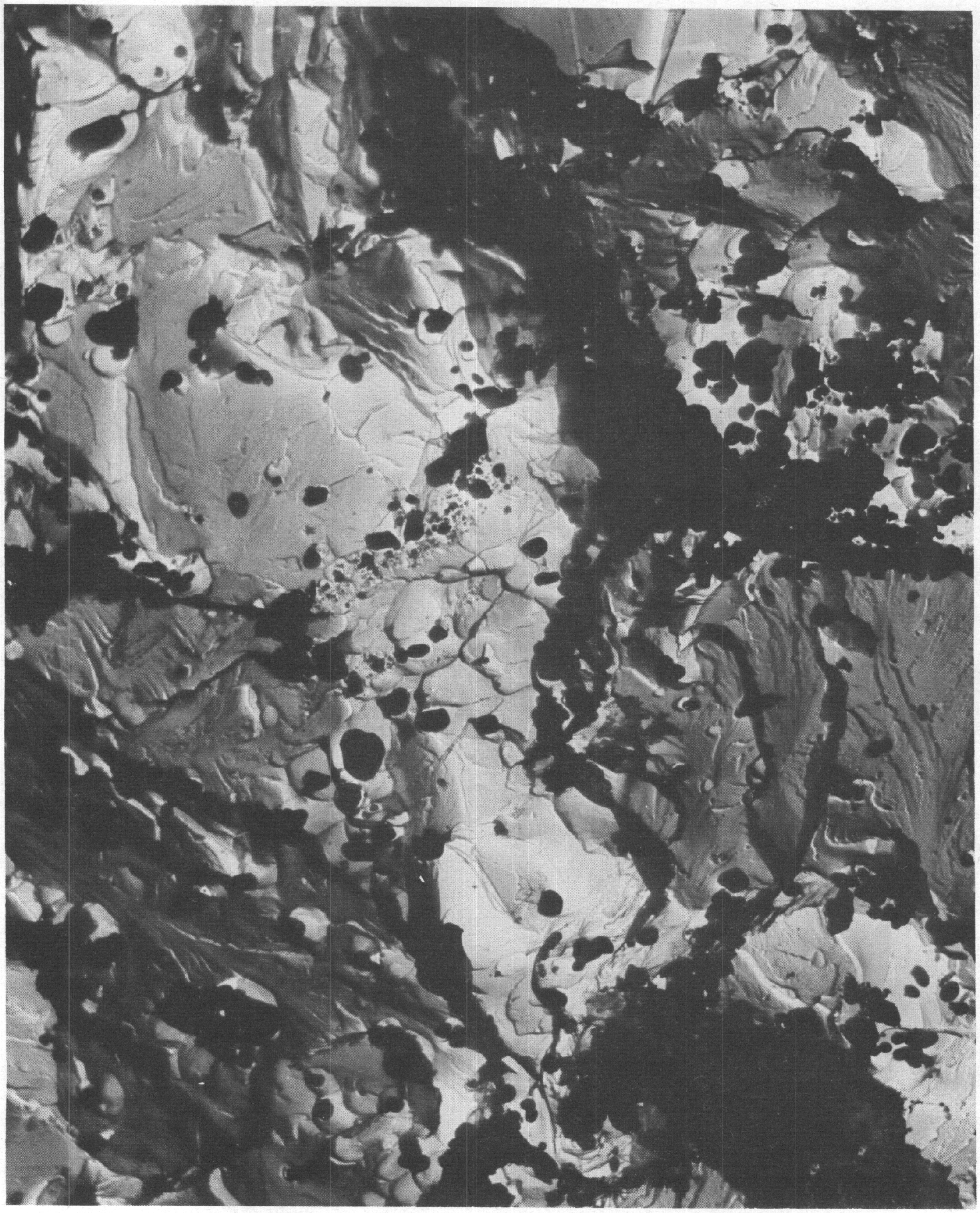

**Fig. 57:** Micro-Fractography.
Alloy 89 (80,1 Fe, 13,9 Al, 5 Mo, 0,5 $Al_2O_3$, 0,5 B)
Electron microscopic x5000.

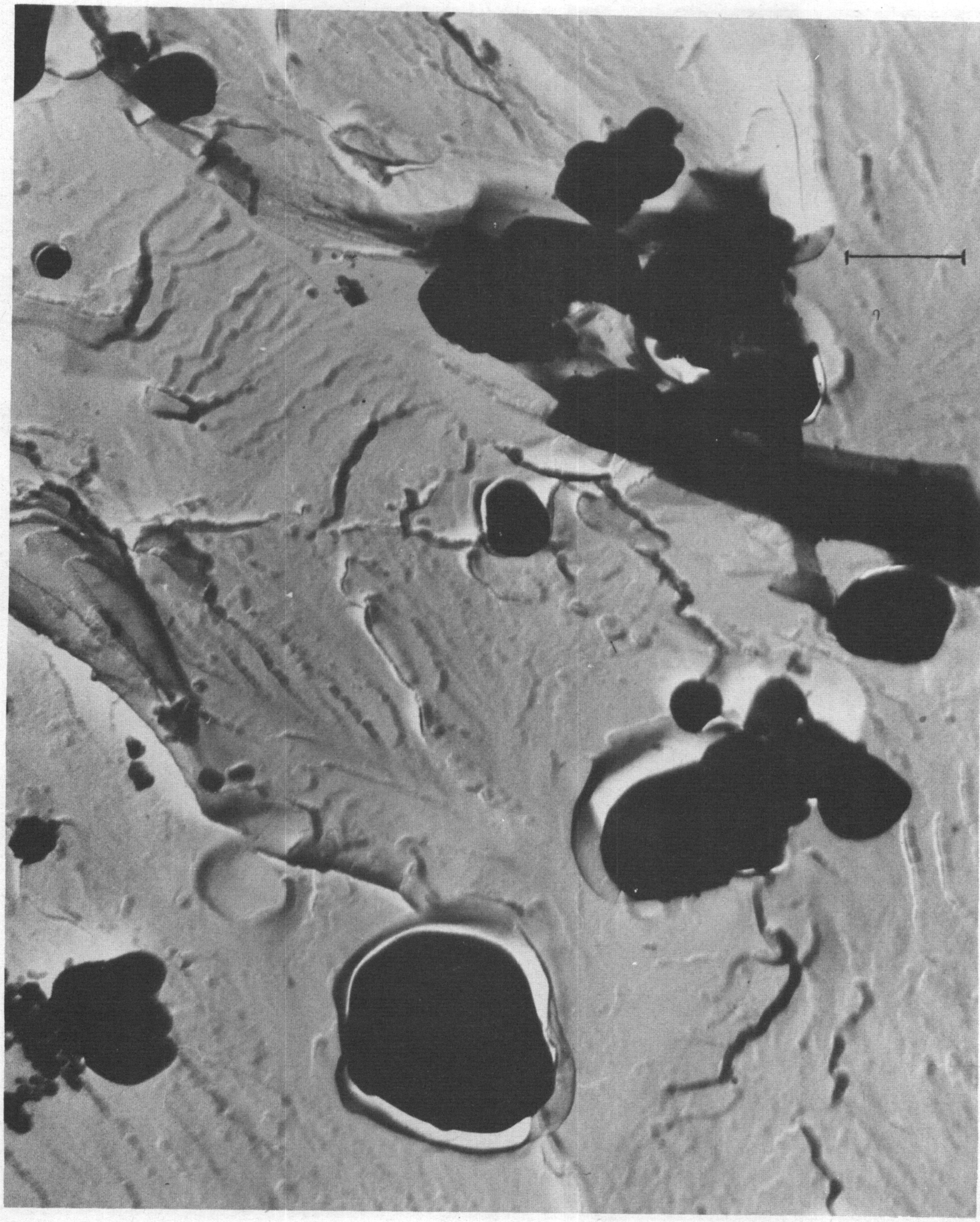

**Fig. 572.** Mico-Fractography.
Alloy 90 (79,8 Fe, 13,8 Al, 4,9 Mo, 1 $Al_2O_3$, 0,5 B)
Electron microscopic x 20.000

| | | |
|---|---|---|
| AF 61(514)-1144 Techn.Note | Metallwerk Plansee A.G. Reutte/Tirol | |

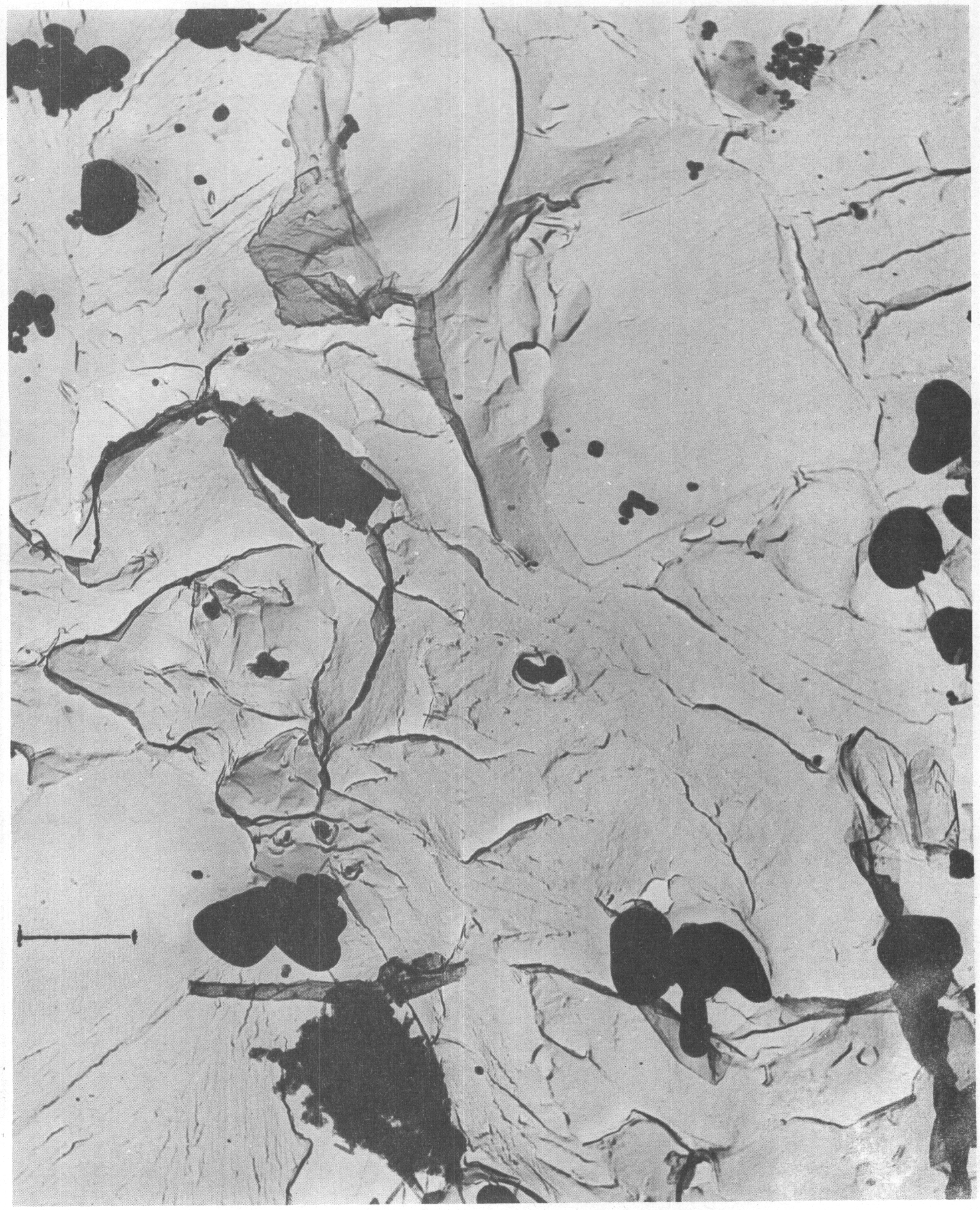

**Fig. 59.** Electron Micro-Fractograph of an Alloy
79,8% Fe, 13,8% Al, 4,9% Mo, 0,5% B, 1% $TiC/Cr_3C_2$
x20.000

Fig. 60: Electron Micro-Fractograph of an Alloy
72,4% Fe, 12,6% Al, 4,5% Mo, 0,5% B, 10% TiC/$Cr_3C_2$
x5.000

| | | |
|---|---|---|
| AF 61(514)-1144<br>Techn.Note | Metallwerk Plansee A.G.<br>Reutte/Tirol | |

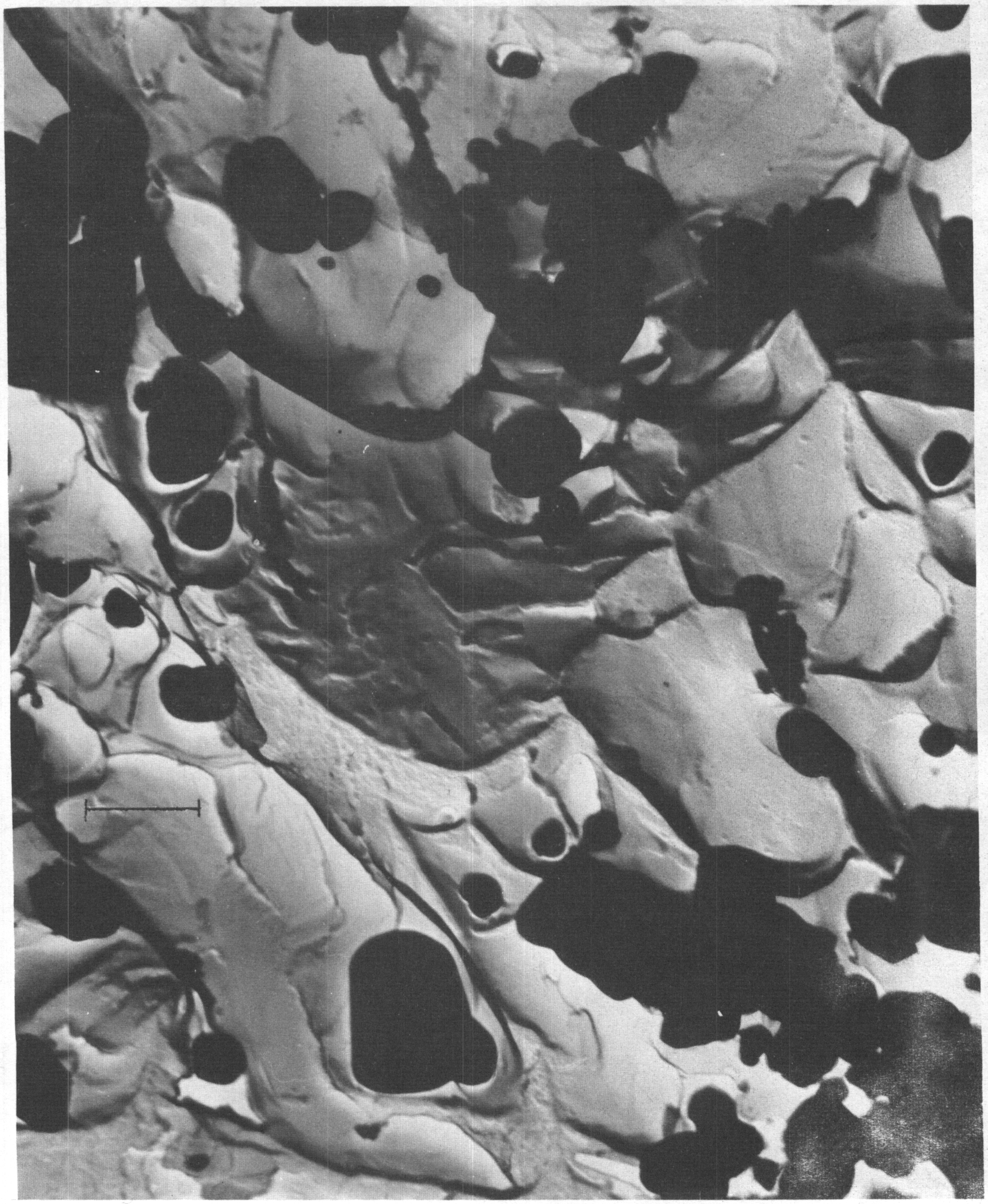

Fig. 61: Electron Micro-Fractograph of an Alloy
79,1% Fe, 13,6% Al, 4,8% Mo, 0,5% B, 2% $Al_2O_3$

 x20.000

more uniform distribution of the dispersion phase, particularly by means of internal oxidation and salt additions from which the dispersed phase is formed during sintering.

## VI. SUMMARY

Wet milled powder mixtures of Fe-Al-Mo 80/14/5-TiC/$Cr_3C_2$ alloys with 0-30% of a 90/10-TiC/$Cr_3C_2$ mixed crystal were sintered in vacuum and their properties examined, density, shrinkage, hardness, tensile strength, transverse rupture strength, impact strength, hot hardness, hot tensile strength, hot transverse rupture strength, hot impact strength, stress-to-rupture strength and oxidation behavior.

With increasing additions of carbide mixed crystal the hot strength increases also, but the alloys become brittle.

Reinforcing of the alloys by means of Ni-Cr, Megapyr or molybdenum wire and nets pressed into the powder compacts raises the impact strength provided that no reaction occurs between the alloy and the reinforcing structure.

Further emphasis was put on the investigation of Ni-Cr 80/20 and Fe-Cr-Al 68/27/4 base alloys and NiAl and CoAl alloys with additions of TiC/$Cr_3C_2$ 90/10 solid solutions. These alloys, with or without reinforcement, were examined as those mentioned above. Alloys with the intermetallic Al compounds were very brittle.

The mechanical properties at room and elevated temperature of Fe-Al (14,18,20)-Mo base alloys with small additions of TiC/$Cr_3C_2$ (1-15%) and NiCr 80/20 as well as Fe-Cr-Al 68/27/4 with 0,5-5% $Al_2O_3$ have been examined in the assintered state and after extrusion of the iron clad alloys. Their stress-to-rupture values for 500°C. being high, the impact strength exhibits a decrease with increasing carbide and alumina content respectively.

Electron microscopic investigations have revealed that mechanical means like milling of the powders are insufficient in attaining the required distribution of the carbide and oxide particles, thus restricting their influence on the stress-to-rupture behavior.